5-2014

NANOLAYER POLYMERIC COATINGS TO ENHANCE THE PERFORMANCE AND SERVICE LIFE OF INORGANIC MEMBRANES FOR HIGH TEMPERATURE-HIGH PRESSURE BIOMASS PRETREATMENT AND OTHER APPLICATIONS

Vincent C. Kandagor
University of Tennessee - Knoxville, vkandago@utk.edu

To the Graduate Council:

I am submitting herewith a dissertation written by Vincent C. Kandagor entitled "NANOLAYER POLYMERIC COATINGS TO ENHANCE THE PERFORMANCE AND SERVICE LIFE OF INORGANIC MEMBRANES FOR HIGH TEMPERATURE-HIGH PRESSURE BIOMASS PRETREATMENT AND OTHER APPLICATIONS." I have examined the final electronic copy of this dissertation for form and content and recommend that it be accepted in partial fulfillment of the requirements for the degree of Doctor of Philosophy, with a major in Energy Science and Engineering.

Gajanan Bhat, Major Professor

We have read this dissertation and recommend its acceptance:

Lee Harry Martin, Thomas T. Meek, Ramesh R Bhave, Claudia Rawn

Accepted for the Council:

Carolyn R. Hodges

Vice Provost and Dean of the Graduate School

(Original signatures are on file with official student records.)

NANOLAYER POLYMERIC COATINGS TO ENHANCE THE PERFORMANCE AND SERVICE LIFE OF INORGANIC MEMBRANES FOR HIGH TEMPERATURE-HIGH PRESSURE BIOMASS PRETREATMENT AND OTHER APPLICATIONS

A Dissertation Presented for the

Doctor of Philosophy Degree

The University of Tennessee, Knoxville

Vincent C. Kandagor
May 2014

DEDICATION

I dedicate this work to my father the late Chief-Cllr. Luka Kandagor Chesire, my mother Christina Kobilo Kandagor and son Spencer Kandagor Chesire.

ACKNOWLEDGEMENTS

First and most important, I want to give glory to God and thank Him for all the blessings and favor that he has granted me throughout graduate school. Good health, strength and favors.

I also like to extend my deepest gratitude to my family and friends for all of their encouragement and support during my studies. Without this personal cheering section, my life would be more difficult and much less fun especially my son Spencer Kandagor Chesire and my mother Christina Kandagor.

Special thank you to my advisor, Professor Gajanan Bhat who chose me to be one of his graduate students, for his advice, wisdom, and guidance, financial support, and the many opportunities for networking that were opened to me during my graduate studies. Professor Bhat has been a great inspiration and mentor, and I felt honored, encouraged, and built my discipline, trust and team work capacity.

Thank you to my co-advisor and mentor, Dr. Ramesh Bhave at Oak Ridge National Lab (ORN) for providing a different perspective to my research, for providing research facility, laboratory space, test samples, and for the financial support. His enormous expertise on membrane technology and science was extremely valuable and helpful. Thanks to Professor Harry Lee Martin, Professor Thomas Meek, and Professor Claudia Rawn for taking their time to be part of my committee and their valuable advice that they offered that made the completion of my program fruitful.

I am also very thankful to Professor Lee Riedinger, the Director of the Bredesen Center for Interdisciplinary and Graduate Education for the great opportunity and honor he accorded me to pursue my PhD through this prestigious program and for the financial support. I also would like to express my appreciation to Larry Powell ORNL for his technical support and valuable advice from his decades of experience.

Many thanks also to current and former group members both undergraduate and graduate students for their support, advice, and empathetic ears especially Kokouvi Akato, Dr. Joshua Fogle, and Stephen Sheriff. Without them, graduate school would have been rather mundane. Last but not least, thanks to my Church family for their prayers.

ABSTRACT

Membrane technology has become increasingly attractive in several applications including water filtration, food industry, oil and gas, and biomedical applications. Most recently the quest for renewable, bioenergy has called for use of membranes in biomass pretreatment and other stages of producing biofuel. The success and advancement of the membrane technology for these various applications has, however, been impeded by the fouling of membranes, which causes the pores in the microporous structure to block, resulting in reduced efficiency, and in some cases, total failure of the membranes system. This challenge leads to a tremendous increase in the cost of using membranes as a separation tool, thus making it uneconomical and therefore inaccessible for many applications that could have taken advantage of this technology.

Whereas most of the researchers have concentrated their work on post fouling techniques, i.e. techniques to clean the membrane after fouling, in this research, an approach was taken to apply a protective ultrathin coating on the membrane's surface. A high temperature stable, and chemically and mechanically robust polymer, polyetherimide (Ultem) was applied on nanoporous membranes using a solution-based coating method. The main objective was to demonstrate the potential success of nanoporous inorganic membranes to perform organic separations with high throughput at high temperatures up to 250 ^{0}C and operating pressures up to 550 psi. The high temperature stable polymer coating will be able to protect the membrane pores to prevent pore fouling during the separation process.

The results have shown that the polyetherimide - Ultem 1010 grade produced by Sabic Innovation Company, when processed into the desired polymer solution for dip coating allows the formation of very thin layer polymer on the surface of the membrane. The Nanolayer polymer coating is chemically resistant to caustic attacks and other acidic environments. The relationships between polymer concentration and the coating thickness and properties were analyzed and the coating process and parameters have been optimized to give the best coating conditions. Although there is a slight reduction in the pore size of the coated membrane, the results have demonstrated that the membrane lifetime, performance, and overall separation characteristics is significantly improved

TABLE OF CONTENTS

LIST OF TABLES

LIST OF FIGURES

Chapter One

Introduction

1.0 Introduction

The use of membranes for filtration has evolved from a relatively simple application to one of the leading separation technologies that can be in scientifically tailored for various uses. This technology has undergone several phases including research and development up to the current state of the art applications in different fields. Research through the years has validated the use of membranes for filtration in different levels as a cost effective treatment and separation route.

Membrane filtration has been defined variously as a pressure or vacuum driven separation process in which a mixture of two or more compositions are separated into individual products, through an engineered barrier, primarily through a size-exclusion mechanism, which has a measurable removal efficiency of a target organism that can be verified through the application of a direct integrity test. Figure 1.1 shows a schematic of membrane separation technology. Membrane filtration technology includes but not limited to microfiltration, ultrafiltration, nanofiltration, and reverse osmosis. [1].

The membrane process can be classified in different ways depending on the application, the type of membrane, and the driving force. Classification by the driving force is the most common. Pressure driven membranes include reverse osmosis (RO), Nanofiltration (NF), Microfiltration process (MF), and Ultrafiltration (UF). All these membranes have different applications because their separation mechanism is varied. The membranes operate at varying pressures ranges and the quality of separation that is achieved is different for each membrane.[2]

The flux through the membrane is approximately inversely proportional to the membrane separating layer and for this reason most RO membranes have an asymmetric structure with a dense top-layer (thickness $\leq$ 0.1 Pm) supported by a porous sub-layer (thickness ~ 50-150 Pm), the resistance towards transport being determined mainly by the dense layer [3].

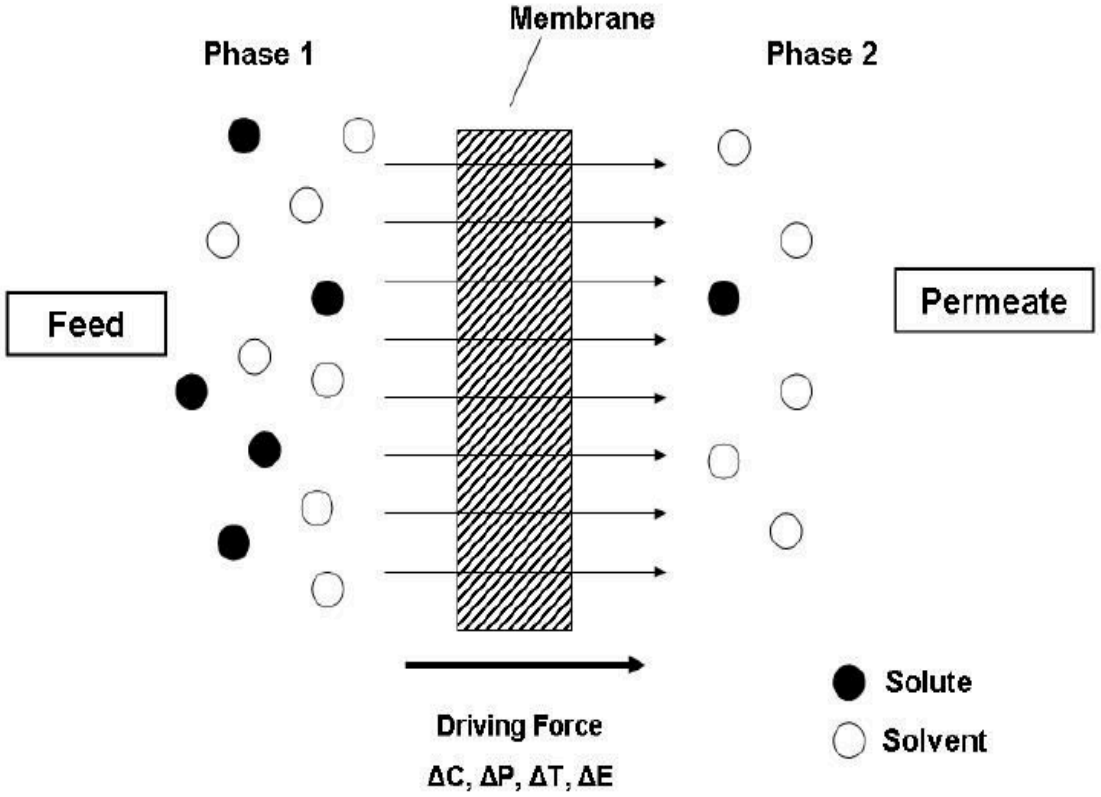

Figure 1.1 Schematic representation of a two-phase system separated by a membrane, where phase 1 is usually considered as the feed while the phase 2 is considered the permeate [4].

An external pressure difference is required to speed up the separation process. Electrical driven membranes have a stack of anion-cation and are operated by applying electrical field across the system stack allowing the separation of ionic species from the feed streams. This is a charge exclusion mechanism, which operates at lower pressure, and the membranes thickness is always higher. Another category of membranes are those that depend on the difference in concentration of the system. Examples of such membranes include dialysis, pervaporation, distillation, and gas diffusion. Here, a membrane separates two cells with different solution concentration, and the separation occurs because there will be a flow of solution from the higher concentration region to

the lower concentration region through the membrane system until an equilibrium is achieved. The concentration gradient across the membrane is therefore the driving mechanism.

Historically, the use of membranes was designed for use in the water processing and treatment industry where water was subjected to a series of membranes in which the main objective was to separate unwanted particles to achieve clean water as the end product. The design was calculated to achieve physical size exclusion where water and small molecules would pass though the membranes so that molecules larger than that of water would be separated, resulting in clean water. The strained solids were then recovered during backwashing or chemical cleaning. The efficiency of each system was however dependent on the design and permeability of the membrane which is determined by the desired water quality.

Over the years, scientific investigations driven by demands for cleaner final products, environmental regulators demands for less contaminating effluents, and the need for nanoscale separation capabilities has resulted in an expansive application of the use of membranes as techniques for separation. The hydrocarbon processing industry for example, which includes petroleum refining, petrochemical processing, oil and natural gas production, is quickly finding the use of membrane technology to be a significantly efficient and a cost effective process. In the oil and gas production industry, which is one of the biggest producer of wastewater stream, also known to produce water that contains salt, heavy metals and other organics brought to the surface, the use of membranes for separation is increasingly becoming the most suitable approach [5, 6].

Currently, trends and interests among researchers and scientists are fast shifting to nanoscale dimensions, and the same their research focus to match the demand for nanoscale technology for various applications in the medical, environmental, and research field. Each function requires different class of membrane materials to fit the specific need. The use of different materials for fabrication of membranes including polymers, ceramics, and zeolite materials, which can be readily dehydrated and rehydrated, and are used as cation exchangers and molecular sieves, is quickly taking root.

Recent advancements in the technological capabilities to view and manipulate in the nanoscale level has transformed how we categorize, analyze and use materials from a generally opportunistic to a specific directed and controlled application. This is very important in the nanoporous application where precise control and perfection over the size of the pore typically to the molecular level is much sought.

Another emerging use of membrane technology is in the biofuel production. In the past few decades, there has been an exponential increase in demand for fossil fuels driven by the increasing economic and population growth worldwide. The high demand for oil-derived fuels has caused their prices to skyrocket. This, coupled with increasing environmental concerns is the potentially damaging effect of the continuous use of fossil fuel, and the fact that the sources of cheap fossil oil supply is finite, has resulted in a worldwide increase in research on alternative source of renewable energy in order to supplement the current high energy needs, and the possibility of eventually replacing the fossil-based fuels. Currently, biofuels from corn, switchgrass and algae among others are being pursued and improved. However, the success of the fuel production from such biomass has been impeded by the high cost associated with the separation of the biomass into different products. One of the alternative avenues for reducing the cost associated with the biofuel production from biomass has been identified to be an efficient separation mechanism. Use of inorganic membranes in the different stages of separation is proving to be of great economic sense [7].

Membranes that are designed for different processes may achieve separation through different passive transportation mechanisms. Membrane pervaporation (PV) has been determined to be one of the most energy saving technologies for use in separation of azeotropic mixtures. Pervaporation is principally an operation on the solution-diffusion mechanism, and many plants use the PV mechanism for alcohol dehydration. The pervaporation process can be categorized into two types: sweep gas pervaporation and vacuum pervaporation. In sweep gas pervaporation, an inert gas such as nitrogen is used on the permeate side to cause a decrease in the permeate partial pressure. On the other hand, the vacuum pervaporation process uses vacuum pump to lower the partial pressure

of the PV permeates. Here, solution to be separated contacts the membrane at the feed side.

Although few existing membranes that are used in different applications are hydrophobic, i.e. ethanol permselective, most of the membranes are hydrophilic. Hydrophilic membranes are mostly water permselective due to water's smaller molecular size. The membranes can be produced from different materials and are therefore categorized into three different main categories: organic, polymeric, and composite or mixed membranes [8].

Although the phenomenon of membrane fouling is an extremely complex and a big draw back to the advancement of the technology, it has not been defined precisely yet. Fouling is still generally used to describe the undesirable deposition of retained particles, colloids, macromolecules, salts, etc., at the membrane surface or inside the pores. The type of fouling that occurs on the membranes is determined by different factors, which includes the kind of separation process, the chemical nature of the foulants, and the chemical interactions between the foulant and the surface of the membrane. The fouling type can be scaling, inorganic, organic fouling and biocolloidal or colloidal fouling [9].

In water application, colloidal fouling is inevitable because natural and process water will have colloids, which are classified into 1) inorganic colloids such as iron oxides, iron hydroxides, and silica, 2) organic macromolecules which includes proteins, polysaccharides, and natural organic matter, and 3) biocolloids such as microorganisms, bacterial, oil suspensions, and viruses. The aggregation of dissolved organic matter into colloidal sized particles is usually facilitated by increased concentration of rejected ions at the membrane surface. In membranes used for biomedical, food industry and biotechnology, the main foulant are proteins.

It has been shown experimentally that strong adsorption of natural organic matter on the surface of membranes can be attributed to hydrophobic fraction characteristics of

the membrane, a factor that results in a sharp decline in the flux. On the other hand, hydrophilic fraction of natural organic matter has a minimal effect on membrane fouling.

Membrane researchers mostly agree that the fouling due to organic micro/macro molecules and biocolloids is largely determined by the foulants ability to adhere to the surface of the membrane which is influenced by the hydrogen bonding, hydrophobic interactions, attractions due to London-van der Wall forces, and electrostatic interactions. In designing the antifouling solution, the strategy is therefore to modify the membrane surface in order to reduce or prevent the adhesion interaction between the surface of the membrane and the foulant, which will then inhibit or reduce the fouling tendency [10].

1.1 Membrane modules

A membrane unit can simply be defined as a unit that consists of membranes, the pressure support structure, outlet and feed ports, and permeate draw-off ports. The membrane modules should be designed so that there is sufficient feed circulation in order to suppress a build up of particle deposit in the system so that concentration polymerization is limited. The modules are also designed so that the membrane surface per unit volume is achieved by maximizing the packing density. This will also ensure that waste due to leaks is eliminated due to leaks between the feed and permeate stage. A simple membrane module should be able to permit easy access during cleaning, disassembly, and have low hold up volume characteristics. There are five major types of membranes, mainly: tubular, spiral wound, capillary, hollow fiber, and plate or frame systems.

1.1.1 Tubular module

Tubular Module Membranes shown in figure 1.2 is the simplest membrane configuration. It is fabricated by casting the membrane inside the support structure of hollow porous tube. Membranes with tubular configuration can handle high turbulent flow with circular velocities of up to 5 m/s. The modules are easy to clean and do not require extensive pretreatment of the feed. The low packing density characteristic of tubular membranes is an economic disadvantage point.

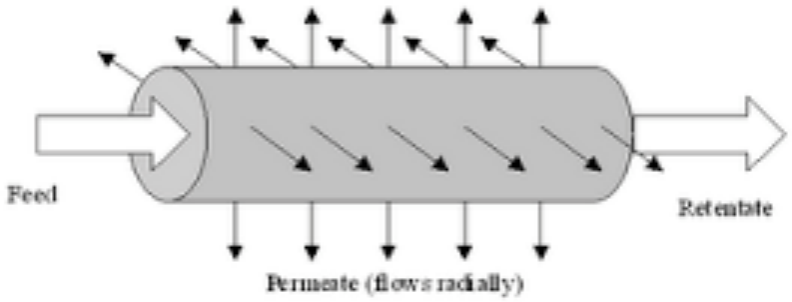

Figure 1.2 Tubular membrane module.

1.1.2 Spiral wound module

This kind of membranes are made by sandwiching two membranes with a flexible permeate spacer between them and sealing the three edges of the module. It is then rolled up onto a perforated tube that acts as the final permeate collector while the open end is connected to the feed side. A system with multiple membranes can also be designed and separated from each other by feeder spacers. The membranes are then fastened to one perforated tube. The feed spacers create an open flow channel for the feed stream, which will cause a turbulence to be created during the flow. The turbulence that is created is usually helpful in reducing concentration polymerization. Spiral wound membranes normally require pretreatment because the feed flow channels formed by the spacers can cause clogging. Spiral wound membrane module is shown in figure 1.3.

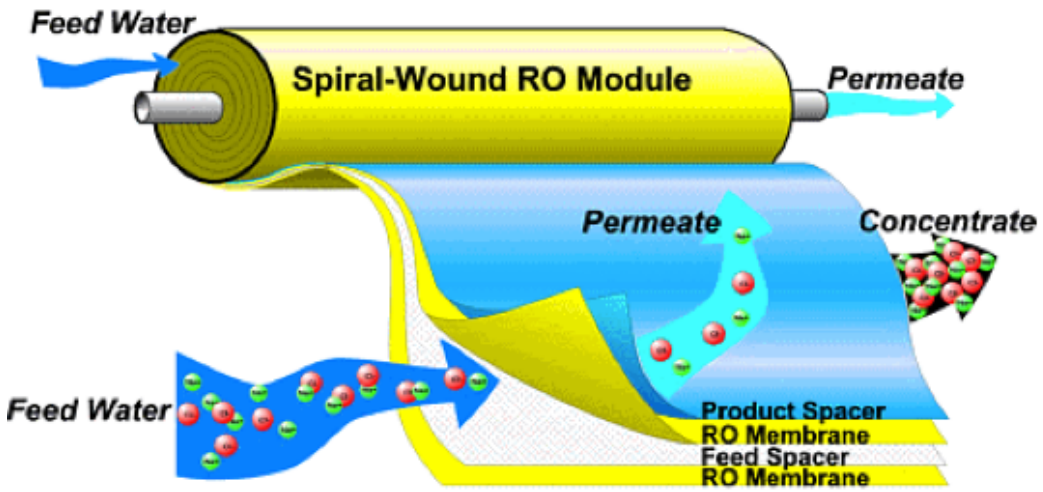

Figure 1.3 Spiral wound membrane module.

1.1.3 Hollow fiber modules

Here, the membranes are cast in the form of hollow fibers and bundled together in thousands or even millions. The feed flow can be connected to the hollow fiber in an inside out or outside in configuration. The packing density of hollow fiber membrane modules is inversely proportional to the diameter, giving this type of membrane a very compact characteristic. Hollow fiber membranes that are designed for ultrafiltration have a packing density of about 1000 m^2/m^3 and those designed for reverse osmosis process have a packing density of about 10,000 m^2/m^3. Hollow fiber membranes can be operated at very low velocities or in some cases it can be operated even at dead end mode. Although the flow rate in hollow fiber membranes is laminar, the shear rate is still high because of the flow channels are very low. Figure 1.3 below shows the schematic of hollow fiber membrane.

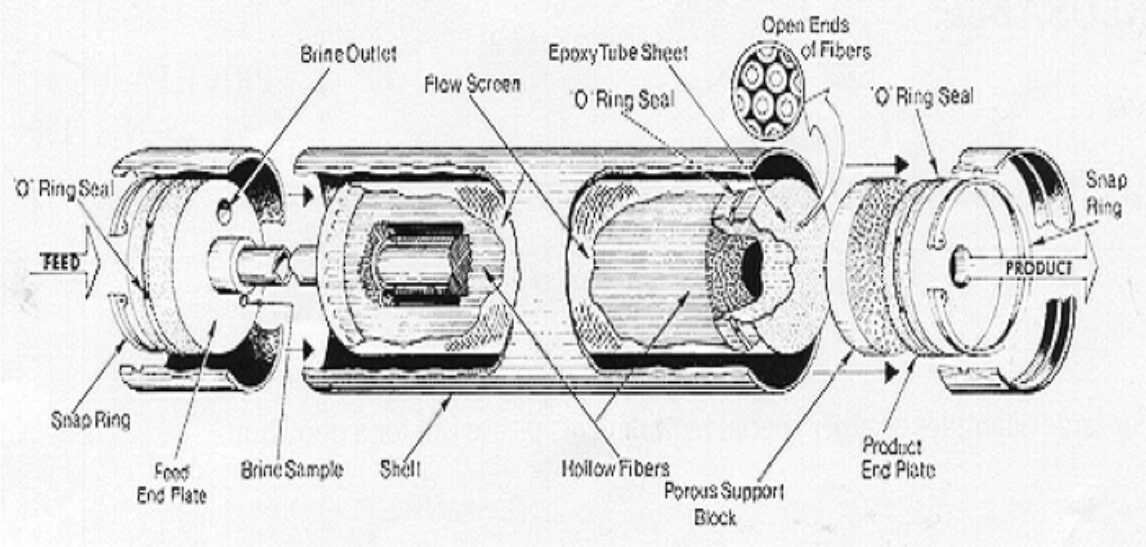

Figure 1.4 Hollow fiber membrane module [2].

1.1.4 Capillary modules

Capillary module membranes are similar to the tubular modules except that the diameter is generally smaller that those of tubular design. Capillary membranes are usually used in ultrafiltration and microfiltration applications. Because of their low dimension and low operating pressure capacity, these modules do not require pressure support. Capillary module membranes are usually designed to operate in cross flow configuration where the feed flow inside the tube, also referred to as shell and tube configuration. One disadvantage of capillary module is that the pressure across the membrane can be very high, which will affect the flow velocity in the membrane lumen, and for this reason, the length of capillary membrane is limited to 1.2 meters.

1.1.5 Plate and frame modules

These membranes are fabricated by stacking flat sheet membranes and support plates. The direction of the feed flow is between the membrane of adjacent plates, and the arrangement is very versatile where the feed circulation can be in series or parallel or a combination of both. The packing density for plate and frame module membrane rages

between 100 m^2/m^3 – 400 m^2/m^3. Because of its simple design, the system is easy to assemble and disassemble and it is easy to clean and replace.

1.2 Membrane performance

The performance characteristic of a membrane is determined by its flux. The flux (J_w) is expressed as the volume or the mass per area per unit time. The volume units can be expressed in grams (g) or cm^3 and so on, and the time in minutes or seconds or hours. The module flux is used to refer to the average permeate flux for a particular module and is expressed in $l/m^2/h$ or $l/m^2/d$. The solute rejection in a membrane can be calculated using the equation

$$R = \frac{(C_{feed} - C_{product})}{C_{feed}} * 100$$

Where: R-is the rejection,

C_{feed} – is the feed solute concentration, and

$C_{product}$ – is the solute concentration.

1.3 Goals and organization of the dissertation

A fouling-resistant membrane has a great potential to increase the overall efficiency of membrane separation system and eliminate the high cost of operation that is typically associated with fouling. Although there exist membrane surface modification techniques reported in literature, these attempts, explained in more detail later, serve as a reference point for the research work that is presented here. The main objective of this research work is to systematically investigate Ultem polymers as a potential anti-fouling coating material for membranes. A deeper evaluation of the chemical, thermal, and solubility properties together with characterization of the polymer coatings will be fundamental in establishing the relationships between the Ultem chemical structure and resulting coating properties. Another objective is to apply these polymer coatings on the surface of the membranes and evaluate their performance as an anti fouling technology. Fouling behavior and the effect of surface properties on fouling were also studied.

This dissertation contains 6 chapters including this introductory chapter. Chapter 2 provides a detailed background and theory of membrane separation systems and the historical perspective. It introduces the previous and current membrane work, models, and explains the anti-fouling technologies that are currently being explored as discussed in literature. Chapter 3 describes the materials and experimental methods used.

Chapter 4 gives an overview of the chemical, physical, and transport properties of the membranes that were used in this research work and discusses the results achieved because of the coating that was applied to the membranes. The fouling characteristics of the membrane before and after coating are also discussed in detail. The subsequent fouling properties and the stability of the polymer coating in different chemical, thermal, and mechanical environments are discussed. The economic, environmental and other benefits are also explained. Chapter 5 closes with conclusions, challenges and chapter 6 summarizes the recommendations for future work.

Chapter Two

State of the Art

2.0 The Historic Perspective of the Development and use of Inorganic Membranes

2.1.0 Introduction:

In the last decade, membrane technology has attracted enormous attention because of its dignified performance as a separation technology, with the major attraction being the fact that it does not require use of chemicals as a mechanism for separation, and it uses less energy. Although initial application of the membranes was extensively for the creation of process water from groundwater, surface water or wastewater, the technology has become increasingly competitive for other conventional applications. The membrane technology is very basic and simple: in the water processing application the membrane acts as a very specific filter that will let water flow through, while it catches suspended solids and other substances. The membranes operation is based on the principle of gradient, which includes pressure gradient, concentration gradient, and in some applications, the introduction of electric potential between the two sides of the membrane. This various methods work by forcing the flow of the medium intended to be separated from one side to another. Membrane filtration technology can be used as an alternative for flocculation, sediment purification techniques, adsorption (sand filters and active carbon filters, ion exchangers), extraction and distillation [11, 12].

It is generally perceived that inorganic membrane technology is a new innovation. But technically, its use and development has been in existence since the early 1940's. The early use of the inorganic membranes was intended for the gaseous diffusion process in the separation of the uranium isotopes applied during the Manhattan Project in the US. Upon this initial technological success, industrial scale membranes were developed for ultrafiltration and microfiltration of process liquid streams. However, recent research on membrane technology has been expanded to a broader application aimed at separation using basic process that includes coupling of catalytic reactions [13].

2.1.1 Development of ultrafiltration and microfiltration inorganic membranes

Organic ultrafiltration for use in the industry resulted from factors that were part of the historic scientific progress in membrane filtration. The need for the know-how was derived by the development of nuclear gaseous diffusion plants. Although the existence and success of use of polymeric membranes for use in the ultrafiltration industries was a step in the right direction, the limitations due to high temperature and pressure applications resulted in the need to develop inorganic membranes.

Use of inorganic ultrafiltration or microfiltration membranes evolved from the same concept of the basic structure of membranes used in gas diffusion described in a number of patents written in the 1970's [13]. However, the use of high mechanical resistance inorganic membranes have been in existence since its development at the Oak Ridge National Lab where zirconium hydroxide mixed with polyacrylic acid was deposited on porous carbon or ceramic base. This kind of dynamically formed nonsintered membranes require continuous regeneration, which later progressed into ultrafiltration membranes of the same kind.

2.1.2 Synthesis of inorganic membranes

The field of inorganic membranes has attracted the attention of many scientists in recent years. The relatively large number of patent applications submitted in the last decade pertaining to this area is a reflection of the development of inorganic membranes. A membrane can be described as a semi permeable barrier between two phases, which prevents intimate contact. These barriers can exist in the form of liquid, gas, or solid and is designed so that it can restrict the movement of molecules in a particular way and must be permselective. As mentioned earlier permselectivity can be achieved in several ways including but not limited to:

- Molecular sieving or size exclusion,
- Differences in diffusion coefficient
- Electrical charge gradient

- Solubility gradient
- Internal surface reactivity and adsorption difference

Since the membrane filtration works on mechanisms driven mostly by pressure or electric gradient, liquid-solid mixtures can be separated using membranes, as well as manipulation of chemical reactions by shifting equilibrium conditions. Manipulation of catalytic reactions can also be achieved by membrane separation technology [14].

Ultimately, the efficiency of a membrane will depend on several factors. The morphology and the microstructure are the most important aspects in determining the quality of a membrane. Depending on the specific application, the membrane will be synthesized to fit the mentioned physicochemical structure. Inorganic membranes can be categorized into a number of groups that are determined by several factors including their application, synthesis method, and characteristics among others [15].

i. Dense membranes: Made from metallic materials and alloys or solid electrolyte developed for diffusion of hydrogen or oxygen. Its mechanism is such that the ions are transported by the metallic electrolyte. Dense inorganic membranes can also consist of liquid porous support.

ii. Porous membranes: Consist of different morphological and microstructures made from porous metals or ceramics, therefore forming different pore systems. Constant pore diameters with pores running from one side of the membrane to the other, with percolated pores consisting of more or less regular shapes with spongy structures.

iii. Dynamic membranes: characterized by nonpermanent property, meaning that the separation layers are formed during the synthesis process in-*situ* on a porous support.

iv. Composite Membranes: Here, the top layer is modified further and consists of intimate mixture of two phases. The technology

employed in modification includes precipitation of a phase from liquid or gases, followed by further treatments, resulting in a decrease in the pore sizes [16].

2.1.3 Modification of composite membranes

The chemical nature of the pores' internal structures, and the decrease in the effective pore structure can be achieved by manipulation of the top configuration. In both cases, there is an increased interaction between the medium inside the pore and the outside layer resulting in improved transport and separation properties of the membrane, i.e. surface diffusion and multilayer adsorption, which ultimately help improve equilibrium constraints in membrane reactors [17].

2.1.4 General Characteristics of inorganic membranes

The effectiveness of an inorganic membrane to perform separation is dictated by different characteristics. The microstructure of the membrane support features such as the pore size, pore density, porosity, tortuosity, and pore shape are distinctive characteristics that must be considered during the fabrication of the membranes. The permeability of membranes can be achieved by the division of the permeate flux by employing the use of transmembrane pressure, where the flux is the throughput per unit are. In inorganic membranes the direction of feed flow relative to the membrane surface is an important factor that determines the flux and retention ability and therefore the efficiency of the membranes. The flow configuration, which includes a through-flow configuration, in which the flow is perpendicular to the surface, and cross-flow configuration, where the feed stream flows parallel to the membrane surfaces, will affect the flow velocity, which will consequently affect the efficiency and retention characteristics [18].

Among the most available commercial inorganic membranes, tubular shaped membranes are the most widely used for various applications, where a module would consist of up to a thousand tubes. While most of such commercially available membranes are asymmetric and composite in existence, some of them are porous glass and metal membranes having a symmetric or homogenous microstructure. These membrane

structures consist of a thin fine pore film for separating components, while the supporting substrate may consist of a single or multi layer with larger pores, mainly for improving the strength of the membrane composite [19].

The main concept in the use of composite or asymmetric structure technology in inorganic membranes is to be able to eliminate the net resistance of the permeate flow path throughout the membrane structure. The rate of flow through the structure relates to the membrane thickness in an inverse proportionality and is directly proportional to the size of the pores in the membrane. A membrane system with defect-free physical integrity, can be achieved by designing and fabricating membranes with thin separative layers, and an extra support which will provide the needed mechanical strength with a negligible hydraulic resistance [20].

In industrial microfiltration applications, backflushing of the membranes is a necessary procedure. This process of backflushing can cause a breakdown of the membranes due to the pressure applied. Membrane structure is therefore a key factor in reducing the effects of such pressures. Additionally, in situations where the antecedent structure of the membrane layers are smaller in comparison to the membrane pore size of the bulk support, the particles of the membranes can significantly penetrate the support pores and therefore causing deterioration of the membrane support due to changes in permeability. This can be avoided by designing the system in such a way that an additional layer with pore size between that of the membrane layer and that of the bulk support is installed

2.1.5 Materials for fabrication of inorganic membranes

Different kind of ceramic materials are currently used in making ceramic membranes. A wide range of commercially applicable and available porous membranes are structured from metal oxides, preferably zirconium oxide, aluminum oxide, and other oxides of titania, silica, and silicium among others [21]. In the academic research environment, however, membranes that are normally not used for ordinary purposes are that of tin oxide. Zeolite and microporous carbon materials are mainly used in designing membranes for pervaporation and gas separation process.

2.1.5.1 Metal membranes

Porous dense membranes are fabricated from metallic material. Stainless steel and other high corrosion resistant metals are commonly used for this purpose. In preparation for the actual fabrication of the membrane, various techniques such as metal powder or template leaching and sintering are used. Dense metal membranes, for example, those based on palladium or its alloys are used for preparation of pure oxygen. But due to its high cost, large-scale use of palladium to fabricate membranes is limited. Silver based membranes have been used for oxygen separation membranes [22].

2.1.5.2 Glass membranes

Glass membranes are usually made from Vycor glass. This involves phase separation process that is followed by leaching. The Vycor glass consists of about 70 wt% SiO2, 25 wt% B_2O_3, and 5 wt% Na_2O. All these materials will become miscible and form a homogenous melt at temperatures of 1400 ^{0}C or more, which when cooled to about 700 ^{0}C, will again separate into two solid phases, one rich in SiO_2 and lean in B_2O_3 and the other rich in B_2O_3 and lean in SiO_2. SiO_2 is very stable and B_2O_3 is soluble in most strong acids at elevated temperatures, and therefore the B_2O_3 rich region can be leached out and a porous structure with rich SiO_2 is achieved. The only disadvantage of membrane rich in SiO_2 is the poor mechanical stability [23].

2.1.5.3 Carbon membranes

Carbon and carbon nanotube (CNT) based membranes have recently emerged to be a leading membrane technology for different applications because of the high flux and very low biofouling, low energy, and low maintenance characteristics. More recently, carbon nanotube membranes have been identified as excellent candidates for fabrication of gas separation membranes because the CNT provides enhanced surface area per volume and weight. CNT can be prepared by chemical vapor deposition, where the substrate is prepared with a layer of nickel particles as catalyst. The substrate is usually heated to about 700 ^{0}C with two gases, nitrogen and hydrogen being fed into the chambers in order to initiate the growth of the CNT [24].

CNT based membranes for water applications are also being explored. The inner walls of the CNT are usually very smooth and highly hydrophobic. The easy movement of water molecules inside CNT based membranes can be explained by the ballistic motion of the water chains due to the strong hydrogen bonding in the water molecules compared to a weaker interaction of the water molecules with the CNT walls. Figure 2.1 illustrates the movement of water molecules across a single walled CNT based membrane. The movement of the water molecules inside these membranes does not follow the conventional fluid mechanics.

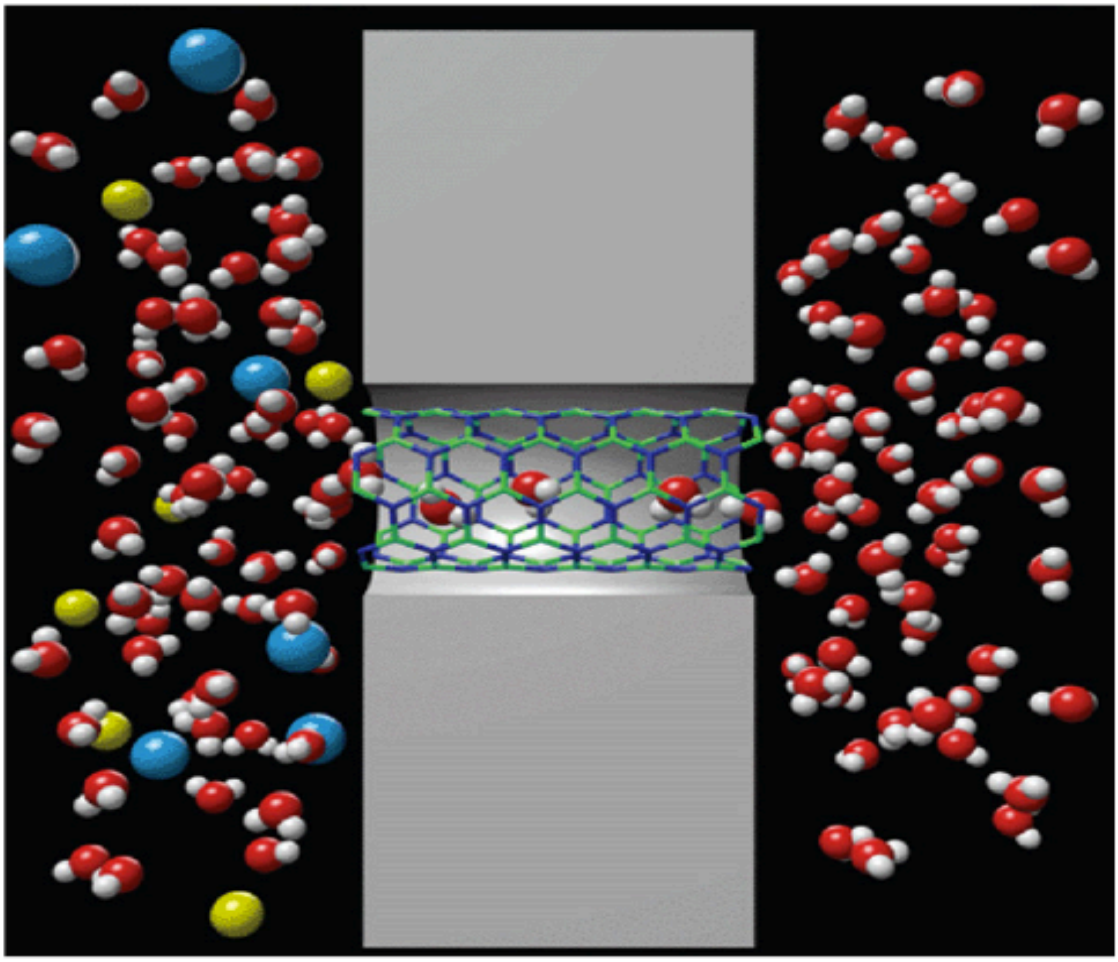

Figure 2.1 Movement of water molecules inside a single walled CNT membrane: (Image permitted by [25]).

2.1.6 Stability of porous ceramic membranes

Ceramic materials are overall known to withstand harsh conditions of temperatures, aggressive chemicals, and acidic or caustic environments where other less expensive polymer membranes cannot withstand. Specifically, the characteristics of ceramic materials are such that they can withstand swelling under extreme heat and acidic conditions due to their high thermal and chemical stability. Since fouling is a problem in membranes, and therefore requires tough solvents to clean, ceramic membranes have an advantage since they can withstand tougher cleaning solvents. The chemical stability of a material can be defined as its resistance towards the effect of liquids that are corrosive and aggressive in nature. During the material formation process of formation of a material, the effective free energy and total energy involved greatly determine the property of the end material, and therefore determining is stability, both thermal and chemical. For example, TiO_2 and ZrO_2 are well known for their chemical stability and therefore are good candidate materials for making membranes [26].

Although membranes fabricated from ceramic materials are generally thermally and chemically stable, the structure of the whole membrane is sometimes complicated and results in the membrane becoming prone to chemical or corrosion attack. This is because the morphology of the membrane consists of grain structure at the surface, grain boundaries, which consist of defects and some impurities. The non-ideal crystal composition and the defects on the boundaries complicate the membrane structure because it contains more energetically favorable positions for dissolution than the bulk material membranes. Consequently, corrosion will occur faster than on other surface structures. The thermal stability of ceramic membranes is unambiguous by nature. The membrane characteristics and parameters such as the grain size, the pore size, and the crystallographic phases can change with change in thermal energy that the membranes. However, in determining the stability of the membrane when there is a change in thermal energy over a wide range, some characteristics of the membranes play a great role. These include, first, the sinter activity of the membrane materials, secondly the transformation at the phase level, and finally the support of the membrane structure [27].

2.1.7 Industrial application of porous ceramic membranes

Several membrane technologies have been developed over the years. Among the most mature technology is the pressure driven membrane process that is used in liquid filtration, and which can generally be classified in four categories based on the size of the solute that can be separated.

- **Reverse osmosis (RO):** which can be used to separate solute up to 0.5nm. (RO) membranes are mainly used in water treatment processes to eliminate salt from water. Nonporous RO membranes have been shown to perform effective selectivity as compared to other filtration membranes that are commercially available. Typically, microfiltration and ultrafiltration membranes remove particulate matter, proteins, and other large species, and then RO is employed to remove dissolved ions. Polyamide thin film composite RO membrane is currently the most widely used RO membrane, which was designed in the early 1970's by John Cadotte. This design of membranes offers a high water flux and a high NaCl rejection relative to other RO membranes like those made from acetate-based materials. The separation mechanism in RO membranes is not sieving because the membranes do not have distinct pore structures. The separation in RO membranes occurs through selective dissolution and diffusion of the components in the membranes, and the flux of the permeate stream is inversely proportional to the membrane thickness. Which means that for a higher flux, the membrane has to be as thin as possible. Figure 2.2 describes the principle of reverse osmosis [28].

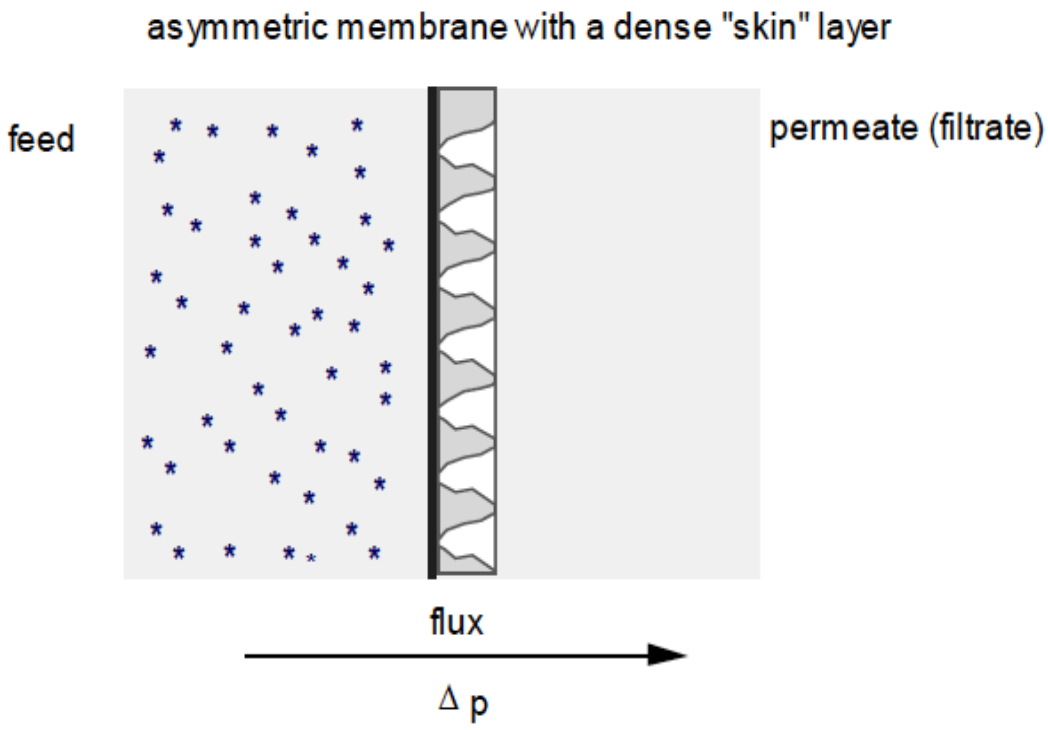

Figure 2.2 Principle of reverse osmosis.

- **Nanofiltration: (NF):** can be used for separating 0.5 nm up to 5nm. This kind of membranes are designed to retain multivalent ions and substances with molar masses higher than ~ 300 g/mol. The retention characteristics are defined and determined by how much free volume there is in the membranes, which can for some membranes be related to the flux. The better the flux of the membrane, the lesser will be the retentive rate [29].

- **Ultrafiltration (UF):** used for processes with solute ranging from 1nm up to 100nm. Typically, ultrafiltration will eliminate high molecular-weight substances, colloidal particles, polymer molecules that are organic or inorganic in nature. However, low molecular-weight organics and ions such as sodium, calcium, magnesium chloride, and sulfate may not be eliminated through ultrafiltration because their particulate size is less than 100 nm. Since only high molecular weight particles are removed, the osmotic differential pressure across

the membrane is very negligible, which means that high pressure in the membrane system is not required to maintain a specific flux. The capital cost in UF membranes can be lower because this membrane operates at low pressure, which permits the use of non-positive displacement pumps and synthetic pipes and components. The principle of ultrafiltration is schematized below and it shows an asymmetric membrane with a thin meso skin layer and macro porous structures.

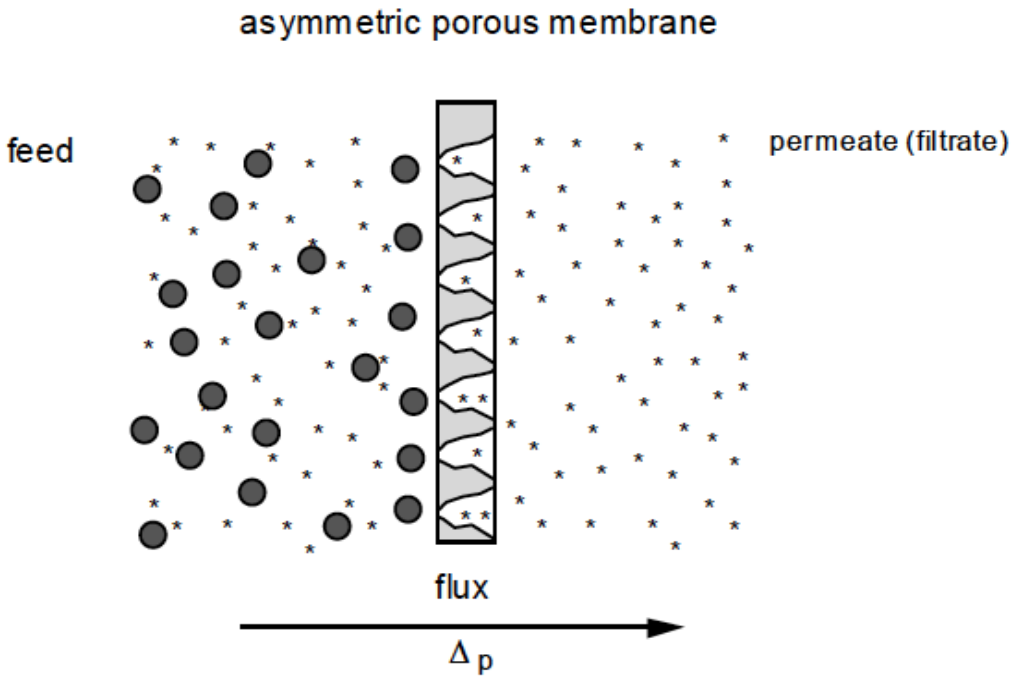

Figure 2.3 Principal of ultrafiltration.

- **Microfiltration (MF):** for processes involving 50nm up to 10µm. MF usually find application in simplified dead end filtration process. As with ultrafiltration, MF systems operate at relatively low pressures and come in a variety of configurations. The most commonly applied process is in the clarification of whole purification process in which macromolecules must be separated from other large molecules, proteins, or cell debris. Since microfiltration is used in performing separations where the particles size are in

excess of about 0.1 μm in diameter, the particle diffusion and osmotic pressure difference between the feed and the filtrate solutions are relatively very low. The mass flux through the microfiltration membranes can therefore be described by the pore-flow model equation:

$$Jv = \sum_i J_i V_i \cong - L_p \frac{\Delta_p}{\Delta_z}$$

Where J_v is the volume flux across the membrane system, and i represent the components in the solution, V is the partial molar volume; p is the system pressure, and the phenomenological coefficient referring to the hydrodynamic permeability of the membrane is represented by L_p, the pressure difference between the feed and the filtrate is denoted Δp, and the membrane thickness is Δz. The principle of microfiltration is depicted below in figure 2.4 [30].

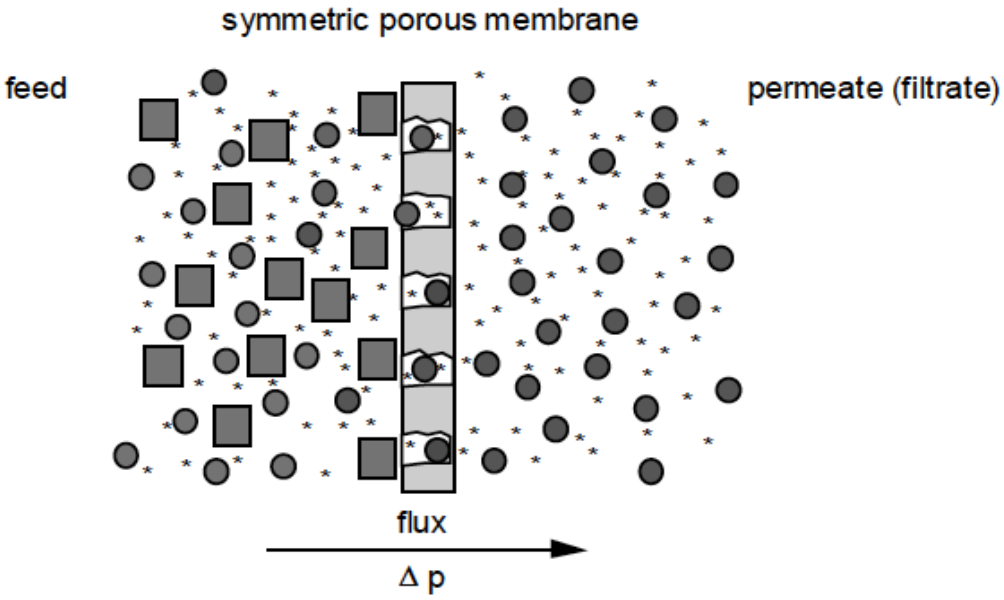

Figure 2.4 The principle of microfiltration; Obtained with permission from Introduction to Membrane Science and Technology [30].

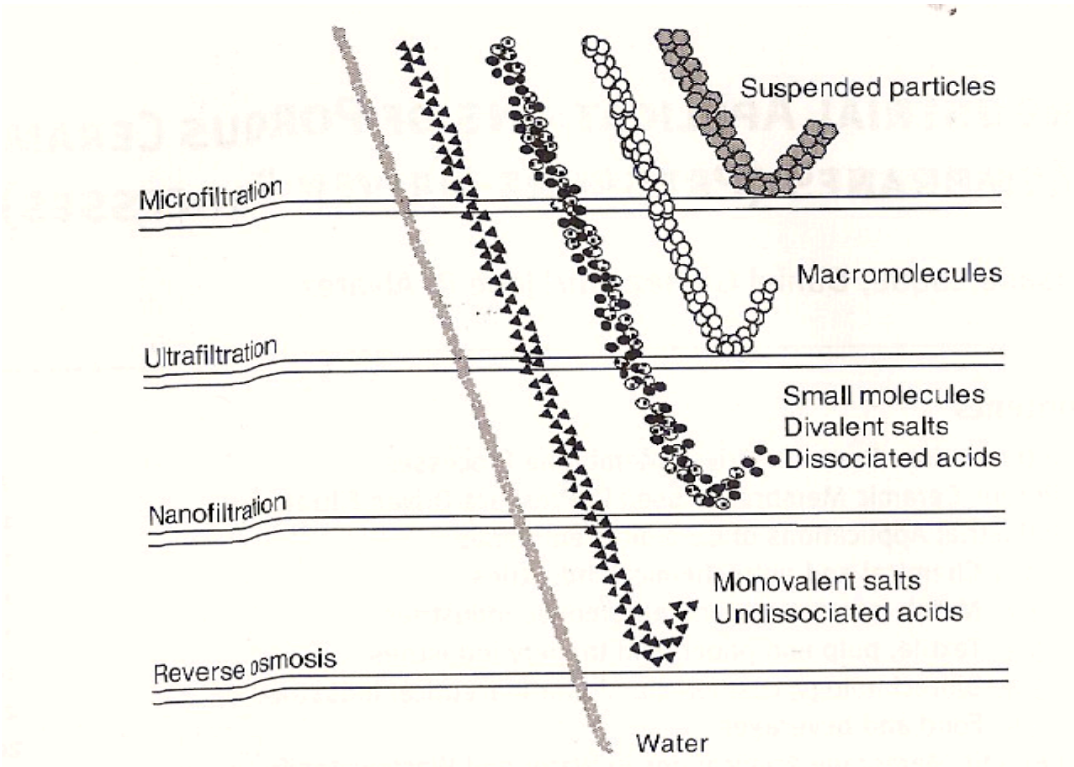

Figure 2.5 Pressure driven membrane process.

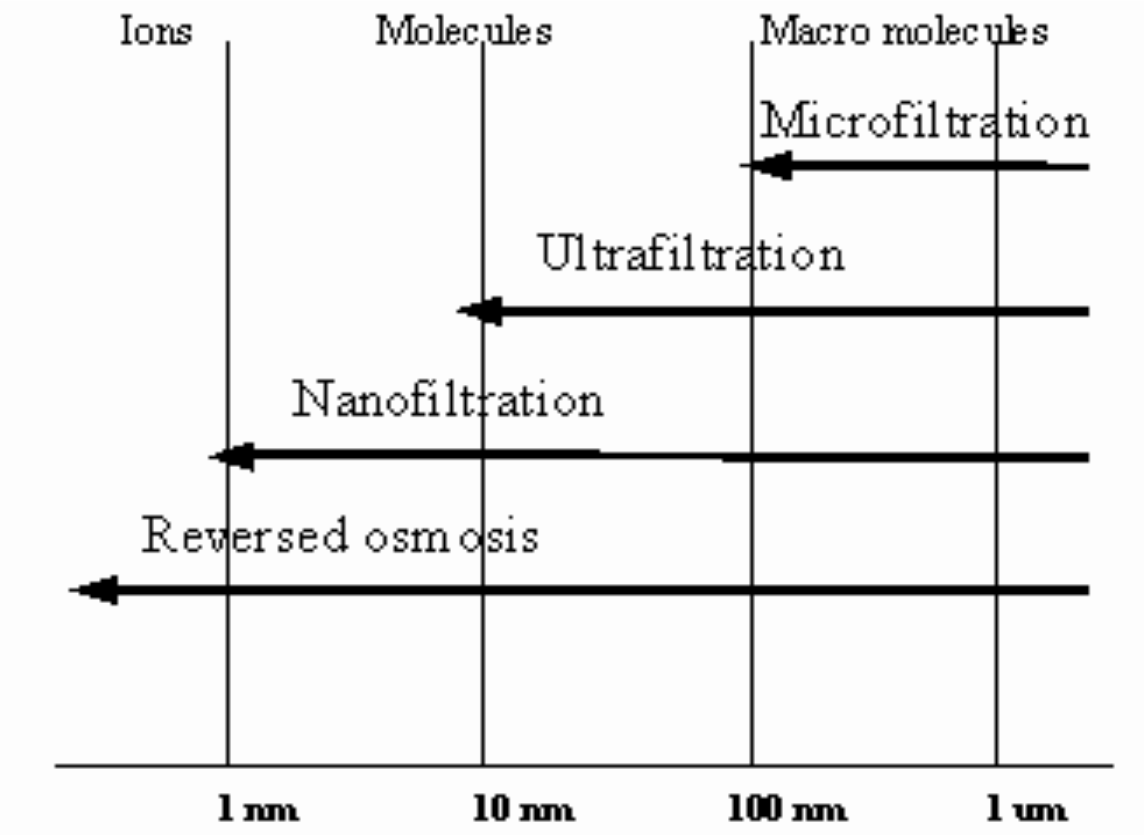

Figure 2.6 Summary of the particle size and their corresponding filtration process.

As the pore size of the membrane decreases, the effective rate of mass transfer through the membrane decreases due to the resistance from the membrane pore structure. An external pressure therefore, has to be applied in order to increase the driving force. In general, pressure driven membrane technology is constantly growing because of its effectiveness and high industrial impact, partly due to its overall high selectivity, lower energy consumption (because no phase change is necessary). It is simpler than other processes, and a continuous operation is always maintained, and the effective cost is much lower compared to similar processes [31].

Ideally, the performance of a ceramic base membrane system can be determined based on the permeation and separation properties, which is directly related to the mechanical strength. The integrity of the selective top layer and the membrane support system on which the top separation layer is coated, greatly determines the overall properties of the membrane. Originally, ceramic-based membranes were designed specifically for use in uranium enrichment projects and also in wastewater treatment. However, the success in its initially intended application and improvements of the technology over the years has resulted in the exploration of its application for possible use in the biotechnology, pharmaceutical, and food and beverage industry, as well as chemical, and petroleum industry [32].

2.2 Characterization methods for nanofiltration membranes

In order to simplify membrane characterization, it is very essential to relate the membrane structural properties to its performance and classify the membranes according to materials and application since these are the features that have the greatest impact on performance. Commonly, two different materials may be distinguished as being frequently used for nanofiltration membranes, namely polymeric and inorganic materials. Most of the polymeric nanofiltration membranes are designed to have cross-linked network structures consisting of ionic groups. These polymeric networks do not contain discrete pores. On the other hand, inorganic membranes do contain discrete meso-pores with different pore sizes.

Membranes for nanofiltration application vary in several ways depending on the material it is made of, the mechanism it employs in separation, and the specific purpose for which it is designed. Membrane characterization techniques can be done based on parameters of the membrane, mainly performance parameters, morphology, and charge parameters. Characterization based on performance involves measurements of the permeability of both charged and uncharged solute since they give direct information on the performance of the membrane in a natural environment.

Due to the different designs of nanofiltration membranes, they do exist in a variety of morphologies and therefore have different characteristics, which will affect the separation of ionic species in any aqueous environment. In membranes that are charged, these features dominate in contributing towards the membrane separation performance due to what is called membrane Gibbs-Donna effect. It is an indication of the distribution pattern of ions between the solute and the membrane, which therefore means that in a situation where the membrane is positively charged, the cations with the same charge as the fixed membrane will be repelled [33].

In uncharged porous nanofiltration membranes especially inorganic membranes, the mechanism by which separation occurs is by sieving. This is mainly based on the pore size to solute size. In membranes with an interfacial polymerized layer, however, separation occurs by solution-diffusion mechanism. The polymeric network and the combined size effects of the polymer determine the efficiency of the operating mechanism and interaction between solute and membranes occurs. Membranes designed for nanofiltration purposes are generally nanoporous with no discrete structures is shown in figure 2.7

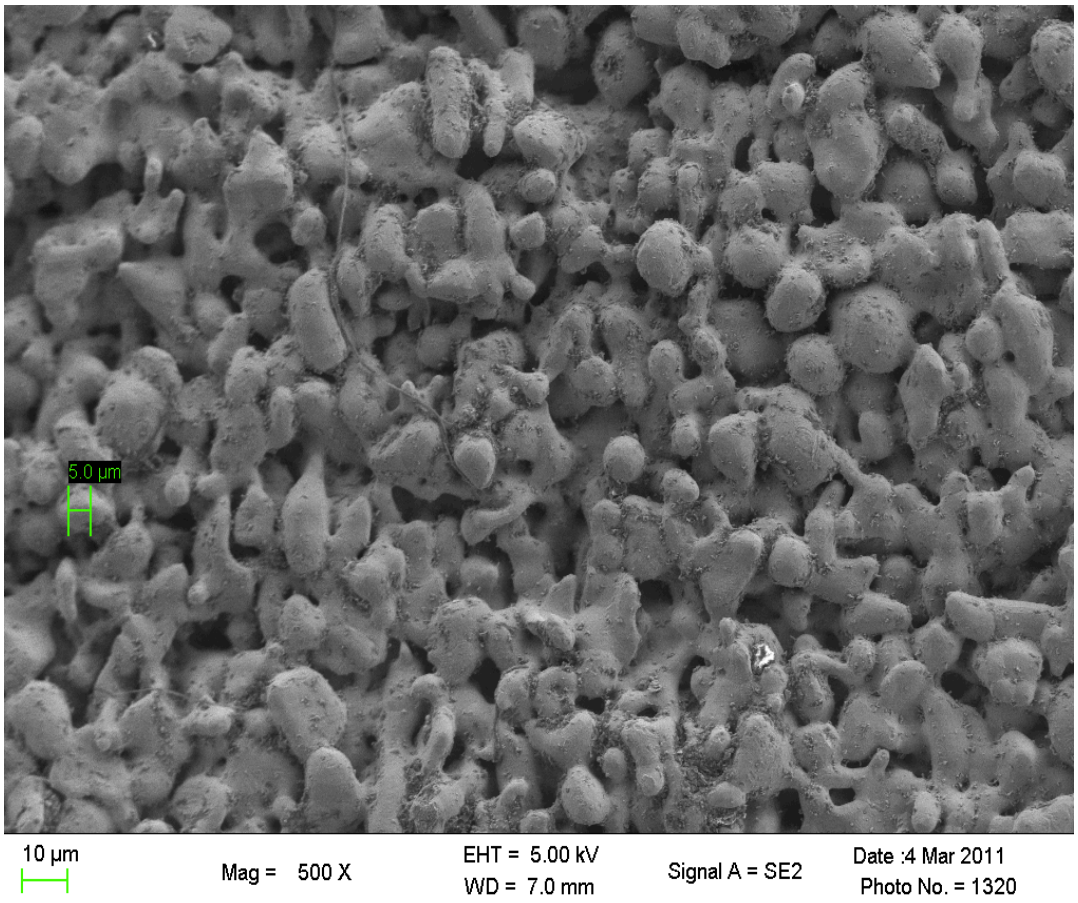

Figure 2.7 SEM picture of membrane.

This structure can also be defined as materials free of void space through which fluid transport can take place. However, a detailed description of a specific membrane and its characterization will fully consider the full and unique description of the pore size characteristics. Other morphology features such as the roughness, chemical structures, and hydrophobicity play a big role in estimating the specific performance of the membrane, which includes the permeability, retention, and fouling.

2.2.1 Surface force – pore flow

In a semi-permeable membrane (i.e. a system that is permeable to solvent, and impermeable to solute) where there is pure solvent on one side and solution on the other side of the membrane, due to high osmotic pressure in the solvent side, the solvent will start moving to the solution side. But if a pressure gradient greater than the osmotic pressure is applied across the membrane, in the direction that is opposite to the osmotic pressure gradient, there will be a reversed flow, where the solution starts moving to the solvent. This is because the solution becomes more concentrated while the solvent in it passes to the solvent rich side. The surface force-pore flow technique is an indirect method of determining the pore size and was proposed by Kastelan-Kunst. Here, the pore size and its density have been determined based on the rate of surface force-pore flow of a solute through the membrane. This method is used in assumption that both the solute and solvent infuse through the membrane skin through a collection of cylindrical pores that are perpendicular to the surface of the membrane influenced by the surface forces. The average pore size and pore size distribution are eventually estimated in comparison with the experimentally obtained separations data for various reference solutes. Apart from these solute-membrane interactions, it has been established that the membrane-based separation process is a function that is very dependent on the pore size. The surface of a membrane contains unique microscopic pores through which a fluid is passed through under force (pressure). The pore dimension and the characteristics of the pore structure also play a great role because they affect the friction factor and therefore the flow characteristics of the membrane separation. The geometrical structure of the pores and the interactions among solute, solvent and pore-wall are explained in the surface force pore-flow. The Modified Surface Force Pore Flow (MD-SF-PF) model was initially used for predicting the performance of the sodium chloride–water and sodium sulphate–water reverse osmosis systems. [34] [35].

2.2.2 Microscopy

There are various microscopic and scattering techniques for different scales of observation that have been used to characterize the morphology of membranes and to analyze the surface and bulk properties of the membrane. There are different microscopic techniques that include Scanning Electron Microscopy (SEM), Transmission Electron Microscopy (TEM), near-field microscopy (Atomic Force Microscopy, (AFM) and Scanning Tunneling Electron Microscopy (STEM). The most widely used among these various techniques are SEM and AFM. The SEM applications are varied and focus on membrane structure characterization, hollow fiber membrane fabrication and the study of the fouling process in membranes [36-38]

2.2.3 Hydrophobicity

2.2.3.1 Contact angle

Hydrophobicity, which is the lack in affinity for water can be determined from the contact angle measurement. This is a technique that has been widely used to determine the affinity of solid materials to water. In porous membrane materials where it is known that solute deposits can occur due to chemical binding, hydrophobicity of membranes, electrostatic attraction and or short-range force as Vaan der Waal, etc, the contact angle is more effective in determining the hydrophobicity.

In the study of membranes, the contact angle expressed in terms of (θ), is a measure of the wettability of the material, which is the capacity of the water that can be absorbed by the membrane. An ideal hydrophobic surface will have a contact angle of zero assuming water as a droplet and not an organic solvent. There are two common methods that are used to measure the contact angle: the sessile drop method and the captive bubble method. In the sessile drop technique, usually performed in air, the liquid drop is placed on the surface of the sample and the angle the drop makes with the surface is measured as shown in figure 2.8 a. The captive bubble techniques use either air or liquids that immiscible. Here, the sample is immersed in the liquid and a drop of the other liquid or a bubble of air is applied beneath the sample. The angle that is made between

the pendant drop and the surface is the contact angle (figure 2.8 b). For both methods, a contact angle of more than 90^0 or more represents hydrophobic surface, and a contact angle of 0^0 is a complete water-wet, hydrophilic surface [39].

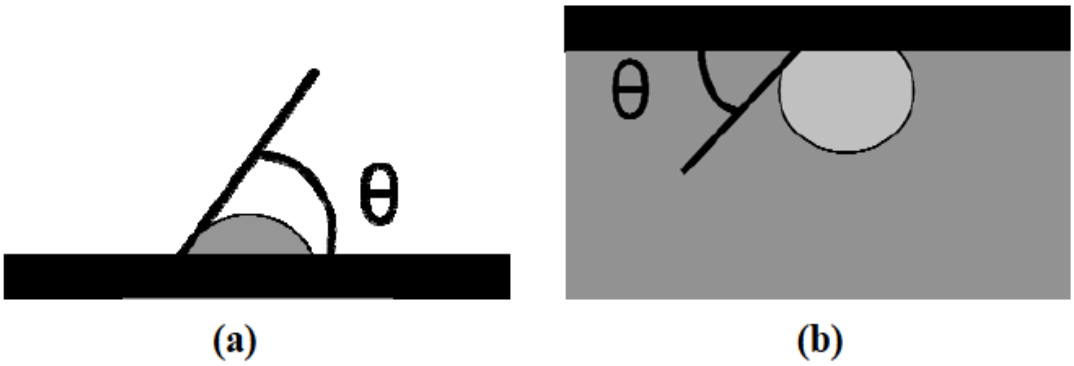

Figure 2.8 a) sessile drop and b) pendant drop contact angle measurements.

2.3.0 Fouling in Membranes

As defined by Koros et al, fouling "*is the process resulting in loss of performance of a membrane due to the deposition of suspended or dissolved substance on its external surfaces, at its pore openings, or within its pores" [40]*. Fouling is an irreversible process which may only be reversed by a chemical cleaning process [41]. This flux decline, as it is also referred to, is different from those that can be reversed by cleaning with only water. Flux decline that can be cleaned with just water is not referred to as fouling.

Due to its negative economic impact on industries that utilize membrane technology, fouling has attracted attention of scientists in such a way that innovative ways of preventing fouling has to be continuously reinvented as the use of membrane technology expands. Fouling in membranes results in increased maintenance cost as a result of increase in energy demand, additional maintenance labor, and cost of the chemicals used in cleaning, hence a shorter lifetime of membranes. This in turn limits the competitiveness of the processes that use membrane technology. It is therefore very important that fouling is detected and controlled at an early stage for effective and

economically viable plants that use membrane technology especially in nanofiltration and reversed osmosis processes.

Staude *et al* have summarized the main possible origin and causes of fouling as:

- Precipitation of substances that have exceeded their solubility
- Deposits resulting from dispersed fines or colloidal matter
- Deposition of compounds that are a result of chemical reactions of the solutes at the membrane boundary layer
- Reaction between the membrane and the solutes may also result in deposition of compounds on the membrane
- In polymer membranes, adsorption of low molecular mass compounds
- Irreversible gel formation of macromolecular substances, and
- Hydrophobic interactions that results in bacterial growth

These factors that contribute to fouling are just a few of the many, and in some cases, they are interlinked, and an indication of how complex fouling can be [38].

2.4.0 Membrane autopsy

Depending on the application of membranes, fouling will occur in different ways and forms. Membrane autopsy is necessary to determine how fouling occurs and the causes of fouling. There can be destructive methods to characterize the nature and location of foulants using predominantly surface characterization. Membrane autopsy technology has been employed to investigate the difference of fouling along the lengths of a membrane by dividing the module into several length sections [42].

Surface characterization techniques including X-Ray Spectroscopy (EXD) mapping or SEM can be used for as a membrane autopsy tool. EXD, for example, has been used to determine what the main foulants are on an NF pre-treatment membranes, while SEM and XRD have been used to reveal the type of species or phases in which

scales are present [43]. Attenuated total reflectance Fourier transformation infrared (STR-FTIR) spectroscopy can also be used to reveal the functional groups of the foulants and the modification of membrane functional groups due to fouling [44].

2.5.0 Membrane fouling mechanism

Membranes designed for different purposes have varying fouling characteristics, and in particular, membranes with tighter features are known to foul to insignificant extent [29]. This is true in that if a foulant is able to permeate through a membrane, the fouling potential is higher as the foulant is able to penetrate into the pores therefore resulting into partial or complete blockage of the pores [45]. In charged membranes, it is desired that the solute be identical in charge to the surface of the membrane in order to promote expulsion of potential foulant through repulsion and therefore reduce the probability of deposition. In some cases, however, even in charged membranes, the hydrophobic interactions between the charged membrane surfaces and the foulant may overwhelm the electrostatic repulsion and deposition may still occur [46]. In general, irreversible fouling results in physical or chemical adsorption, which cause pore plugging or solute gelation on the membrane, whereas reversible fouling does not result in a permanent blockage of pores, and can be reversed by cleaning.

In membrane science, the process in which accumulation of solutes continues to be retained on the membrane boundary layer is referred to as concentration polarization, a phenomenon that was first described by Sherwood [47]. As a result of the polarization, there results a gradient in the solute concentration at the surface of the membranes compared to the bulk solution. This results in the solute being brought to the boundary layer by means of convection and may be removed by a process of slower back diffusion. The process of back diffusion of the solute from the membrane surface has to be in equilibrium with the convective transport mechanism. For fouling and retention studies, the solute concentration gradient is very important [48]. Figure 2.9 shows the schematic representation of the concentration gradient effect.

In nanofiltration, the concentration polarization is assumed to be fast in the beginning arguably due to increased osmotic pressure or retained ions and the formation

gels due to the accumulated organic molecules. The phenomenon of concentration polarization can introduce a degree of confusion and complexity in the membrane performance parameter retention, and is generally considered as a reversible processes that can be manipulated. For example, by crossflow velocity, ultra sound, permeate pulsing, or by applying electric field across the system [49].

However, membrane fouling can occur without concentration polymerization. When there is adsorption of certain components if the surface of the membrane within the membrane structure as a result of hydrophobic interactions, electrostatic forces, van der walls forces, and in some cases where the hydrogen bonds with the surface of the membrane. The general phenomenon of membrane fouling is very complicated and complex to describe or predict using theoretical models. Membrane fouling results in changes in the membrane separation characteristics, which depend on the process parameters such as the material from which the membrane is fabricated, the structure feed solution constituents, and the concentration or applied driving force. The membrane operation time is a affected by membrane fouling. Due to all this factors, it is very difficult to develop a general relationship into a model or phenomena of membrane fouling [50].

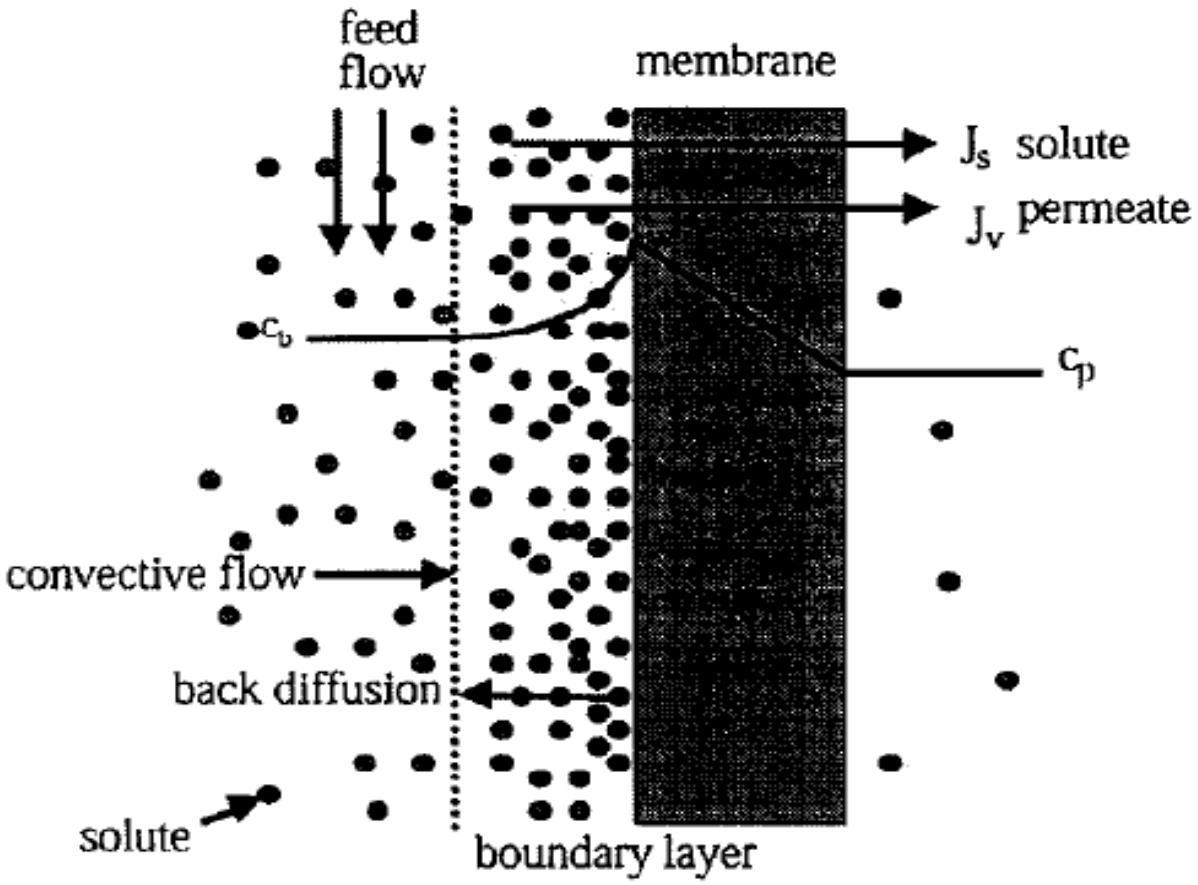

Figure 2.9 Schematic representation of concentration polarization [48].

2.6.0 Adsorption in membranes

The interaction between the membrane surface and the solute even without convective flow through the membrane is referred to as adsorption [51]. As expected, the adsorption occurring in the presence of flux will be higher than that which occurs in the static flux environment [52]. Since adsorption can occur at any point where there is a contact between the membrane surface and the solute, it may occur in pores as well as the back of the membrane. In this case the pore size is greater than the solute, and therefore pore penetration is possible and therefore the adsorption of the solute occurs at the surface of the membrane including the back, as well as at the pore surface. When the solute size is larger than that the size of the pores then the pore penetration is impossible and the adsorption occurs only at the surface of the membranes.

Mathematically, the adsorption characteristics of a particular membrane can me described and measured by determining the coefficient *K* between the bulk phase and the membrane where

$$K = \Gamma \div M \bullet c[Lm^{-2}]$$

Where: Γ is the volume of the organic adsorbed ($\mu g\ m^{-2}$), ***M*** the molar mass of, the adsorbing compound (g/mol), and is the ***c*** the concentration at equilibrium for the solute ad solution ($mol\ l^{-1}$)

2.7.0 Gel layer formation

Gel formation in membrane is almost similar in nature to the concept of fouling. Gel formation involves precipitation of organic solutes on the surface of the membrane and does not necessarily mean irreversible reduction in flux. The process of gel formation normally results when the overall membrane wall concentration polarization is greater than the solubility of the organic as illustrated below in figure 2.10

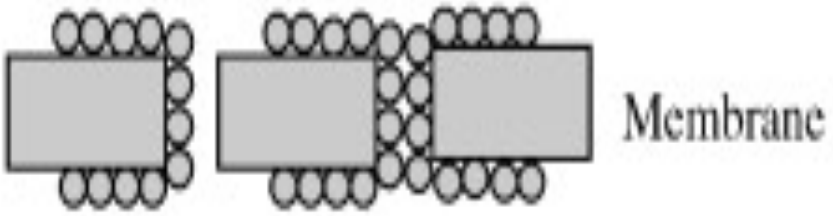

Figure 2.10 Schematic of pore narrowing/ constriction due to adsorption of protein molecules.

Here, the solute size is much less than the pores size and solute penetration is possible, resulting in gel formation on the surface of the membrane as well as on the surface of the pores.

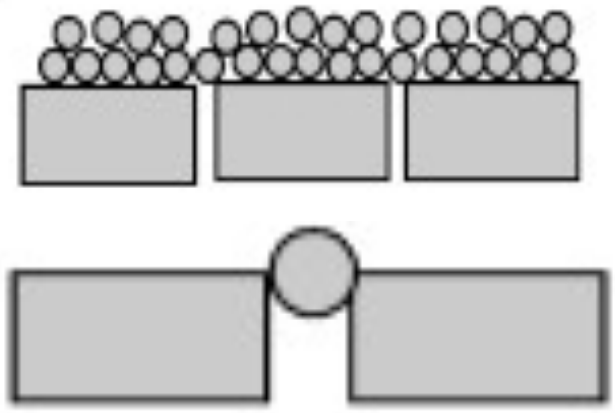

Figure 2.11 Schematic of gel layer formation on the membrane with solute larger than pores.

In figure 2.11 above, the pore penetration is not possible because the pore size is less than the solute size hence the formation of the gel is primarily on the surface of the membrane.

2.8.0 Pore blocking

In nanofiltration, and microfiltration, there are stages of fouling of macromolecules [53]. The stages significantly depend on the size and can be described or categorized as:

1. Fast internal sorption of macromolecules,
2. Build up of a first sub layer,
3. Build up of multi-sub-layer,
4. Densification of sub layers, and
5. Increase in bulk viscosity.

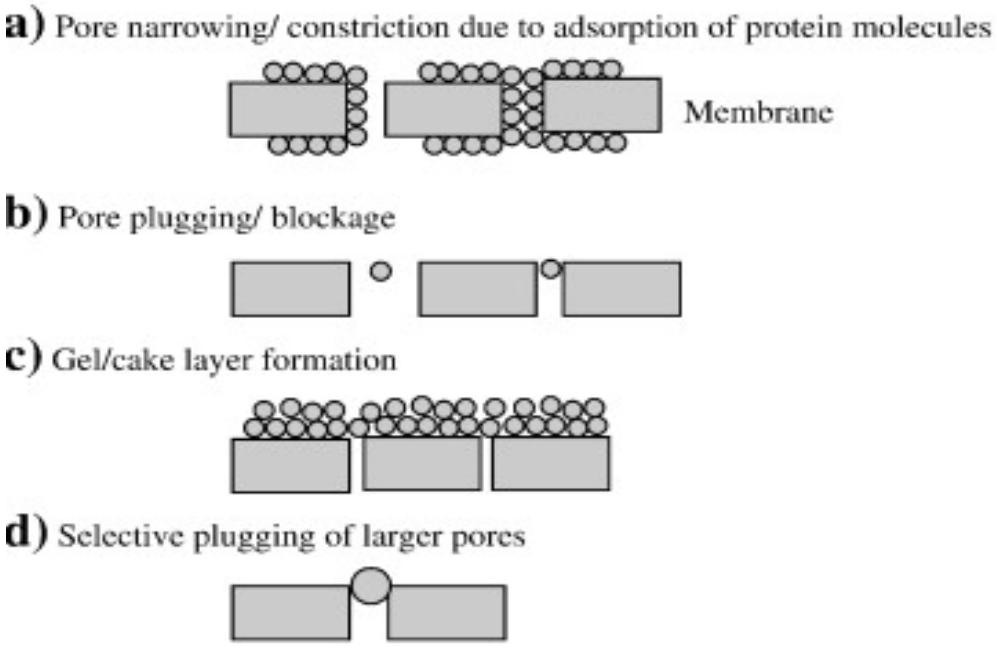

Figure 2.12 Schematic of various membranes pores blocking and size reduction mechanism.

The fifth stage is inapplicable or negligible for solutions that are very dilute e.g. surface water. In the case of solutes that are very small compared to the size of the pores in the membrane, continuous deposition internally, may result in eventual loss of pores. But in a situation where the solute size is exactly comparable to the pore size, immediate pore blockage occurs. Solute with particles in the size larger than the membrane pores results in deposition of a "cake", where the characteristics of the porosity will be dependent on factors, which include; particle size, aggregate structures, particle size distribution, and compaction effects. In general, pore plugging due to particle size where single particle can completely block the pores, is a faster process compared to pore blocking due to adsorption in the pores. The rate of decline in flux, characteristics of membrane performance, is more severe in the latter case. For nonporous membranes, deposition of solutes occurs on the surface of the membranes with relatively smaller solutes forming less permeable deposits [54].

2.9.0 Membrane operating conditions and critical flux

Critical flux is defined as the minimum flux strength below which, a decline in flux over time does not occur. This concept can be illustrated in a number of ways. The main concept, however, originates from the idea that the strength of the drag force towards the membrane is directly proportional to the strength of the flux. Similarly, the higher the concentration, the stronger the polarization, and therefore a higher boundary layer thickness, and the higher the flux, the dispersion of the deposits will be more difficult [55].

In comparison to other membrane transport phenomenon for particles between 10nm and 10μm, it has been variously shown that the surface interactions are responsible for fluxes compared to diffusion and convection. In the case where the transport phenomenon is induced by surface interaction, the critical flux is defined as the flux required to overcome particle repulsion and leading to coagulation on the surface. Flux is also classified into two: strong and weak flux. As defined by Field et al, The strong form is the flux at which the transmembrane pressure starts to deviate from the pure water line, which is a linear relationship, while the weak form there is the assumption that there is a very rapid fouling on start-up, and is the point at which this line becomes non-linear, and the transmembrane pressure-flux relationship is below that of pure water as shown in figure 2.13 below [55, 56].

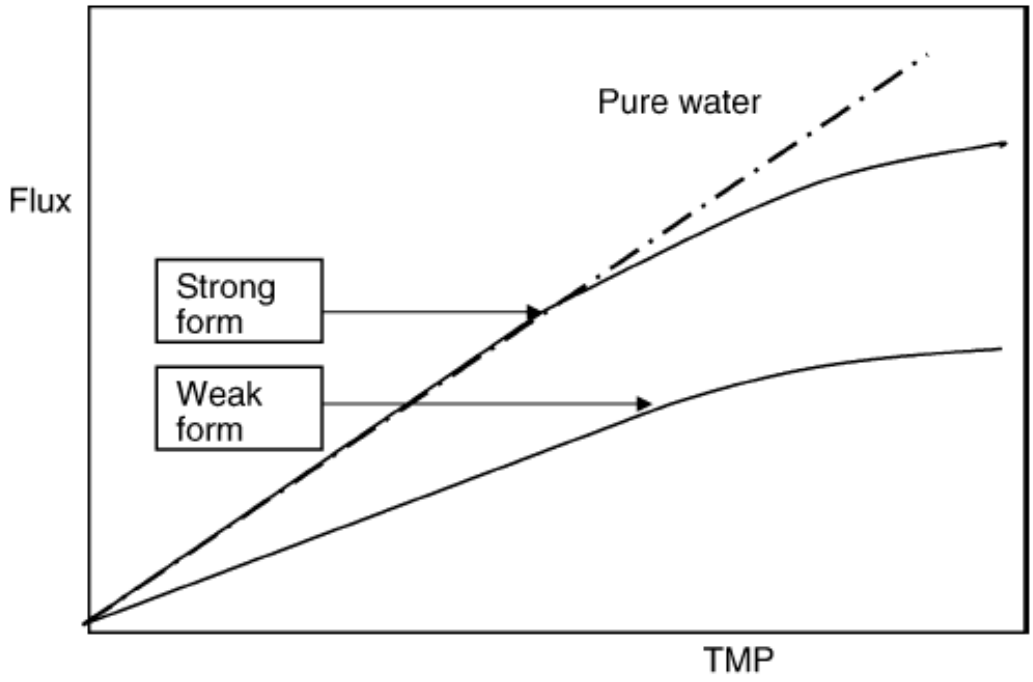

Figure 2.13 Forms of critical fluxes.

The relationship between the flux and the membrane pressure measured by pressure or flux stepping can be analyzed to give the specific critical flux of a membrane system. The mass particle balance can also be directly observed throughout the membrane. The flux-pressure data can be obtained by either imposing a flux on the membrane and measuring the pressure or by imposing a pressure and measuring the flux. In the case where the pressure is imposed, it allows the determination of steady state flux, which is time independent, and the results are more accurate, compared to the steady flux experiments, which can be affected by the fouling which can occur during the experiment. For a fixed flux, the variation of resistance with time will allow the determination of the fouling rate and also the dynamic data can be analyzed to establish the sustainability of the process [57].

A membrane with a suitable permeability can also be subjected to either constant pressure or constant flux operations and then critical flux can be determined this way.

The constant flux is achieved my pumping permeate through the membrane and the pressure measured. This pressure will remain constant at each flux with time. An increase in the pressure will be an indication of the onset of fouling at which point the critical flux will have been exceeded. The total resistance should be calculated at each step in order to make sure that the resistance remained constant throughout. Similarly, in constant pressure experiments, the flux should remain constant with an increase in pressure until when fouling begins to take place, at which point the flux will begin to drop. In both cases, the critical flux will have been achieved at the point where the flux-pressure relationship is no longer linear.

The critical flux can also be determined by analyzing the particle concentration in the out stream. The adsorption of particles is first determined without any flux and then any additional reduction in the particle concentration will be because of deposition. The deposition rate at different fluxes is measured and plotted in a graph and extrapolated. The point at which the deposition rate equals zero is the critical flux. Each method of determining the critical flux has its own advantage and advantages and where it can be applied as shown in Appendix B [58].

There are several operating parameters that affect the flux in a membrane: pressure, feed concentration, temperatures, and turbulence in the feed channel. The feed concentration effect is described in the film theory model, which states that the flux will decrease exponentially with increasing feed concentration. The relationship should hold true regardless of the type of flow or the degree of turbulence or the temperature.

Assuming there are no unusual effects occurring simultaneously, such as fouling of the membrane due to precipitation of insoluble components at higher temperatures or denaturation of proteins, an increase in temperatures will generally lead to higher flux in both pressure controlled regions and in the mass transfer controlled regions. In the pressure controlled regions, the effect of temperature on flux may be due to its effect on fluid density and viscosity since the activation energy of both flux and viscosity are similar in the region of room temperature to about 50 ^{0}C. In practical terms therefore, it will take a temperature rise of between 30-40 ^{0}C to double the flux [59].

2.9.1 Organic fouling

The chemical interaction between membranes and organics is complicated in nature. This makes it difficult to pin point a specific or individual interaction mechanism because these interactions are dependent on various aspects and properties of the membrane as well as the chemical characteristics of the organic molecules and affinity between the two. Organic fouling is an irreversible process of flux decline due to deposition or adsorption of dissolved or colloidal organics. Organic fouling due to deposition of colloids on the pores, or the formation of gel on the membrane surface, can be severe and persistent because it can penetrate into the membrane [60].

The presence of organics in a membrane system will play a greater role in membrane fouling. One such way is that the organics present on the surface of the membrane may be adsorbed and deposited on the membrane, which will result in change in the surface characteristics such as the morphology and hence fouling behaviors. Microorganisms that are likely present on such surfaces will feed on the organics that will facilitate biofueling a mechanism that will promote fouling. Similarly, adsorption of the organics by colloids will cause stabilization of smaller colloids hence causing them to harden, a process that will make it difficult to be removed during pretreatment [61], [62].

Adsorption, which is normally the first step towards membrane fouling, can be described as the formation of a conditioning film in the pores and membrane surfaces, which allows the attachment of bacterial and therefore biofueling [39]. When the adsorption of organic molecules into the pores and on the membrane surface occurs, the overall membrane matrix changes as a result of change in the free volume, and depending on the kind on the molecule-surface interaction, an increase or decrease in volume will occur with a similar change in flux [29]. In itself, adsorption can result in extreme fouling or it can be the precursor to rigorous fouling layer. When organic compounds are adsorbed, it can also lead to a significant change in the surface characteristics of the membrane which can create charge or increase hydrophobicity, for example, resulting in flux variation [41].

2.9.2 Particle and colloidal fouling

Fouling can occur when suspended matter is agglomerate on the surface of the membranes. Clogging can also occur due to silting, which will cause a significant reduction in the flux because of increased hydraulic resistance. Internal pore blocking can also occur when finer particles in the feed enters into the internal membrane pore structure. Fouling that occurs in this way results in a rapid increase in the trans-membrane pressure, a process that occurs in the first stage of a multi-stage membrane process. The term biofouling originates from fouling that occurs from biocolloids, where active biological organisms are involved. It is a dynamic process of microbial colonization and growth resulting in microbial biofilms formation on the surface of the membrane, which is normally and irreversible adhesion.

2.9.3 Crystalline fouling

Crystalline fouling also know as scaling occurs when soluble minerals are deposited on the membrane surface due to the high concentration of the salts in the feed stream when the solution passes across the membrane surface. When the retentate becomes over concentrated precipitation begins to occur, resulting in the commencement of nucleation of crystals and crystal growth on the surface of the membrane as a scale. The scaling will result in dramatic decrease in the salt rejection capability, a moderate increase in the trans membrane pressure, a slight loss in production, which will be manifested in the last stage of a multi-stage membrane process.

2.9.4 Cleaning of foulants and fouling prevention

Frequent cleaning of membrane is not recommended because it results in wear and tear, which will normally reduce the lifetime of the membrane. Instead, different kind of pretreatment is recommended, and this can help reduce or delay fouling. By reducing or delaying such processes as biofouling, it in essence prolongs the time between cleaning, consequently maximizing the overall lifetime of the membrane [63]. An alternate method to avoid or prolong time before cleaning of the membrane is surface modification. Surface modification can, for example, result in the surface becoming more hydrophilic, or in other cases, the surface can become electrically charged [64]. However, since surface modification results in overall increase in material in the membrane, a reduction in flux could occur because of the space taken up by the surface modification material. A compromise has to be reached between the flux and fouling, which is one of the most challenging balancing required in membrane science [65]. Surface modification can be done by UV irradiation or UV-assisted graft polymerization, where such treatments on the surface of the membrane have resulted in increased hydrophobicity of the membranes, and this can be attributed to the formation of hydroxyl groups on the surface of the membranes. These techniques will result in less fouling, but at the expenses of decreased retention [66].

In situations where fouling has occurred, the membrane has to be cleaned using mechanical force to remove foulants or using chemicals that can dissolve it. Physical cleaning methods may include:

- Flushing (back flush, forward flush, and reverse flush) and hydraulic energy cleaning. This is a techniques used by subjecting the membrane to high energy and high velocity in the feed channel.

- Scrubbing
- Air Sparage
- Vibration
- Sonication, and
- Carbondioxide Back Permeation

Although these techniques may be the only necessary methods to remove foulants, these have potential negative effects on the surface characteristics of the membrane surface. Of all the methods listed above, sonication is the most effective and relatively novel method that can be used to remove foulants without damaging the membrane structure [67]. In particular, sonication is useful in removing cake deposits but it does not work very well in reversing pore blockage. As a result, over time, sonication alone becomes ineffective because the primary goal of cleaning the membranes is to be able to maintain the pore effectiveness by preventing or removing pore plugging. The use of sonication, chemical cleaning, and backwashing has been adopted as a more reasonable combination that effectively achieve the cleaning of membranes [68].

In order for chemical cleaning to be more effective, the reaction between the chemical and the foulant should occur in such a way that the particular deposit will be dissolved, which means that the bond that precipitated in its formation will now be broken. The solvent used should be able to break the bonds and cohesion forces between the foulant and the membrane and possibly the bond between the foulant itself [69]. The chemical reactions may occur in the form of:

- Saponification, a term used to describe the chemical reaction that occurs when vegetable and animal fat are mixed with alkaline chemicals which results in the formation of soap and glycerin. Advance solubilization of the foulant will increase the chances of the breaking of the ester bonds between fatty acids and glycerol of triglycerides into the free fatty acids and the glycerol. Chemical cleaning works by breaking down the foulant structure causing the foulant species to be solubulized. As mentioned earlier, the downside of chemical cleaning is the possibility of bonds collapsing within the macromolecular species.

- Peptisation – This is the process where precipitates are converted into colloids. It is the process in which coagulation is reversed by breaking down the bonds and forces between the membrane and the foulant and
- Solubilization,
- Hydrolysis

- Other processes includes dispersion and chelation

Table 2.1 and 2.2 below show a summary of methods used in cleaning NF, RO, MF and UF membranes [70].

Table 2.1 Cleaning techniques for RO and NF membranes.

Foulant	Cleaning reagent	Process condition	Reagent action
Fats and oils, proteins, polysaccharides, bacteria	0.5N NaOH + 200 ppm chlorine	30–60 min at 25–55°C	Hydrolysis and oxidation
DNA, mineral salts	0.1M–0.5M acid (acetic, citric, nitric)	30–60 min at 25–55°C	Solubilisation
Fats, oils, proteins, biopolymers	0.1% sodium dodecyl sulphate, 0.1% TritonX-100	30 min overnight, 25–55°C	Wetting, emulsifying, suspending, dispersing
Cell fragments, fats, oils, proteins	Enzyme detergents	30 min overnight, 30–40°C	Catalytic breakdown (proteolysis)
DNA	0.5% DNAase	30 min overnight, 30–40°C	Enzyme hydrolysis
Fats, oils, and grease	2–50% ethanol	30–60 min at 25–55°C	Solubilisation

Table 2.2 Chemical **c**leaning techniques for different foulants in membranes.

Foulant	Example	Chemical cleaner
Scale (pH adjustment and/or scale inhibitor)	$CaCO_3$, $CaSO_4$, $BaSO_4$, $SrSO_4$, SiO_2	Citric acid, 0.2% (wt.) HCl, 0.5% (wt.) phosphoric acid, or EDTA-based solution; Clean silicate-based foulants with ammonium bifluoride-based solutions
Colloidal clays/silt (filtration and/or charge stabilisation)	SiO_2, $Fe(OH)_3$, $Al(OH)_3$, $FeSiO_3$	EDTA- or BIZ-type detergents at high pH; Clean silicate-based foulants with ammonium-bifluoride-based solutions
Biological (sodium bisulphite addition or chlorination)	Iron-reducing bacteria, sulphur-reducing bacteria, mycobacteria, pseudomonas	EDTA- or BIZ-type detergents at high pH; Shock disinfection with hydrogen peroxide, peracetic acid
Organic (filtration)	Polyelectrolytes, oil, grease	Detergents/surfactants, isopropanol

During the designing and fabrication of membranes for a particular purpose, the manufacturer will have to partner with manufactures of cleaning agents in order to determine the most effective cleaning process and chemicals that will work well in cleaning the potential foulants that may be formed for that particular membranes, because the membrane cleaning protocol is both membrane and foulant dependent [71], [72].

As part of the membrane fabrication process, the testing of the membranes is performed in order to determine various aspects of the membranes including its efficiency, pore clogging and foulants among other things. It is at this stage that the type of foulant can be established, so that the appropriate surface modification can be determined and the best choice of foulant removal is established. The choice of cleaning the membrane is normally approached by a trial and error process [67]. The frequency of cleaning is usually determined by rate of foulant build up or by the rate of loss of flux or declined performance. Although cleaning the membrane at a predetermined schedule is more favorable, it is important also that cleaning be done at the earliest sign of fouling formation rather than when the fouling is well established, making it harder and more expensive to clean. The manufacturer will usually give a recommended cleaning interval or specific suggestions. Ultrafiltration and microfiltration process membranes require more cleaning compared to nanofiltration membranes because detrimental plugging of the pores occurring in ultrafiltration and microfiltration is insignificant in membranes used in nanofiltration processes [73], [74].

2.9.5 Effectiveness of the cleaning protocol

To ensure that the most effective membrane cleaning protocol is chosen, the efficiency of the membrane has to be determined after cleaning, and the results compared to its virgin state performance. The simplest way to determine the success of the membrane cleaning protocol is of course to observe if the original steady state flux is recovered after cleaning. If the ratio of the flux after cleaning to the virgin flux is close to one, the better the cleaning protocol.

For water, figure 2.14 below has been used to illustrate the variation of flux recovery as a result of successive cleaning protocols. Here, sodium hypochloride has

been specifically used because of its ability to cause swelling of the membranes therefore increasing its cleaning effectiveness [65].

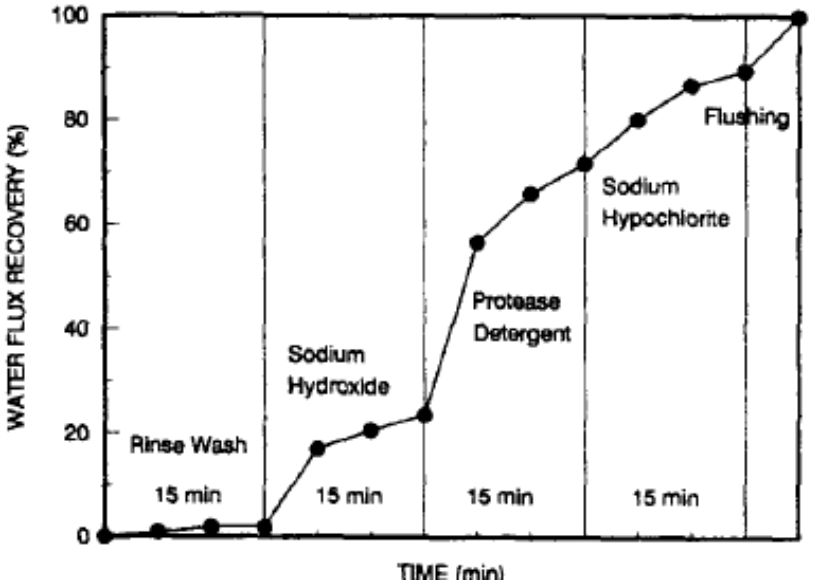

Figure 2.14 Flux recovery due to successive cleaning steps [65].

The effectiveness of the choice of cleaning can also be established by the change in the composition of the cleaning solution. Visible changes such as precipitates may indicate that scaling has been removed and so on. Exact quantification of the can be achieved by chemical analysis and observation of the cleaning solutions [75]. This analysis can give information about the effectiveness of the cleaning protocol, and give information about the reversibility of certain foulants [42].

Physical investigation of the membrane surface after cleaning can also reveal whether the specific cleaning protocol is the best choice for cleaning. This technique will reveal the degree to which the original condition of the membrane can be restored. In most cases, it has been observed that even in situations where there is a complete flux recovery, it doesn't necessarily mean that all the foulants have been eliminated [76]. The surface characterization techniques, however, are similar to those methods mentioned in

membrane autopsy which includes contact angle measurements, FTIR, SEM, and measurements of the steaming potentials just to mention a few. A combination of the methods is sometimes used to ensure a correct analysis is made. Most of the surface characterization techniques are, however, destructive in nature [77].

2.9.6 Membrane regeneration and the theoretical aspect of backflushing

Flux decrease will occur during the membrane filtration process because of the accumulation of rejected particles on the membrane surface. Although the cross-flow configuration filtration is helpful in reducing the build up of foulants, it does not eliminate this problem. Backflushing can help remove some of the build up foulant and minimize the decrease in flux. This involves the application of periodic counterpressure on the permeate side of the membrane in order to push a small amount of permeate through the support back to the feed of the module.

Extensive studies of membrane based filtration process have shown that some form of periodic cleaning to eliminate the build up foulants should be carried out. This can be done by chemical attack or dissolution of the foulants deposited on the surface of the membrane and those foulants that are embedded within the internal structure of the membranes. Since inorganic membranes are resistant to attacks by organic solvents or oxidizing agents even at high temperatures, it is possible to design several effective membrane regeneration procedures. Inorganic membranes can also be sterilized or autoclaved using different approach [78].

Several commercially available cleaners are available depending on the foulant that is targeted. Acid cleaning will work best for mineral foulants, whereas alkaline cleaners can clean soluble organic foulants. In cases where membranes have been severely fouled internally and externally, stronger chemical, complex agents, wetting agents, and surfactants is required for effective cleaning, which can compromise the integrity of the membrane structure. A low transmembrane pressure must be maintained during backflushing, and it is recommended that the permeate pores be closed during the first half and of the cleaning cycle and be open during the other half [79].

Cleaning solution with dissolved air or gases must be avoided at all cost because the dissolved air or has been known to promote membrane fouling. This is because in the microporous membranes, a positive pressure is required to dislodge the bubbles or entrapped gases. This pressure increases with the decreasing size of the membrane pores diameter. The quality of the cleaning water should also be of low fouling index, low hardness, and love concentration in minerals such as silica, iron, and manganese, which can also contribute to fouling [30].

2.10 The use of membranes

Until mid 1940's the use of microporous membranes was mainly focused on the removal of macromolecules from liquid and gaseous streams and in some research applications, it was used to estimate the size and shape of particulate matters intended for diffusion studies. Membrane processes have also found increasing application in industrial and laboratory applications, which include the purification and concentration of pharmaceuticals and food products, in the production of base chemicals, and in the energy industry for fuel cell devices. In the medical applications, processes such as blood oxygenation and haemodialysis greatly utilize high-tech hybrid membranes that are designed using conventional technologies, which minimize the environmental impact and operate at high-energy efficiency. Although membrane development for more technical application began in the laboratory, key inventions such as the development of high efficiency and cross flow membrane elements consisting of large surface areas enabled the laboratory to commercial realization after the 1960's. The invention of new materials and capabilities to control them to the molecular level enabled the fabrication of membranes with tailored morphology that was capable of controlling microscopic transportation a phenomenon that promoted manufacturing of economical and reliable membranes [80].

2.10.1 Membrane for gas separation

Advancement in the development of inorganic and organic materials for separation processes has brought a significant cost benefit for energy and environmental related processes. This is particularly important considering the significant rise in the cost of energy and the environmental degradation to gaseous waste. Currently, conventional gaseous separation techniques that include removing of condensable organic vapors from a mixture of gases using condensation technology, cryogenic distillation of air, and removal of acid gases such as CO_2 from natural gases by means of amine absorption, are processes that require gas-to-liquid phase change. The phase change process presents challenges that results in increased energy cost. Gaseous separation using membranes has become an emerging solution because the energy cost of the process is significantly reduced, and the simplification of the process is enabled because of the reduced footprints [81].

Today, membrane for gas separation is finding application in the hydrogen separation, for example in the separation of hydrogen and nitrogen in ammonia producing plants, and in the petrochemical industry its application includes separating the hydrogen and hydrocarbon from the petroleum products. It is also widely used in the separation of CO_2 from CO_2/CH_4 as shown in figure 2.15. Although there is a wide range of emerging new materials used in fabricating membranes, the most used for gas separation are polymer membranes. The ability and easiness to process them into hollow fibres of high surface areas combined with the relatively low cost makes it an attractive option. Membrane for gas separation processes are designed to operate under steady state conditions with three streams. The feed stream is a high pressure mixture of gases that passes through ones side of the membrane, then another gas that is used to sweep the permeating molecules comes from another side, and then finally the non-permeating gas molecules that remain on the feed stream side are then removed from the membrane as the retentive stream. The permeation process is driven by the pressure differential across the membrane.

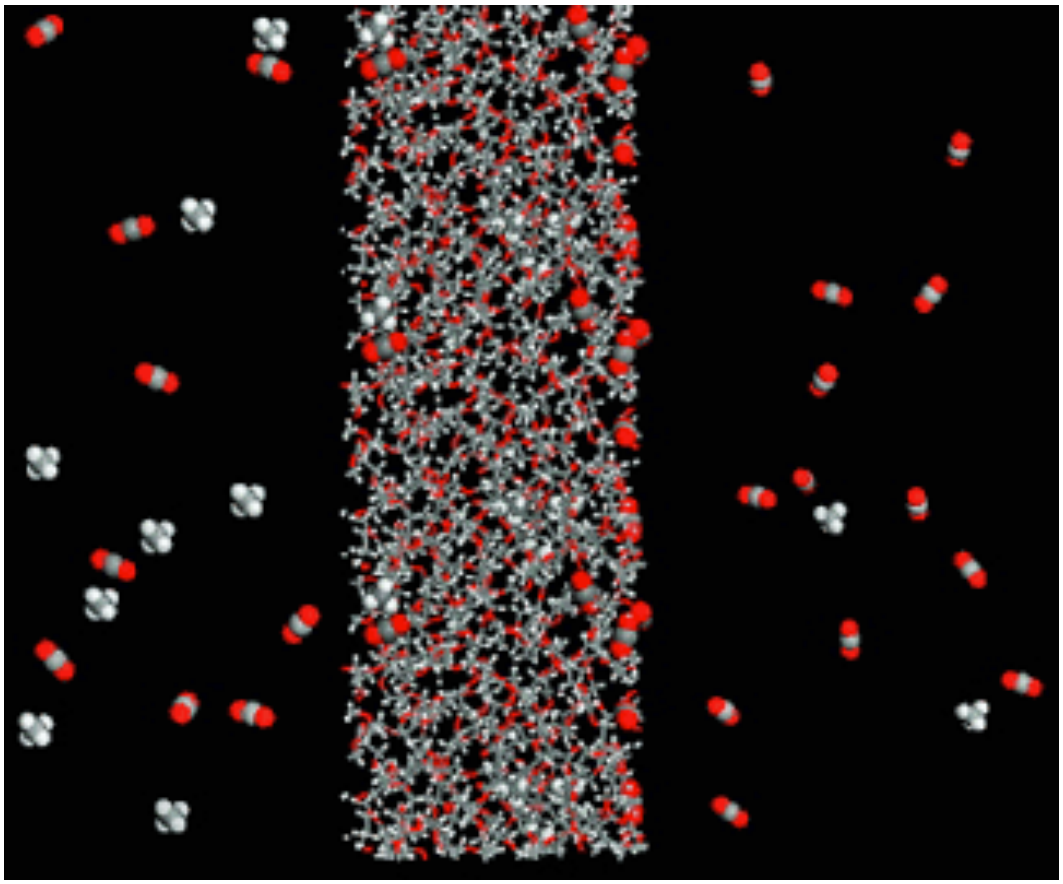

Figure 2.15 Solubility-selective polymer membrane developed by Freeman's group removes CO_2 from CO_2/CH_4.

It has recently been demonstrated by various research groups that membranes made from rigid polymers have become very efficient for separation of CO_2 from the atmosphere because of the high diffusion selectivity, a property that makes membranes made from rigid polymers an attractive option. The challenge for this alternative is that in the case where the pressure of CO_2 builds up to partially high levels, and environments with high level of hydrocarbon contaminants, the membrane separation capability is impeded and the separation process will deteriorate to levels that render membranes inefficient. For more practical purposes, membranes for gas separation should be designed such that the selective layer is as thin as possible so that the flux is increased therefore improving the performance of the membrane. Highly selective polymer membranes will exhibit low permeability and vice-versa, which means that the trade off relationship is of high importance.

2.10.1.1 Gas permeance through porous membranes

Viscous gaseous flow through porous membranes is normally characterized by the fact that there is a more interaction between the gas molecules than the interaction that occurs between the walls of the membranes and the gas molecules. However, in the case of liquid permeation through porous membranes, the same is true when the diameter of the permeating liquid is much smaller than the membrane pore diameter. For gas permeance, when the free path length of the gas molecules permeating is larger than the pore diameter, the interaction between the gas molecules and the membrane pore walls may be lower or of the same magnitude as the interactions between the gas molecules even if the pore size is much larger than the diameter of the gas molecules. Under such conditions, the permeation of the gas through the membrane is not by viscous flow, but the transport mechanism of the gas through the membrane is referred to as Knudsen diffusion. The difference in this two-gas transport mechanism through the porous membrane is illustrated in the figure 2.16 b. The figure shows the different interactions that occurs in membranes with pores of different diameters with a number of gas molecules inside the pores ad their interaction between each other and the pore walls [82].

The mean free path length of a gas (λ) is defined as the average distance a gas molecule will travel before it will collide with another molecule. The mean free path of a gas molecule will depend on the pressure, the temperature, and the nature of the gas where:

$$\lambda = \frac{\kappa T}{\pi d^2_{gas} \sqrt{2}}$$

Where: κ is the Boltzmann constant, d_{gas} is the diameter of the gas molecule, *T* is the absolute temperature and *p* is the pressure of the system.

At room temperatures and atmospheric conditions, the mean free path of gases is in the order of couple of nanometers. Knudsen diffusion will occur in conditions when the gases inside the pores have a mean free path length that is larger than the pore diameter [83].

2.10.1.2 Gas separation by molecular sieving and surface diffusion

Some gases especially vapors are usually adsorbed at the surface of membrane, which leads to a build up of higher concentration of the adsorbed gases in the membrane pores than that of the inert gases that ere not adsorbed and thus a the flux of the adsorbed gases will be higher. In cases where the pore size in the membranes have reduced to a certain size due to the adsorption, a phenomenon referred to as capillary condensation will occur, resulting in complete blockage of the pores and no inert gases will flow. In Knudsen diffusion, inert gases with smaller molecule size such as H_2, He, N_2 etc., have higher permeability than gases with larger molecular size. However, the flux of these inert gases can be drastically reduced because of capillary condensation that is caused by the adsorption of the larger gas molecule onto the surface of the membrane pores. This can result in an increase in the permeability of the larger molecule gases where the surface condensation and capillary condensation may occur compared with the permeability of small inert gas as show in figure 2.16 a and b [84, 85].

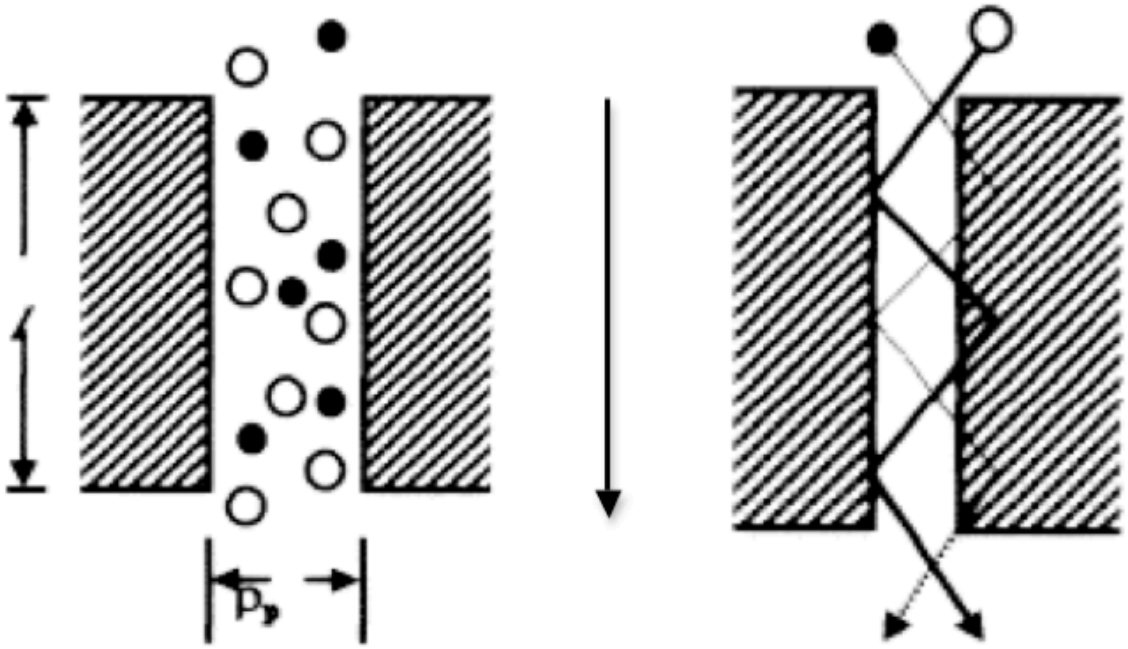

Figure 2.16 a) Viscous flow and b) Knudsen Diffusion of gas through two different size membrane pores. The arrow shows the direction of the hydrostatic pressure flow.

2.10.2 Membranes for making potable water

Desalination, which is the process of desalting seawater, is becoming increasing necessity, especially in the third world countries that have continually been faced with the challenge of access to clean potable water but are surrounded by long shoreline. Desalination can be used to bridge the gap in the accessing clean water. Desalination process dates back to the fourth century when sailors used evaporative technique to obtain potable water from seawater. Electrodialysis and reverse osmosis is a membrane technology, which has been used extensively to separate dissolved salts from the water. In Electrodialysis, desalination occurs through an electrochemical process in which the target water passes through the anion cation membrane system where the salt passes through the membrane, allowing clean water to be retained. The dissolved salt in the water will either be positively or negatively charged. Desalination in the membrane is therefore achieved by the selective passage of the ions, as they are attracted to electrodes with an opposite electric charge as shown in figure 2.17. In electrodialysis, the recovery rate is between 75-90 percent of the original stream, making it a very efficient process [86].

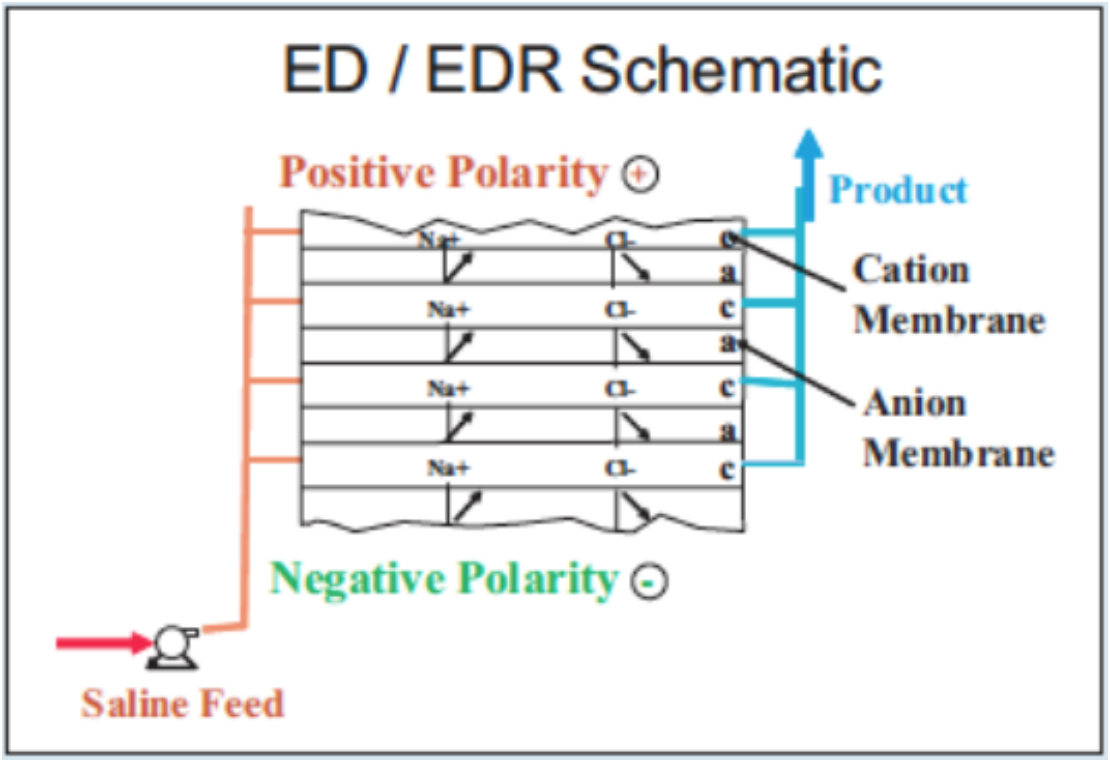

Figure 2.17 Schematics of electrodialysis membrane technology.

In reverse osmosis, separation is achieved through diffusion where the salty water will move from the high concentration (of salt) to areas of low concentration until an equilibrium is reached, which is when the differential hydrostatic pressure that is due to the concentration changes on each side of the membrane is equal to the osmotic pressure of the salt as shown in the schematics below in figure 2.18.

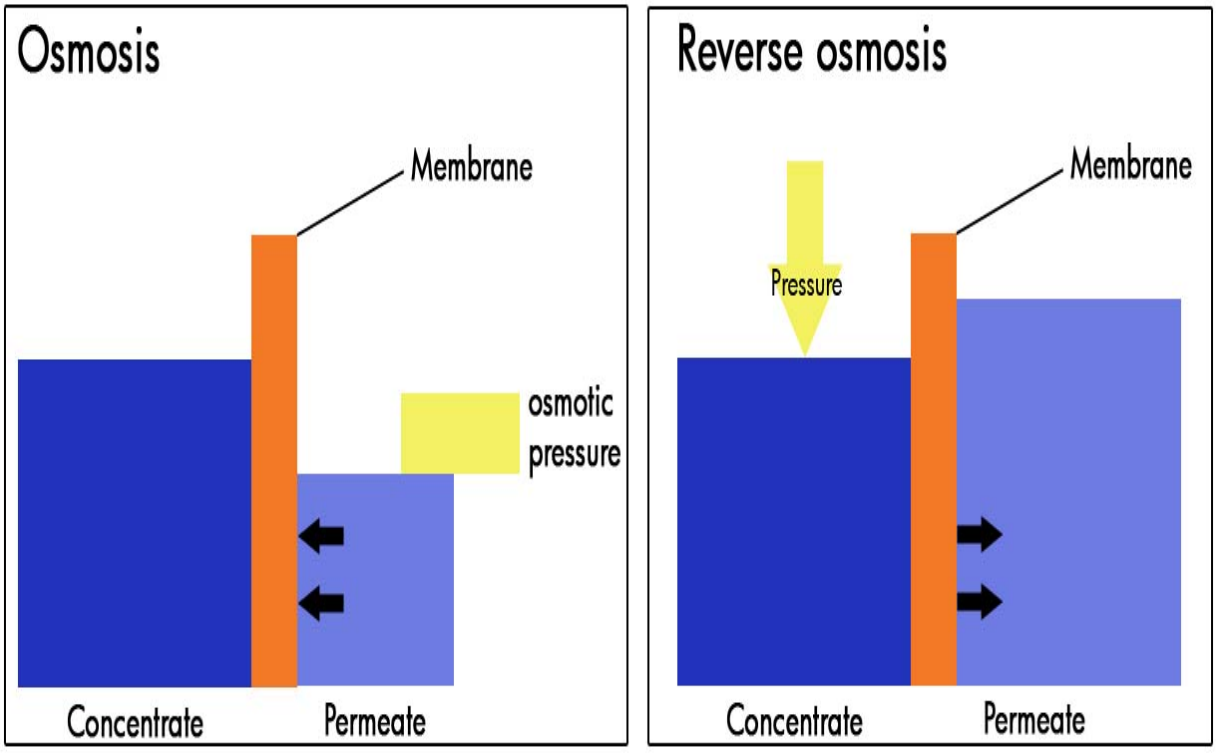

Figure 2.18 Schematics of reverse osmosis.

2.10.3 Membranes for biomass pretreatment

The production of ethanol and other biofuels from lignocellulosic biomass presents an attractive alternative for green energy efforts. However, the pretreatment process which plays a greater role in achievement of this milestone because of the enormous cost that is involved and the complicated steps within the conversion of the biomass, has been faced with great challenges due to the of the structure of the biomass. The advancement of the membranes technology for pretreatment process shows potential for improved efficiency and great reduction in cost. Oak Ridge National Laboratory has become a leader in the development of inorganic membranes that have been configured into tubular design for the separation of organic compounds obtained in solution form the pretreatment reactor. This process involves heating of water to temperatures in the range of 200-260 ^{0}C to generated steam pressure of up to 550 Psi that is then passed through the solubulized organics. Then the exit steam, which will contain the organics is directed towards the specially designed nanoporous inorganic membranes resulting in the generation of retentate with an increased concentration of reactive solids, which will also remove inhibitors such as monolignols and phenolic acids. By using step-wise temperature increases in the flow-through process through the membrane, organic fractions that solubilize at different temperatures can be separated using this technology. Membrane application for biomass pretreatment allows high temperature processing and is therefore a highly energy efficient process [87].

2.11 Membrane design guidelines

Membrane manufactures have over the years attained the capability to fabricate membranes to tailored parameters and finishing for any application defined by the end user. The parameters that define the manufactures guidelines in the manufacturing process include:

- The expected maximum flow rate and applied pressure of the system,
- The permeate flow rate, which should be directly proportional to the driving pressure.

Fouling tendency and the feed parameters are also important. The fouling characteristics are usually directly proportional to the characteristics of the pretreated feed. The resulting concentration of the foulant on the surface of the membrane will increase with increase in the permeate flux.

The framework of the membrane operating conditions is of great consideration in the designing of membranes. A membrane system should be designed so that minimal fouling is achieved and excludes the element of mechanical damages on the membrane. The operating conditions of the various elements are defined by the expected maximum recovery, the flow rate of permeate, the defined maximum feed flow rate, and the minimum concentration of the permeate flow rate. Systems that have a higher tendency to foul will result in strict design guidelines. Since membranes are defined by what they do rather than what they are, when designing a membrane, it is therefore very important to understand the function that the membrane is supposed to accomplish so that the designer can have a full understanding to be able to devise a membrane with accurate parameters such as the separation mechanism, and the affinity for the membrane material [88].

2.11.1 Solute losses during membrane filtration process

In reverse osmosis membrane filtration process, for example, water desalination, the product is the filtrate, or the product is retentate in cases where there is a concentration of proteins and the separation is through ultrafiltration. Membranes that are strictly not semipermeable allow the solute in the solution to permeate through the membrane with the solvent. This will result in a compromise of the quality of the filtrate that may lead to product loss in the retentate. In some cases, the solute loss can be significantly high even in membranes that have a relatively higher solute rejection when the retentate concentrations are desired.

2.11.2 Reverse osmosis design guidelines

In the designing and construction of a reverse osmosis system, there are main parameters that must be put into consideration that will define the effective performance of the plant. This includes the concentration of the feed, permeate, and the retentate solutions and their flow velocities parallel to the surface of the membrane. The recovery rate is also a very important factor to be considered and so is the concentration polymerization. The characteristics of the membrane permeability of the solvent and the solute must be analyzed also. Most of these parameters are coupled. The feed flow velocity, for example, will determine the concentration polymerization characteristics and the recovery rate, while the retentate concentration is a function of the feed concentration of the recovery rate and the membrane properties. Other parameters such as the membrane properties, i.e. the permeability, and the true membrane retentions are constant [89].

2.11.3 Ultrafiltration and microfiltration design guidelines

There exist a lot of similarities between the design guidelines for ultra- and microfiltration processes and that of reverse osmosis design. The major differences between these systems is that the membrane flux in reverse osmosis at constant applied pressure is a function if the osmotic pressure of the feed solutions, which in itself is a function of the concentration polymerization effects and the recovery rate. While the reverse osmosis and the ultrafiltration process are operated continuously at certain rate of recovery, microfiltration are normally operated as dead end or cross floe filtration systems. Microfiltration is usually more applicable in the removal of large components such as bacteria, viruses, or other large particles in liquid and gas feeds. The concentrations of these particles are generally low or can be trace elements in the feed streams, and therefore the recovery rate in microfiltration process is generally very high, especially for dead end filtration where the recovery rate almost approaches unity because virtually all the permeable components are obtained in the filtrate. The diagram below illustrates the dead end and cross flow systems as shown in figure 2.19 a and b [90].

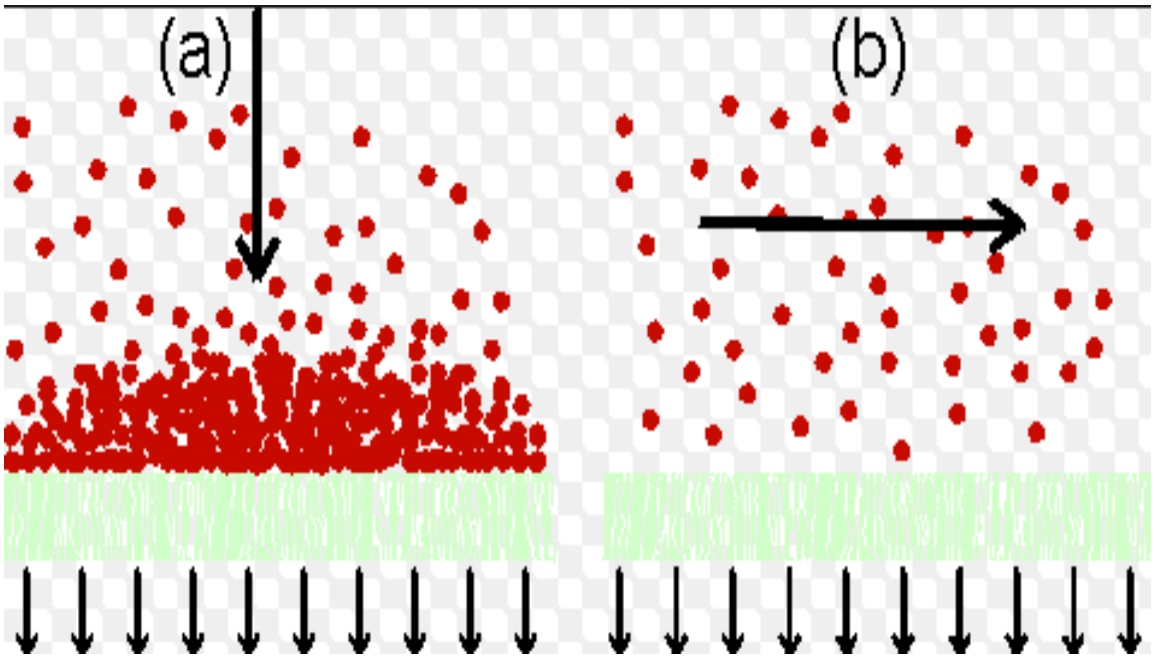

Figure 2.19 Illustration of a) dead end filtration and b) cross flow filtration.

The fluid flow in dead end filtration is perpendicular to the membrane surface while in cross flow filtration, the fluid flow is parallel to the membrane surface.

2.12 Filtration process operation models

Practical membrane filtration can be described in three models of operations, namely batch process, continuous process, and feed-and-bleed process. In the batch process, a defined feed volume is placed in a pressure container. The system is then subjected to certain hydrostatic pressure and the components; mainly the solvent will permeate the membrane and is collected as filtrate. The components that are retained will build a concentration, and when a certain concentration is achieved, the process is shut down.

The continuous process derives its name because of the continuous feed solution that is fed into the filtrate device, which consist of membrane-channeled tubes. When certain system hydrostatic pressure is achieved, permeation of some components will occur, which is collected as the filtrate that is removed from the membrane through designed ports. The concentrated components are retained in the membrane at the end of the process. Depending on the solution flow velocity in the feed, the filtration rate, and the geometric characteristics of the membrane system, certain recovery rate will be achieved. If a lower recovery rate is obtained through one process, a higher recover rate can be achieved by subjecting the system to the so-called feed-and-bleed operation mode. This will cause part of the retentate to be recycled back to the feed system. Increased recovery rate can be achieved depending on the ration of the retentate that is recycled into the feed [91].

2.13 Membrane chemical resistance

Generally, inorganic membranes are characteristically more stable to several chemicals with ranging pH values compared to organic membranes, which is a valued advantage. These properties of inorganic membranes, particularly those fabricated from ceramic materials, is derived from the compactness of the crystal structures, the chemical bonding and the high field strengths associated with the relatively small and highly-charged cations in ceramic materials. Ceramics with larger total energy of formation and large free energy are especially the most stable from a thermodynamics point of view,

and therefore membranes made from aluminum, beryllia, titania, and zirconia are some of the most chemically stable.

But because of their application, most membrane will undergo regeneration procedures where interaction with different kind of corrosive chemicals such as strong acids and bases for an extended periods of time. This kind interaction with the surface of the inorganic membranes results in a chemical attack, which must be addressed. At high temperatures, inorganic membranes will not tolerate an extended period of exposure to oxidizing environment. Even though there is no quantitative data available on the kinetics of chemical dissolution of ceramic membranes as a guide for chemical corrosion considerations, it is generally known that various ceramics membranes posses differing degrees of acid/base resistance depending on the pH value [92].

2.14 Hydrogen permeance

The hydrogen transport through the membrane can be described by the total flux, which can be defined as the rate at which the hydrogen passes through the membrane per unit area. The generalized equation governing the movement of the hydrogen through the membrane is shown below, and is based on the assumption that the rate-limiting factor is in the hydrogen transport mechanism is the diffusion. It is based on the assumption that the transport is unidirectional. The hydrogen flux can therefore be described as:

$$N_{H2} = -k\frac{\left(P_{H2,ret}{}^{0.5} - P_{H2,perm}{}^{0.5}\right)}{X_M}$$

Where: the hydrogen flux is defined by N_{H2}, k is the membrane permeability, X_M is the thickness of the membrane and $P_{H2,ret}$ and $P_{H2,per}$ are the partial pressure of hydrogen on the retentate and permeate sides of the membrane, respectively. Because the hydrogen flux is inversely proportional to the membrane thickness, a thinner membrane should be maintained if the flux is to be increased. However, the mechanical integrity must also be maintained and a minimal thickness is required to maintain mechanical integrity, depending on the physical conditions to which the membrane will be subjected.

The gas permeability of a membrane material is a function of temperature, and the Arrenhius-type equation show below describes the relationship.

$$k_P = k_o \exp\left(\frac{-E_P}{RT}\right)$$

Where the k_p is the membrane permeability, k_o is the pre-exponential membrane permeability constant, the activation energy for permeation is defined by E_p, and R and T are the gas constant and the absolute temperature of the system respectively.

Chapter Three

Research Objective and Approach

3.0 Introduction

The potential success of the membrane technology in various applications is very promising in terms of cost effectiveness, energy savings, efficiency, and the simplification of the separation processes. This has made the membrane technology a center of attention in the filtration and separation science since its commercialization. One of the major challenges to successful use of membranes is the problem of fouling. As cited earlier, the adsorption of naturally occurring organic materials to membrane surfaces has been variously defined as the primary source of chronic fouling in membranes. The nature of fouling has been continually misunderstood and is therefore a key impediment to developing improved methods for membrane anti-fouling and cleaning technology and techniques. In order to obtain a lasting solution to membrane fouling, specific effort that will directly address the nature of interactions between natural organic matter, ionic components of the feedstream matrix, and the membranes in the fouling process have to be investigated and understood.

The major properties of the fouling material that determines the propensity to foul the membranes includes the natural affinity to the membrane surface, the functionality, the molecular weight of the foulant, the material of the membrane surface, and the conformation characteristics. It has been shown elsewhere that those membranes that are hydrophobic in nature are more likely to be fouled by streams of organic materials because of the greater charge density property of hydrophilic materials. In this effort we seek to understand the nature of organic foulant and membrane interactions as a basis for selecting improved strategies for treating the membrane surface in order to prevent or slow down the fouling characteristics on the membrane pores, which will improve the performance characteristics of the membranes and also makes the post fouling treatments easy. The main aim is to increase the lifetime of the membranes, which in turn will

improve the efficiency and the overall performance of the membrane separation technology [93].

3.1 Current antifouling technology

Some of the existing antifouling technologies includes one that was developed by a researcher at Cornell University for water purification membranes [94]. The approach involves modified RO/FO thin-film composite membranes with antimicrobial nanoparticles deposited on the surface. The surface modification creates a uniform, durable coating and results in charged groups that prevent microbial build-up, while maintaining permeability and salt rejection. Their work demonstrates a novel technique for covalently or ionically tethering antimicrobial nanoparticles to the surface of UF membranes. Membranes that use reactive barrier as the main mechanism for separation have also been improved by imparting novel nanomaterials on the surface of the membranes, which gives the target membranes multifunctional and tailored properties that will improve the reactive separation mechanism as shown in figure 3.1. This ongoing development includes coating membranes with biocidal, photocatalytic, adsorptive carbonaceous, and zero-valent iron materials that have been shown to eliminate targeted foulants with a great degree of success.

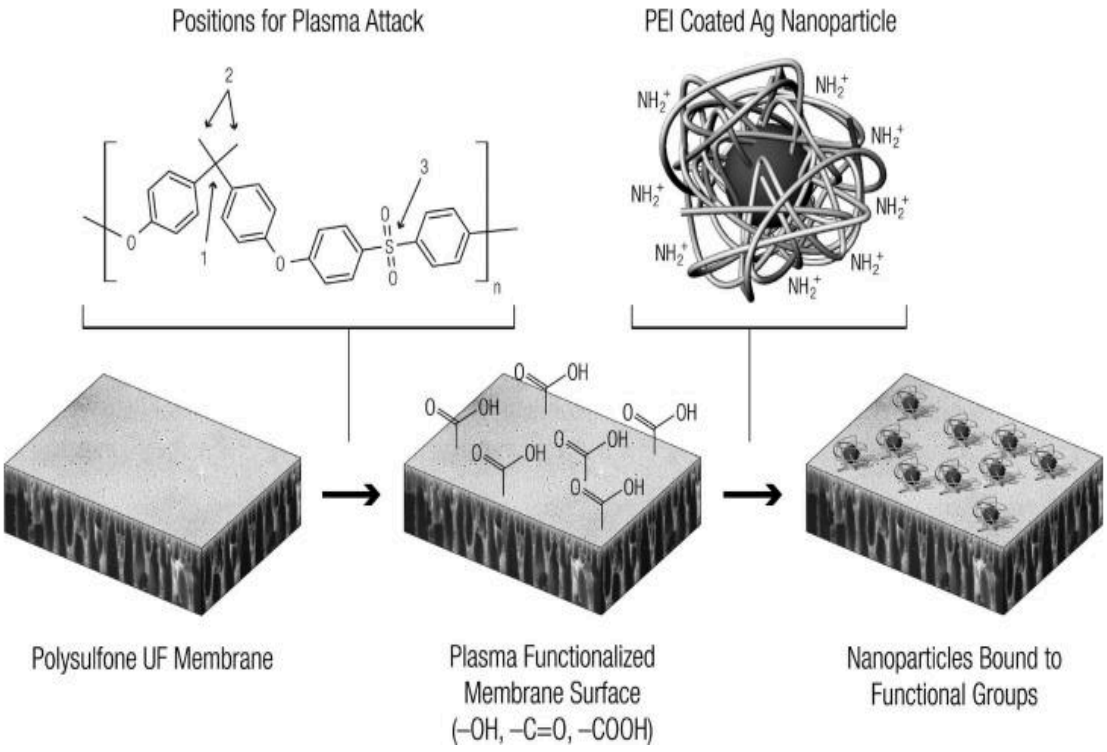

Figure 3.1 Post-synthesis grafting processes for the fabrication of reactive membranes.

In the fabrication of reactive micro- and ultra- filtration membranes, another emerging technology involves predominantly incorporating nanomaterials into the membrane casting dope or synthesized *in situ* through chemical reduction of metal ions. The high density of nanoparticles achievable in mixed matrix membranes with continuous distribution throughout the membrane cross-section enhances contact with the reactant and improves the lifetime treatment capacity of the membranes. In other reactive separation processes, particularly those related to the destruction of foulants in the feedstream, concentration of the nanoparticles at the membrane surface is advantageous. The only major drawback of these antifouling fabrication techniques is in the complexity of controlling the placement of the nanomaterials in the membrane cross-sections [95, 96].

3.2 Proposed monolayer coating of high temperature stable polymers

3.2.1 Background

Currently, ongoing research work continues to demonstrate the potential of nanoporous inorganic membranes to perform organic separations with high throughput at high temperatures up to 250 ^{0}C and operating pressures up to 550 psi. Whereas various research institutions and manufactures are developing inorganic membranes, there is a definite need to protect these membranes with high temperature stable materials to prevent pore fouling during the separation process. This work intends to propose, identify, and research the monolayer coating of a high temperature stable, chemically and mechanically robust engineering polymer on nanoporous membranes using various solution-based coating methods. This idea of modifying the surface of inorganic nanoporous membranes that have sieving properties as compared to dense membranes that rely on diffusion through the separative layer with a monolayer coating of high temperature stable polymers is novel and complementary, compared to other surface modification techniques discussed and researched by other groups. The proposed technique offers a simple yet robust and more effective antifouling option that will also help in prolonging the lifetime of the membrane and make cleaning easier [97].

3.2.2 Research objective

In this research, we propose to deposit monolayer coatings of a high temperature polymer on these inorganic membranes to decrease pore fouling and increase their service life. The specific objectives are:

- To evaluate high temperature stable engineering polymers such as Ultem as coating materials
- To apply monolayer coating of these polymers on nanoporous membranes by dilute solution approach [98].
- To investigate the effect of solution concentration and other process variables on coating thickness

- To evaluate the properties and performance of such coated membranes, and
- To optimize the processing conditions for efficient coating of such membranes

In this project, several nanoporous membranes, both commercially available and those fabricated at ORNL with pore sizes in the range of 1 to 5 nm are being investigated. One of the critical challenges is to be able to perform separations at high temperature with minimal surface or pore fouling. The success of this work would help reduce membrane fouling and also aid in the ease of membrane regeneration. Both of these aspects are important considerations for process scale-up and to reduce capital and operating costs.

3.3 Research approach

The proposed research involves the following approach:

- Solution preparation and characterization
- Coating of membranes
- Characterization of the uniformity of coating, coating thickness and porosity of the coated membranes
- Optimization of the coating process
- Evaluating of the robustness of coating, and effect of coating on membrane fouling

For this research, Ultem 1010 and 1040A obtained from Sabic was investigated. Methylene chloride was used as the solvent. The polymer solutions were prepared in low concentrations such as 0.25, 0.5, 1, 2 and 5% by weight of the polymer. Dip coating was initially investigated. Later on, forced flow method was also investigated to see whether the technique will help in controlling the coating thickness. The coated membranes were

then dried to remove the solvent before characterization. After drying, the thickness of the polymer coating was evaluated using microscopy, and other physical measurements. The important test is to make sure that the coating does not cover the pores of the membrane. For this, the permeability characteristics and pore size measurements will be done on the membranes. Other characterizations to be done include resistance to steaming, flow weighted pore size distribution, and water and gas permeance to determine the membrane integrity before and after coating.

3.4 Experimental

3.4.1 Materials

Several polymers were evaluated in this research work in order to determine the best cost effective, simple to process, and one that requires minimum storage conditions without degradation. ULTEM resin grades 1010, 1285, 1040A and also polyethylene imine (PEI) with 10,000 MW were investigated.

3.4.2 Properties of ULTEM 1010

Ultem, a polyetherimide resin marketed by Sabic Innovative Plastics and formerly by General Electric Plastics, is a copolymer with ether molecules between imide groups. Being an amorphous thermoplastic polyimide, the Ultem resin combines the high performance associated with exotic specialty polymers and the good processability of typical engineering plastics. In addition to high strength, high modulus, and heat resistance, the polymer has high dielectric strength and broad chemical resistance. Ultem 1010 is categorized as a multipurpose, unreinforced, high-flow grade PEI. It has been observed elsewhere that Ultem is soluble in methylene chloride, one of the solvents easier to work with. This was the basis for proposing dilute solution approach to achieve monolayer coating, as the melt will have very high viscosity [99].

Ultem has the molecular formula of repeating unit of PEI $C_{37}H_{24}O_6N_2$ and its molecular weight is 592 g/mol. and density of 1.27 g/cm^3. The base polymer Ultem 1010

resin has amber brown color, it is transparent, and, is manufactured by the polycondensation process and has the following chemical structure shown in figure 3.2.

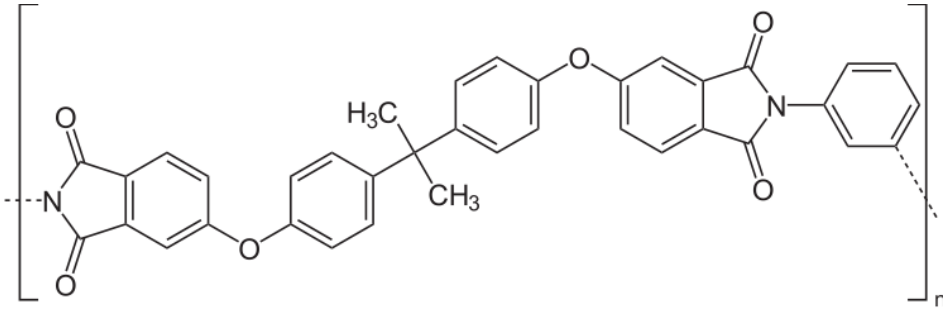

Figure 3.2 Structure of ULTEM.

The electrical properties of ULTEM 1010 will vary with the temperatures at which the polymer is exposed to. The dielectric constant will decrease as the temperature increases typically from 3.15 at room temperatures to about 3.02 at 174 ^{0}C if the frequency is maintained at 130 Hz. Exposure to gamma rays of up to 500 x 106 rads can reduce the tensile strength but not more than by 6%. This loss in the tensile strength is very small compared to the loss in other polymer materials. It has also been shown elsewhere that ULTEM 1010 exhibits high tensile strength at room temperature and retains a significant portion of this strength at elevated temperatures, and most of the physical properties are also maintained at higher temperatures. This high performance characteristics and design flexibility allow ULTEM 1010 to be used for a wide variety of applications ranging from tableware to aircraft, coating of different thickness and in automotive industry where glass fibers further increases high-temperature strength. Generally, organic solvents even at elevated temperatures do not affect ULTEM 1010 but it can be dissolved in methylene dichloride [98].

3.4.3 Solvent – Methylene Chloride

Methylene chloride, also known as dichloromethane is an organic solvent with a chemical formula CH_2Cl_2 and structure shown below. It is commonly used as a solvent because of its unique properties enabling it to dissolve a wide range of organic compounds. The methylene chloride used in this research was obtained from Sigma Aldrich and was used without further purification

3.5 Processing

3.5.1 Polymer solution preparation

The PEI and the solvent have been mixed in the respective proportions of 1, 2 and 5% by weight of the polymer. The PEI was optimally dissolved in the solvent after by sonication in a water bath for 40 minutes at a bath temperature of 60 ^{0}C. Due to the fibered nature of the polymer, the resulting solution was filtered using a 5µm filter to remove the undissolved polymer.

3.5.2 Coating

Two distinct coating techniques; spray coating and dip coating were used to deposit the thin layer polymer coating on the clean surface of the membrane.

3.5.2.1 Dip coating

Dip coating is a technique that has been used successfully to apply thin layer coating on surfaces especially where the control of the deposited layer is very crucial. Deposition occurs when a substrate is withdrawn from a liquid bath and the resulting characteristics of the deposition will be determined by the withdrawal speed, gravitational acceleration, and the physical properties of the solution which is a function of the viscosity, surface tension and density. The typical dip coating process entails two main steps, the dipping and the withdrawal, and different research groups have reported that the coating thickness is highly dependent on the approximate withdrawal speed. Schroeder *et al* showed that the thickness is dependent on the withdrawal speed to the

two-thirds power, while the work of Yoldas *et al* reported a 0.5 power relation [100, 101].

The dip coating was carried out immediately after the polymer solutions were prepared in order to minimize the change in viscosity of the polymer solution due to the evaporation of the solvent that may cause unintended change in the concentration of the polymer solution. The withdrawal has been carried out at a calculated speed of .3, 0.6, and 0.9ms^{-1} in each of the polymer solution concentration (0.25, 0.5, 1, 2, and 5%). The coated surface was then dried at room temperature, but was covered in clear perforated polythene environment to allow the solvent to evaporate slowly so as to protect the coated surface from the damages that could result from the drop in surface temperatures associated with rapid evaporation of the methylene chloride. The combinatorial pattern of withdrawal speed and the concentration of the polymer solution are done in order to investigate their influence on the resulting coating thickness on the coated surface.

3.5.2.2 Spray coating

Spray coating was carried out on the membranes for the purpose of establishing the best coating technique that gives the best results in terms of simplicity, time management, and low cost-high quality coating. We have used an airbrush purchased from central pneumatics model number 95630. It operates at a pressure of 60 PSI and is capable of depositing a thin layer of the polymer. The principle of the spray coating is based on a flow of air carrier gas causing suction in a very thin capillary containing the polymer solution. In this way, a solution is pushed out to the spray nozzle, where it is atomized into droplets. The airbrush was kept at a certain small angle with respect to the vertical position during spray coating to avoid large droplets landing on the membrane surface. Spray coating was performed in air and at room temperature. Different parameters of spray coating were investigated including the distance between the membrane and the nozzle of the airbrush, and the angle of spraying. This profile will help to establish the best combination that will achieve a monolayer coating. After spray coating, the membranes are left to dry in air before heat-treating.

3.6 Curing of the polymer coating

The coated membranes are specifically to be used in the biomass pretreatment process and expected to operate at temperatures above 200 ^{0}C. Heat treatment of the coated membrane is therefore a necessary step to ensure that the coating can withstand such operating temperatures. The heat-treated membranes were also evaluated to determine if the treatment affects the structure of polymer coating. The heat treatment was completed in an tubular furnace from room temperature to 260 ^{0}C at a heating rate of 2 ^{0}C per minute.

3.7 Characterization

3.7.1 Polymer solution viscosity

The viscosity of the polymer solution is a very fundamental characteristic, which plays an important role in the polymer coating process. An Ubbelohde OB-K361 viscometer was used to determine the viscosity of the different polymer solution concentration in a constant temperature bath of 31 °C. The same measurement was repeated after the solution was stored for four months in order to determine if the integrity of the polymer solution was affected after a period of time.

3.7.2 Thermogravimetric analysis (TGA)

TGA was used to characterize the thermal stability of the plain and coated membranes. The TGA model SDTA851e was used to measure the amount and rate of change in the weight of the samples as a function of temperature and time in a controlled nitrogen atmosphere. The sample was heated at three or more different heating rates. The use of different heating rates changes the time scale of the decomposition event. The higher the heating rate, the decomposition temperature will be higher. This approach will establish a link between time and temperature for the polymer decomposition and this information can be used to model the decomposition kinetics

3.7.3 Scanning electron microscopy (SEM)

Uncoated membranes and several of the coated membranes have been characterized in order to determine the presence of coating on the membranes, and also to determine if the pores in the membranes have been blocked. LEO 1525 SEM has been used to study the surface characteristics of the coated and the plain membranes while ARUGA SEM with *in situ* milling capability was used to study the pore characteristics before and after the coating in order to determine if the thin polymer coat on the membrane was deposited on the surface or also into the pore structure.

3.7.4 Fourier transform infrared/attenuated total Reflectance (FT-IR/ATR) analysis

ATR-FTIR is a well-established, nondestructive method for determining the chemical composition of materials based on their chemical bonding. Compared to other characterization techniques such as the XPS, ATR-FTIR resolves chemical bonds of polymers more clearly. ULTEM has more variation in chemical bonding and therefore using this technique would be useful compared to determining its elemental composition. In addition, it is much faster than more common thickness measurement techniques, requiring no sample preparation, pump down, or sputtering. We effectively used ATR-FTIR to determine the presence of the ULTEM coating on the surface by detecting the chemical composition of the ULTEM based on its chemical bond and structure.

The resulting respective peaks were analyzed and compared with theoretical ATR-FTIR scans of Ultem in order to confirm the presence of the polymer coating on the membranes. For correct measurements to be possible, we have also assumed that IR penetration depth at the wavelength of the peak that is unique to the ULTEM will be greater than the thickness of the coating. The ULTEM coating throughout the substrate and on the membrane surface is also assumed to be chemically stable through the testing procedure, and that the ATR-FTIR depth of penetration, $d_{p,}$ will be constant for each sample to be characterized.

3.7.5 Permeability and selectivity measurements

Permeability measurements for both liquid and gas were completed on the membrane before coating and after every successive coating in order to determine the effects of the coating on the membrane pore size and on the permeance. The ceramic membranes that were used were obtained from Inopre and have an intermediate support structure and outside support structure made of alumina and the membrane layer made of TiO_2 with outside diameter (OD) of 0.4 inches, an inside diameter (ID) of 0.275 inches and a length of 10 inches. The permeability results was used in combination with other results to determine the approximate thickness of the polymer coating and also to establish the optimized coating conditions and polymer solution concentration and coating application method that will give the desired membrane performance. Typically, the pressure differential was established by introducing one of the permeate gases at a known pressure into the volume outside the membrane tube and monitoring the pressure increase inside the tube, which was at a very low pressure with respect to time. The schematics of gas permeance measurement set up is show in figure 3.3. The rate of increase of pressure dP/dt inside the tube was then plotted against the pressure difference created across the membrane. The slope of this plot was converted to permeability coefficients (mol/cm*min*atm) for each of the permeate gases. This calculation was done based on the known dimensions of each membrane, the volume of permeate chamber, and the temperature during the measurement. Selectivity was obtained from permeability ratios.

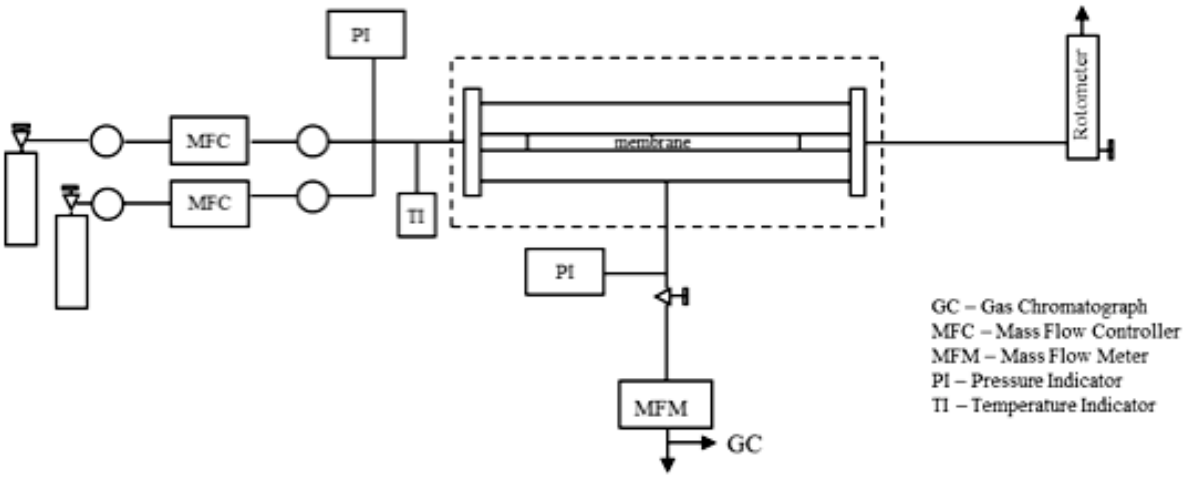

Figure 3.3 Schematics of the gas permeance test set up.

A cross flow cell was used to measure the water flux of the membrane with the effective surface area of 54.86 cm^2. This measurement was performed at room temperatures. The schematic of the flow cell shown in figure 3.4 consist of a water vessel, a feed pump, the membrane, water pressure indicator, and a water flow indicator. The feed flow pressure was varied between 30 and 60 bars and the corresponding time and volume of permeate was recorded. The water flux was calculated using the equation

$$J = \frac{V}{S \times t}$$

Where J is the flux of the membrane measured as $lm^{-2}\ h^{-1}$, V the permeate volume measured in liters (l), S is the membrane active surface area (m^2) and t is the time in hours it takes to permeate across the membrane (h) [102].

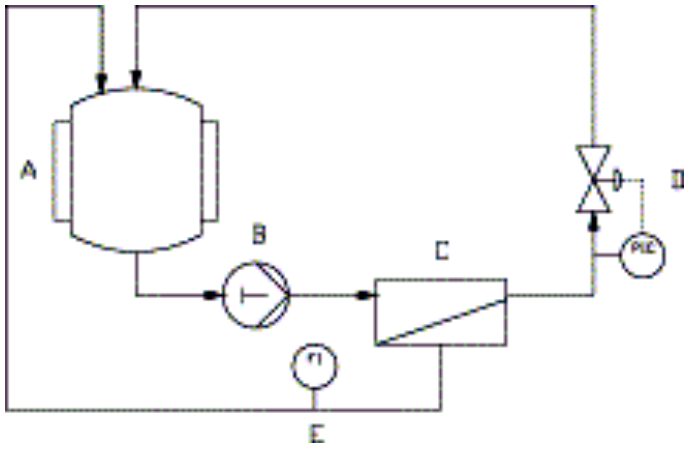

Figure 3.4 The schematics of the cross flow model for flux measurements showing a) the vessel, b) feed pump, c) the membrane, d) the pressure indicator and controller, and e) the permeate flow indicator.

The performance of the membrane before and after coating was measured by filtering the 10% lignin solution. The lignin solution was prepared in 2% caustic solution and the membranes were used to perform the separation. Several factors were varied in order to measure the performance of the membranes at different pressure, temperature, filtration time, lignin concentration, and flowrates. The flowrate was varied between 1 and 3 Gallons Per Minute (GPM) and the temperature of the lignin solution was varied between 50-90 ^{0}C. The trans-membrane pressure (TMP) of the system was also changed between 20 and 60 PSI, and the concentration of the lignin solution that was used was between 2-10% of the lignin weight. All these variables were combined in a combinatorial pattern that enabled a wide range of membrane performance to be established. Deionized water was used for rinsing steps, which were performed before and after each fouling experiment occurred, while 2% sodium hydroxide solution was used as the cleaning agent and cleaning performed at 50 °C. The cross flow velocity during the cleaning steps was higher than that at which fouling of the membrane occurred in order to enhance removal of the fouling layer from the membrane surface. The laboratory set up is shown in figure 3.5.

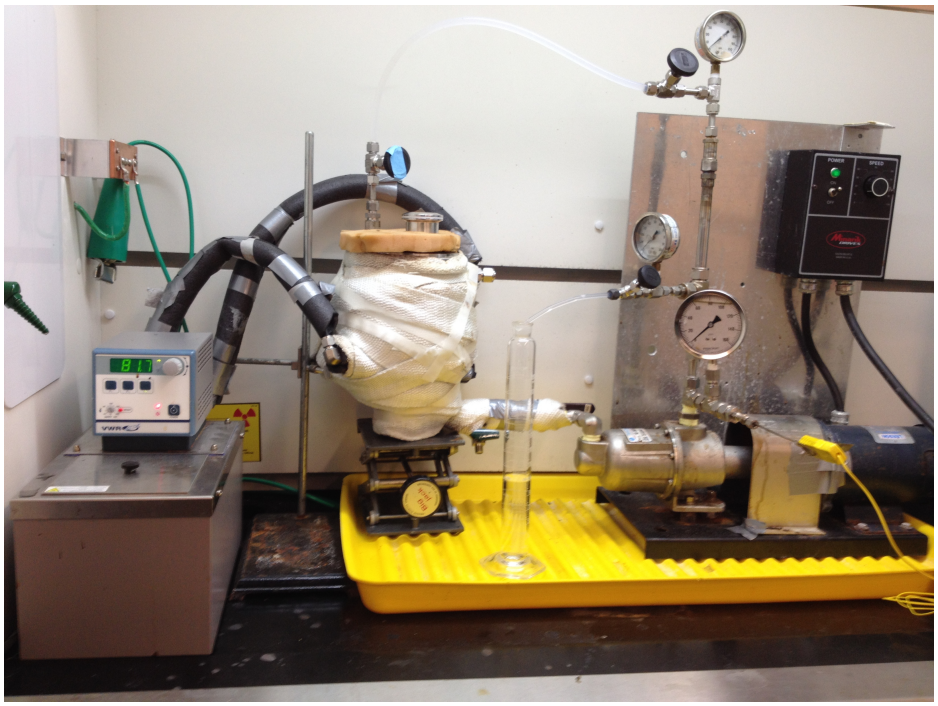

Figure 3.5 Experimental setup for the lignin separation using the membrane.

3.7.6 Thermal curing and chemical resistance test

Since the coated membranes will be operating at conditions of up to 200 ^{0}C, it is necessary to cure the polymer coating. Thermal curing was completed on the coated membranes. The heat treatment was carried out in a furnace with the temperature being increased from 25 ^{0}C to 200 ^{0}C at a rate of 2 ^{0}C/min. The heat-treated coated membranes were then tested to determine if the polymer was stabilized after the heat treatment.

These membranes will also be potentially exposed to operating conditions that may result in chemical attacks. The coated membranes were therefore subjected to various solvents and acidic environments in order to establish stability of the polymer coating and performance in such extreme environments. This test was performed by separately immersing the coated membranes in dimethylformamide (DMF), methylenechloride, and sodium hydroxide solutions for a period of 7 days, and by observing the changes in the surface morphology.

Chapter four

Results and Discussion

4.0 Polymer solution characterization

Experimental results have shown that Ultem forms a thin layer coating on the substrate, with the thickness of the coating determined by the concentration of the Ultem in the solvent. Reproducible experimental data consistently show that the thickness of the coating increases in a direct proportion with the percentage amount of the ULTEM in the solution as shown in figure 4.1.

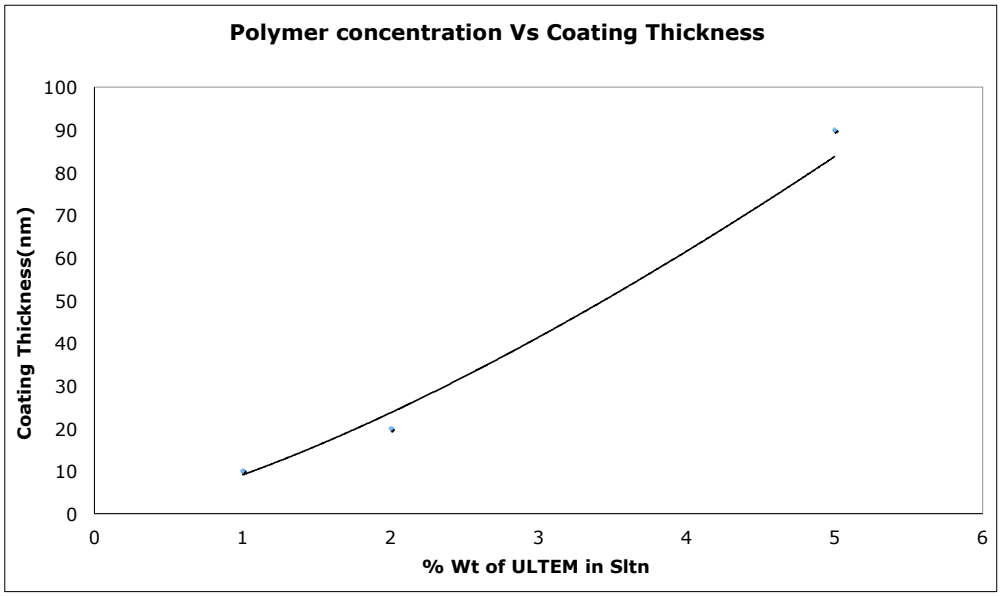

Figure 4.1 Coating thickness as a function of the Ultem concentration.

It was established that the polymer solution did not deteriorate over time, as the viscosity remained the same over a four-month period. Since it is extremely difficult to determine the concentration of the polymer in the solution after filtering using the 5µm filter (because the un-dissolved fibers that are greater than 5µm in diameter in the polymer solution are removed during filtration), we have used a normalized kinematic

viscosity equation, where the fluid head term is eliminated so that the viscosity is described by the relationship ν = (area/ time). If the area remains the same, then the viscosity can be estimated or described by the measured time the known volume takes to go through the viscometer. Table 4.1 below shows the time it took for the same volume of various Ultem solution concentrations and grades to go through the viscometer. Experiment one shows the initial time measurements while experiment two is the time measurements of the same solutions done after four months of storing it at room temperatures. This result shows that there is a negligible change in viscosity of the polymer solution as shown in table 4.1.

Table 4.1 Representation of viscosity as a function of time for ULTEM 1010 and ULTEM 1285.

	ULTEM 1010		ULTEM 1285	
	1% by Polymer wt.	2% by Polymer wt.	1% by Polymer wt.	2% by Polymer wt.
Time (s)				
Experiment 1	96.32	150.52	96.80	134.08
Experiment 2-	96.07	150.28	96.03	134.04

4.1.1 Dip coating

The thickness of the coating has been optimized against several parameters. The temperature and time at which the polymer fully dissolves in the solvent was determined and optimized at 60 ^{0}C in the sonicator bath for 40 minutes. Below this temperature and time, the polymer does not completely dissolve. Table 4.2 below summarizes the relationship between the coating thickness, the withdrawal speed, and the solution concentration by weight of the polymer. The thinnest polymer layer was obtained at the lowest polymer concentration and at high withdrawal speed.

Table 4.2 Correlation between the resulting coating thickness and other parameters.

Amount of ULTEM	Withdrawal speed (ms^{-1})	Coating Thickness (nm)
1%	0.9	7.7
	0.6	11.8
	0.3	14
2%	0.9	20.9
	0.6	22.4
	0.3	24.0
5%	0.9	88.7
	0.6	91.4
	0.3	120.4

The SEM micrographs in figures 4.2, 4.3, and 4.5 show the same relationship where the thickness of the polymer coating for each of the polymer concentrations is shown. The minimum thickness has been achieved with the lowest concentration of 1% of the polymer weight, with a withdrawal speed of 0.9 m s^{-1}.

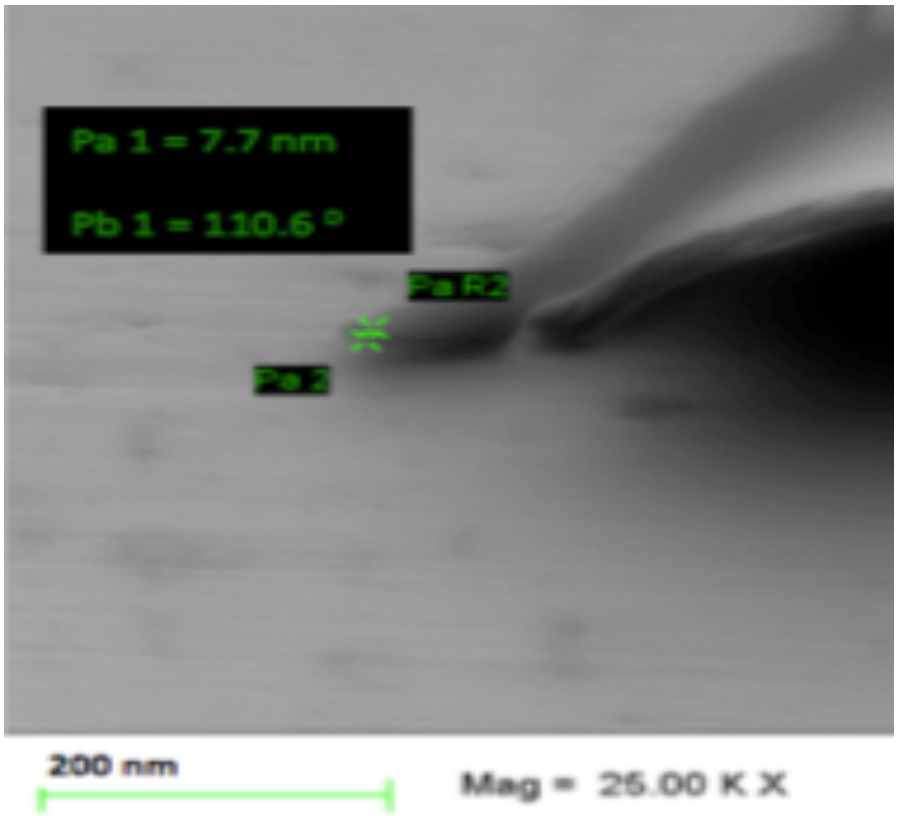

Figure 4.2 SEM micrograph showing the resulting thickness for the 1% ULTEM coating.

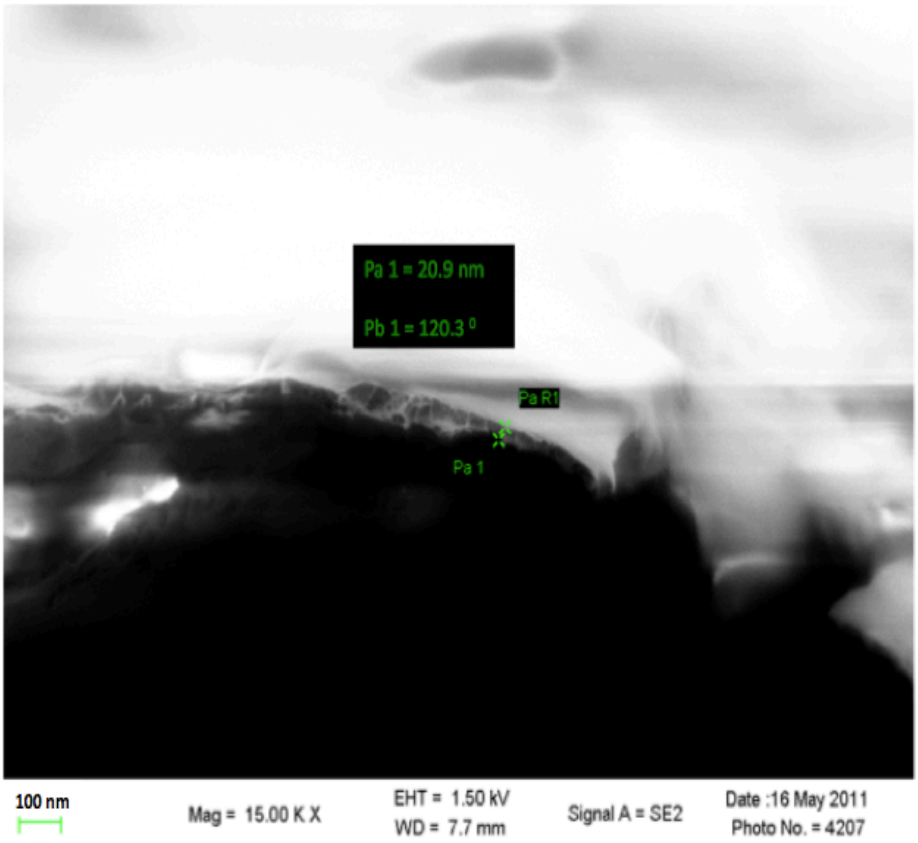

Figure 4.3 SEM micrographs showing the resulting thickness for the 2% ULTEM coating

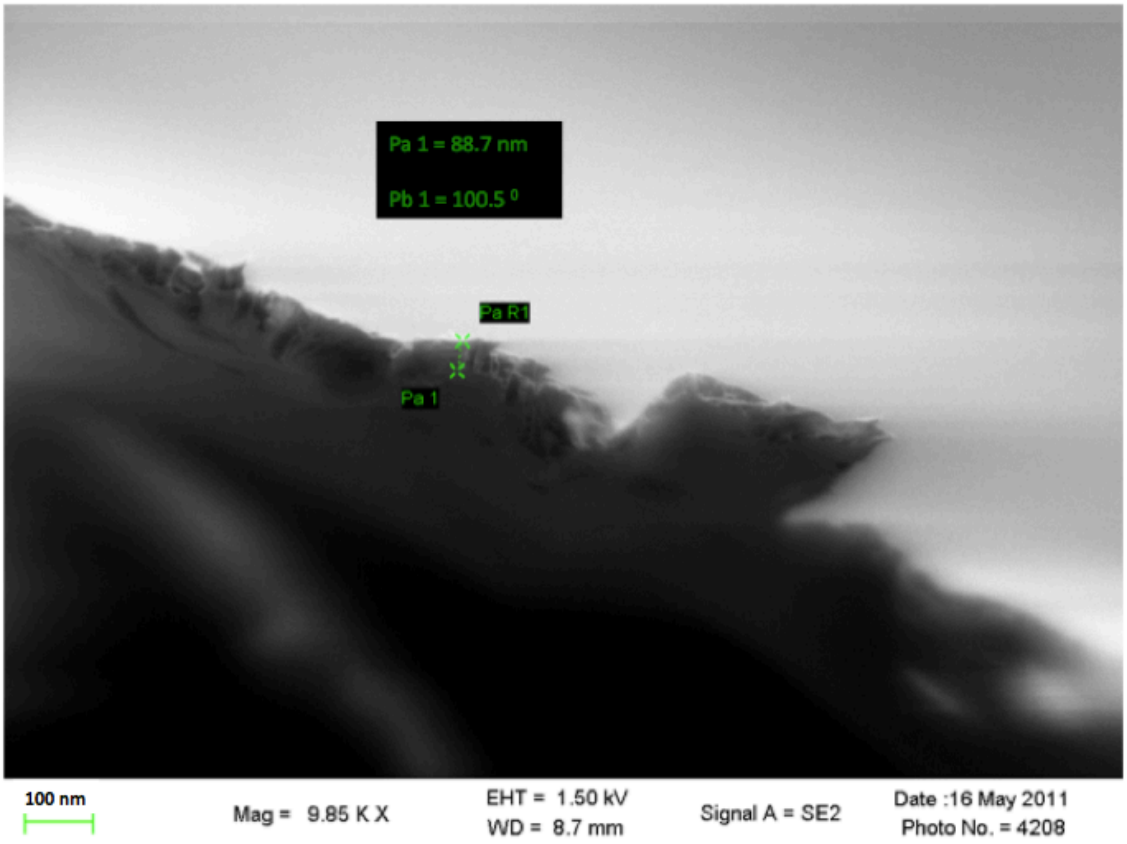

Figure 4.4 SEM micrographs showing the resulting thickness for the 5% ULTEM coating.

4.1.2 Spray coating

We have also proposed and developed a simple ultrathin coating method for depositing the polymer on the surface of the membrane. Here, a specialized nebulizer-like commercially available airbrush has been used to spray the polymer solution. The principle of the airbrush is derived from a pressure differential caused by the flow of compressed carrier gas that causes suction in an ultra thin capillary containing the polymer solution. The solution is forced through the nebulizer nozzle and atomized small droplets are dispersed and deposited onto the desired surface forming a monolayer coating. The Central Pneumatic designed airbrush with an air outlet capability of 0-60 PSI has a carrier rate of ≈ 0.64 l/min and a yield droplet size of 1-5 μm range for aqueous medium.

The distance between the airbrush and the surface has been established to be one of the main factors that can effectively control the thickness of the polymer coating. In order to deposit a monolayer of the polymer on the 1cm x 1cm surface, 10-15 μl amount of the polymer solution with 1, 2, and 5 % of the polymer by weight was introduced into the brush. This amount was optimized in considering the spraying geometry (the distance between the surface and the airbrush), so that the loss due to conical dispersion of the spraying beam is compensated. It was observed that for a short distance between the spray and the surface, the surface is visibly wet and appears similar to drop coated surface. Since the polymer was dissolved completely, no clusters have been formed. It has been established that the optimum distance between the airbrush and the surface, which results in a near monolayer coating is about 10-12 cm. SEM images show a uniformly distributed coating on the surface under these conditions.

The effect of ULTEM concentration on the thickness of the polymer coating was also studied. The viscosity of the polymer increases with the amount of ULTEM in the solution thus increasing the size of the atomized droplets. Although the range of concentration studied has shown increase in the coating thickness, there was no significant change in the qualitative appearance of the morphology. This could be attributed to the fact that as the solution droplets set on the surface and the solvent

evaporate, the droplet size shrinks and the gaps between the polymer molecules remain the same and independent of the polymer concentration and therefore the surface morphology does not change. Only the amount of the polymer deposited on the surface increases with the polymer concentration.

The process of spray coating involves the dispersion of the atomized ULTEM solution from the airbrush followed by the deposition of the droplets onto the surface of the membranes by the steering flow, and then subsequent evaporation of the solvent. Since the coated surface is porous with estimated pore size of about 5 μm, and the intended purpose of coating is such that the pores are not covered, coating by means of spraying plays a very important role in that as the atomized polymer droplets are dispersed and settle on the surface, only the intended surface is coated and with the pores left open allowing a precision in thickness control. The figures 4.5 a and b and 4.6 below shows SEM micrograph of the surface of a membrane before and after coating. Although both the dip coating and the spray coating techniques were effectively used to achieve thin layer coating on any surface, the dip coating was used more in this research because it was an easier method to coat the inside of the membrane tubes.

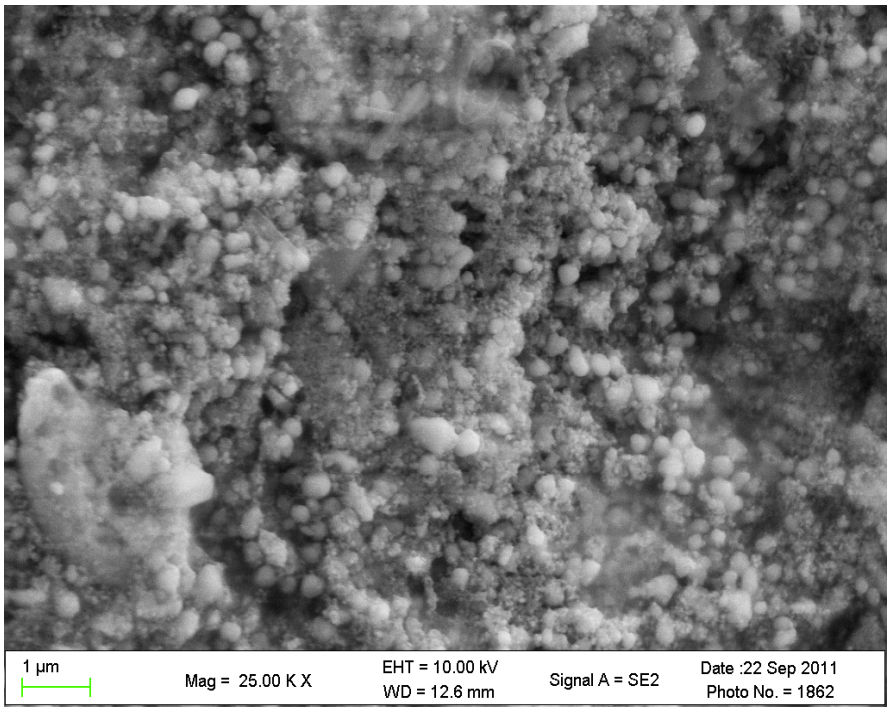

Figure 4.5 a) SEM micrograph of the uncoated (5µm diameter pore size) membrane.

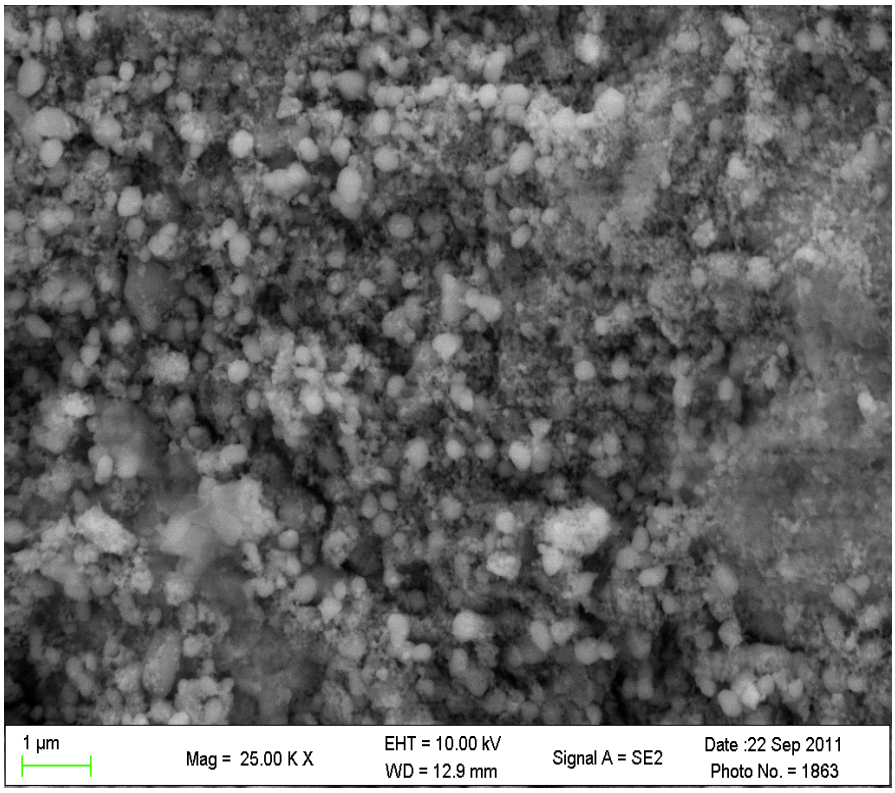

Figure 4.5 b) SEM micrograph of the membrane (5µm diameter pore size) coated with 1% ULTEM solution.

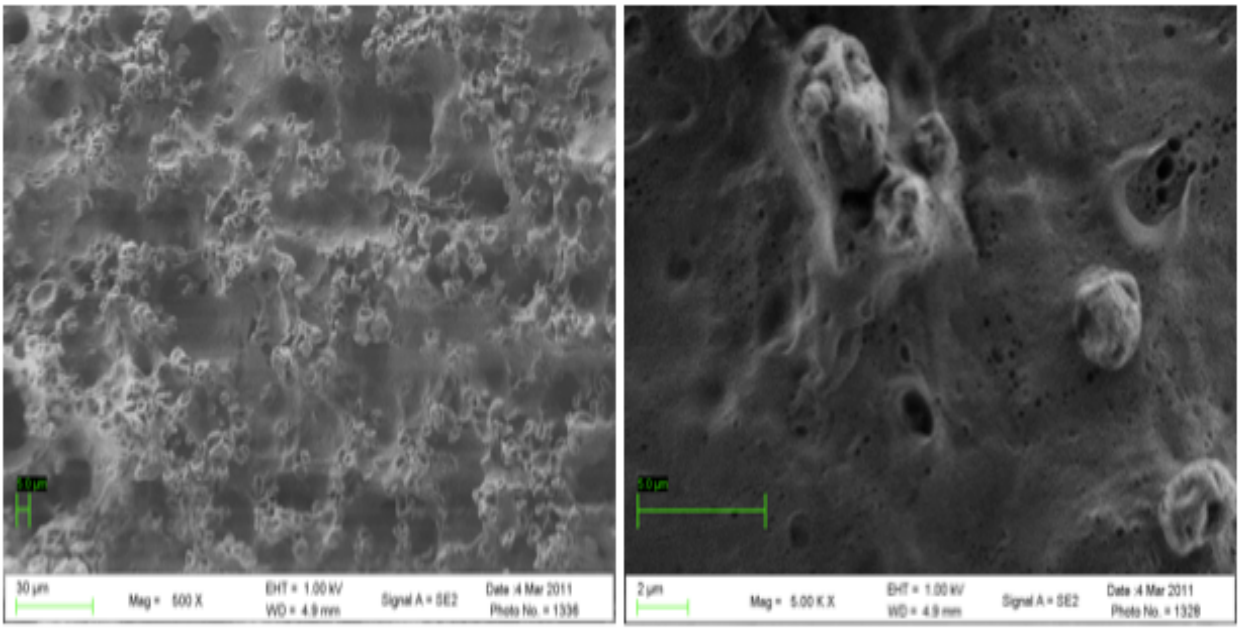

Figure 4.6. SEM micrograph of the membrane coated with 2% and 5% Ultem solution.

It is uniquely evident that the increase in the polymer concentration in the solution results in a thicker coating on the membrane, and only in the 1% concentration does the pores remain unblocked. When the concentration increases to 2%, the pore structures are still visible but the effective pore performance is greatly affected and does not appear to be porous. With 5% solution, the surface of the membrane is completely covered and the membrane does not appear to be porous.

As previously mentioned, membranes coated with unfiltered Ultem solution show that the undissolved fibers from the Ultem result in the fibers deposited on the surface of the membrane (figure 4.7) and therefore affecting its overall performance. Filtering the solution with a 5µm filter eliminated the problem and does not affect the overall thickness of the coating deposited on the membrane. Figure 4.7 a and b shows the surface of the membrane coated with the filtered and unfiltered polymer solution

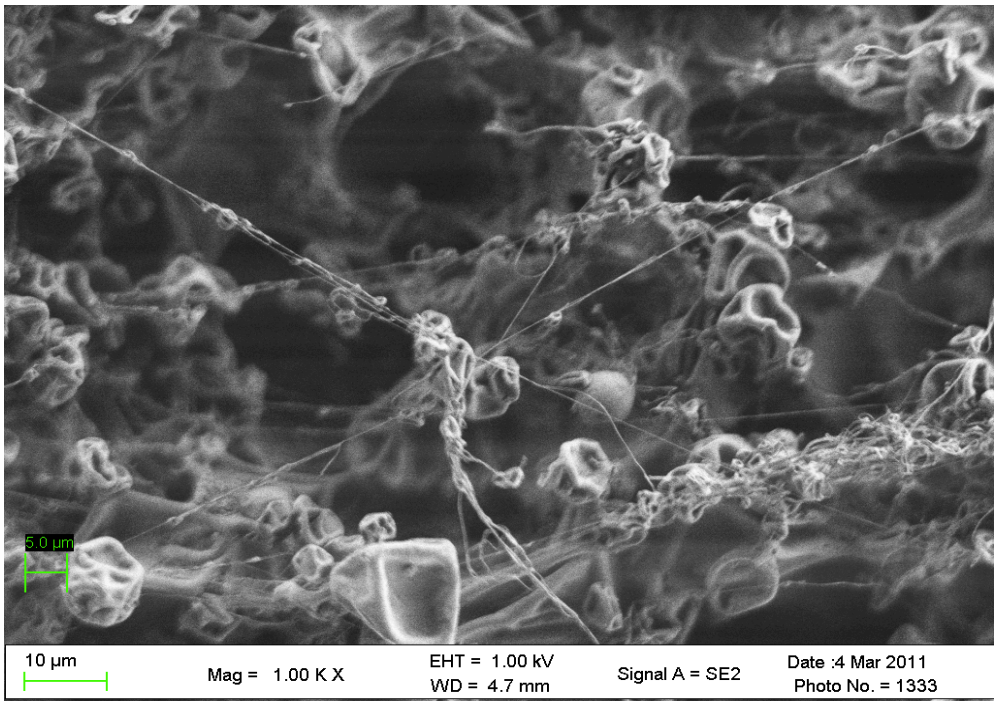

Figure 4.7 a) SEM micrograph of the membrane surfaces coated with unfiltered 5% polymer solution.

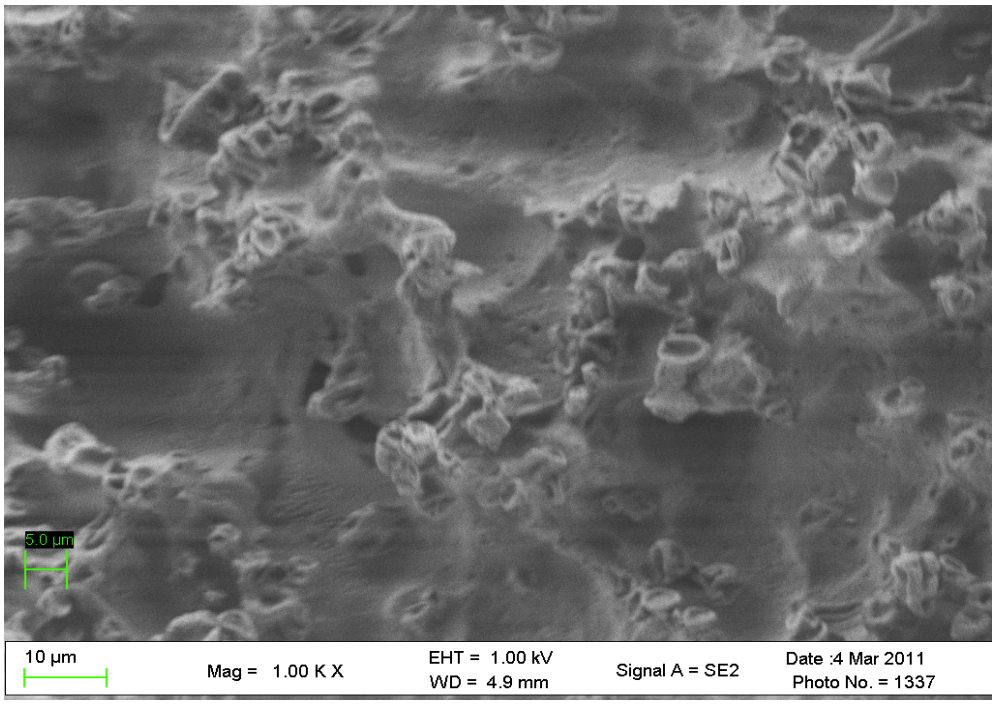

Figure 4.7 b) SEM micrographs of the membrane surfaces coated with filtered 5% polymer solution.

4.2 Fourier transform infrared/attenuated total reflectance (FT-IR/ATR) analysis

Attenuated total reflectance-infrared spectroscopy was used to confirm the existence of the polymeric coating on the surface of the substrate and the membranes. ATR-FTIR, a non-destructively tool, was used to determine the composition of the surface coating by detecting the chemical composition of the Ultem based on its chemical bonding and structure. Ultem has a wide variation in chemical bonding and therefore the use of ATR-FTIR plays a big role. The ATR-FTIR results have showed consistency with theoretical expectations, and it was demonstrated that Ultem is indeed present on the surface of the target.

Figures 4.8, 4.9, and 4.10 show the ATR-FTIR spectrum obtained at an incidence angle of 60^0. We have identified the characteristic bonds occurring at different wavenumbers and are summarized in table 4.2. Ultem has been deposited on the surface of stainless steel and the varying amounts of polymer have been evident by the difference in peak intensity.

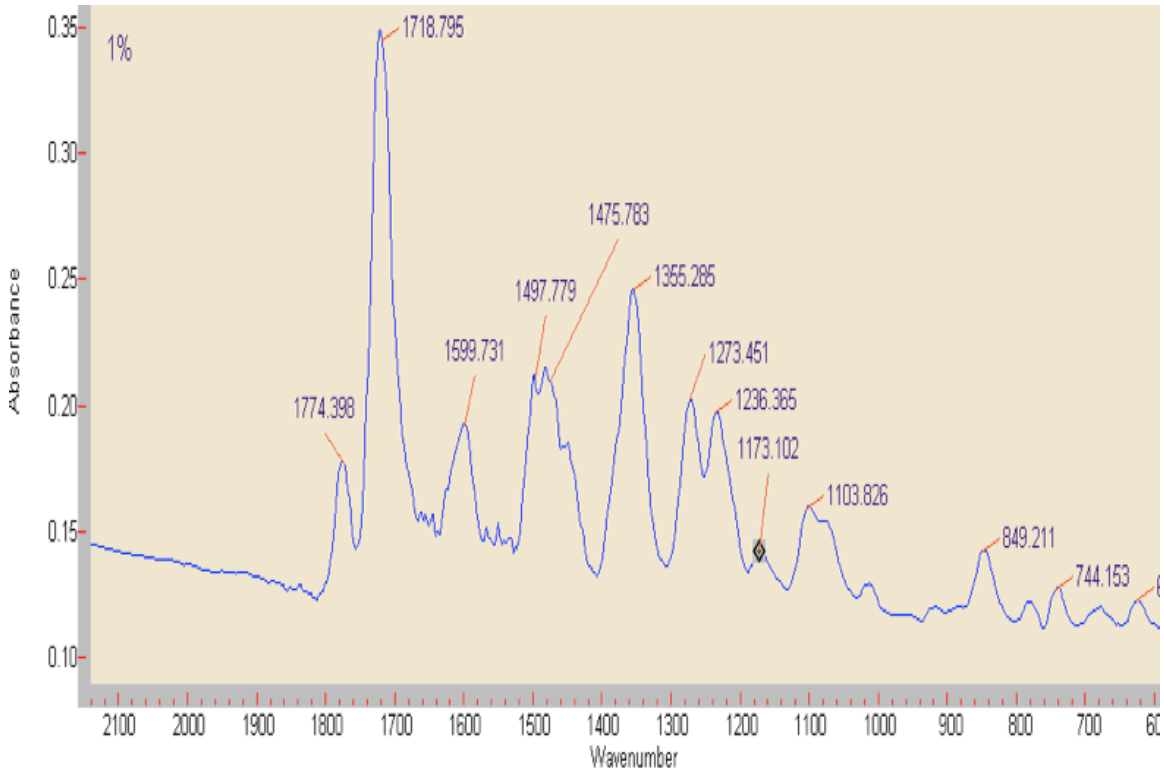

Figure 4.8 ATR-FTIR graph of 1% Ultem coated on the membrane.

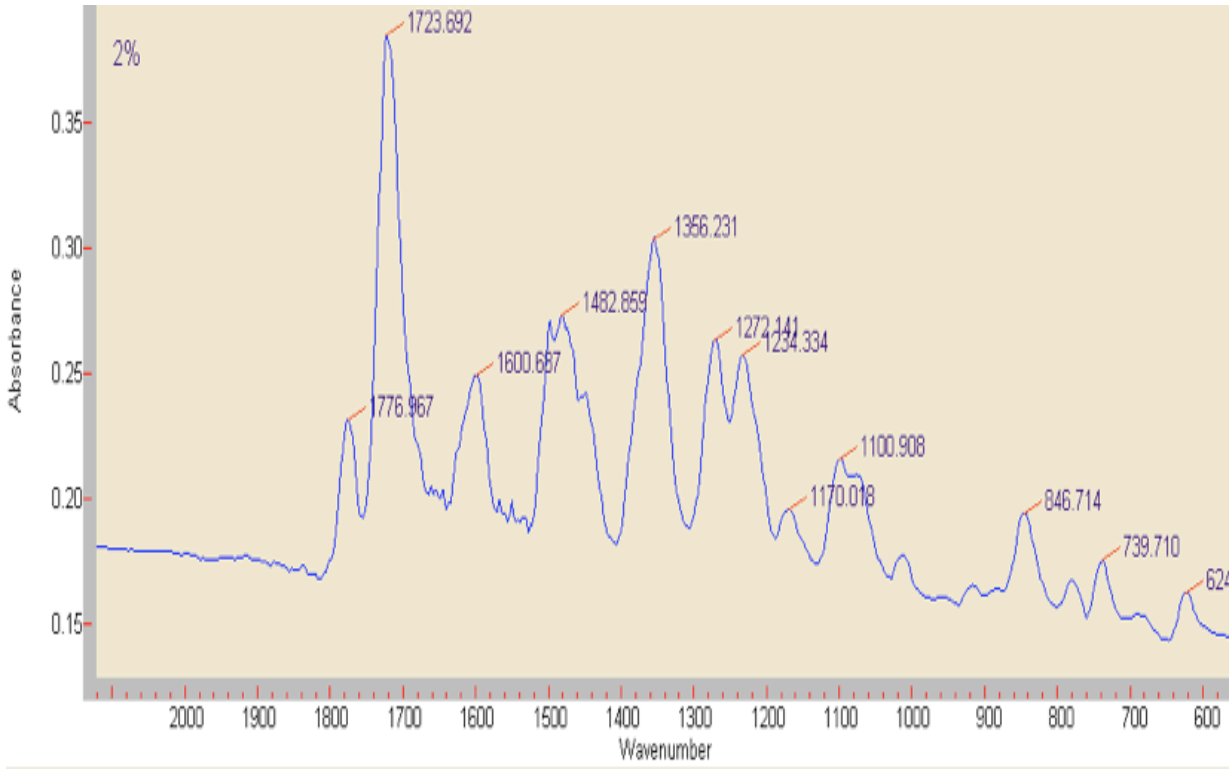

Figure 4.9 ATR-FTIR graph of 2% Ultem coating on the membrane.

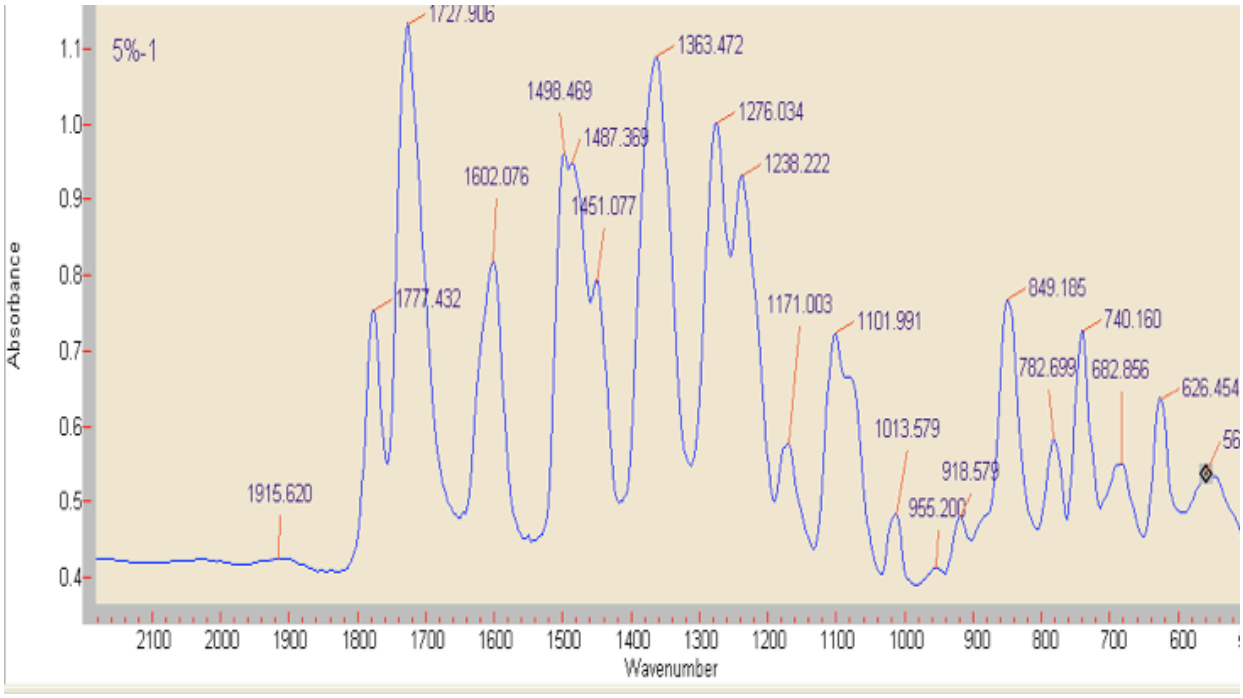

Figure 4.10 ATR-FTIR graph of 5% Ultem coated in stainless steel.

Table 4.3 Tabular representations of the ATR-FTIR infrared absorption band characteristics of Ultem.

Literature Peak	**Experimental Peaks for Weight % of ULTEM**			**Vibration Band Assignment**
	1%	2%	5%	
672	624	624	623, 682	Phenyl (Mono Substituted)
739	744	739	740, 782	Imide Ring
834	849	846	849	CH_2 from plane wagging
1064	1103	1100	1101	C-O-C stretching
1166	1173	1170	1171	C-N
1209, 1263	1236, 1273	1236, 1272	1238, 1276	C-N stretching, -o-aromatic, CH_3
1476, 1596	1475,1497, 1599	1482,1473, 1600	1498,1487, 1602	C=C ring stretch
1715	1718	1723	1727	C=O symmetric stretching
1775	1774	1776	1777	C=O asymmetric stretching

4.3 Thermogravimetric analysis (TGA)

TGA has been used do characterize the thermal stability of the plain and coated membranes. As shown in the Figures 4.11 and 4.12, the coated membrane has exhibited a decrease in weight at about 600 ^{0}C. The 5% Ultem 1010-coated membrane has experienced a relatively higher weight reduction compared to the other polymer coatings. These results may be an indication of the difference in thermal stability of the two polymers.

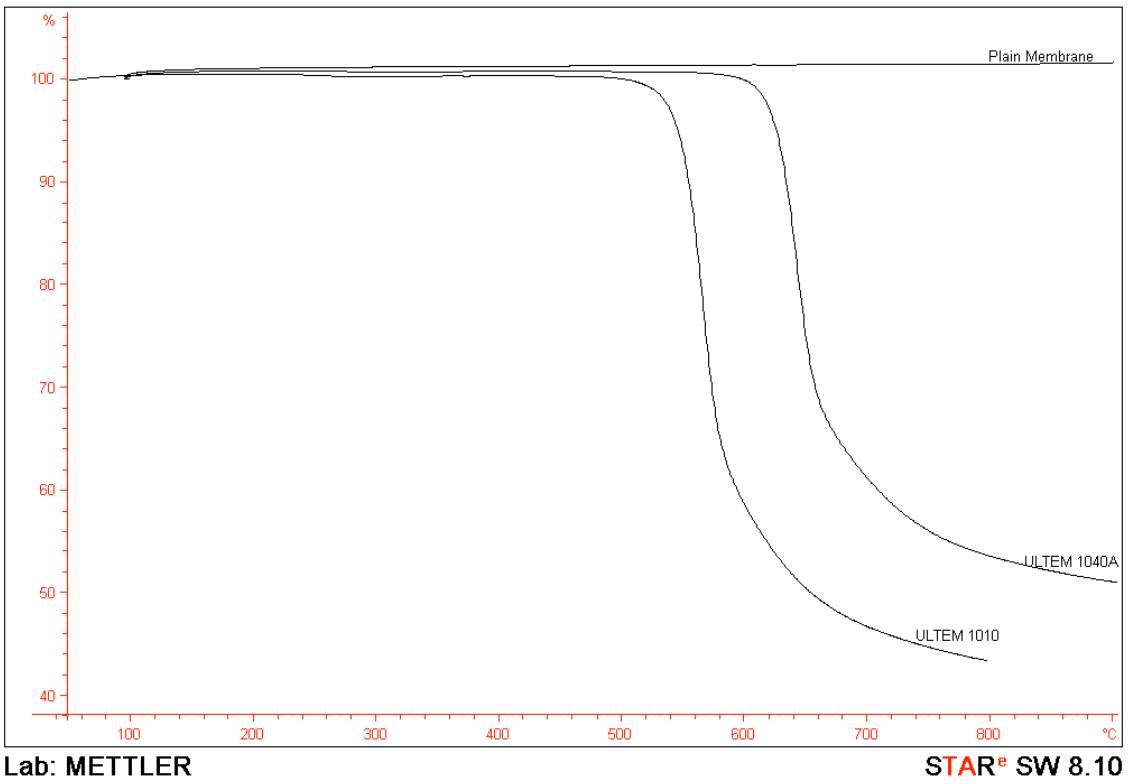

Figure. **4.11** TGA Graph showing percentage weight loss as a function of temperature for polymer Ultem 1010, Ultem 1040A and uncoated membrane.

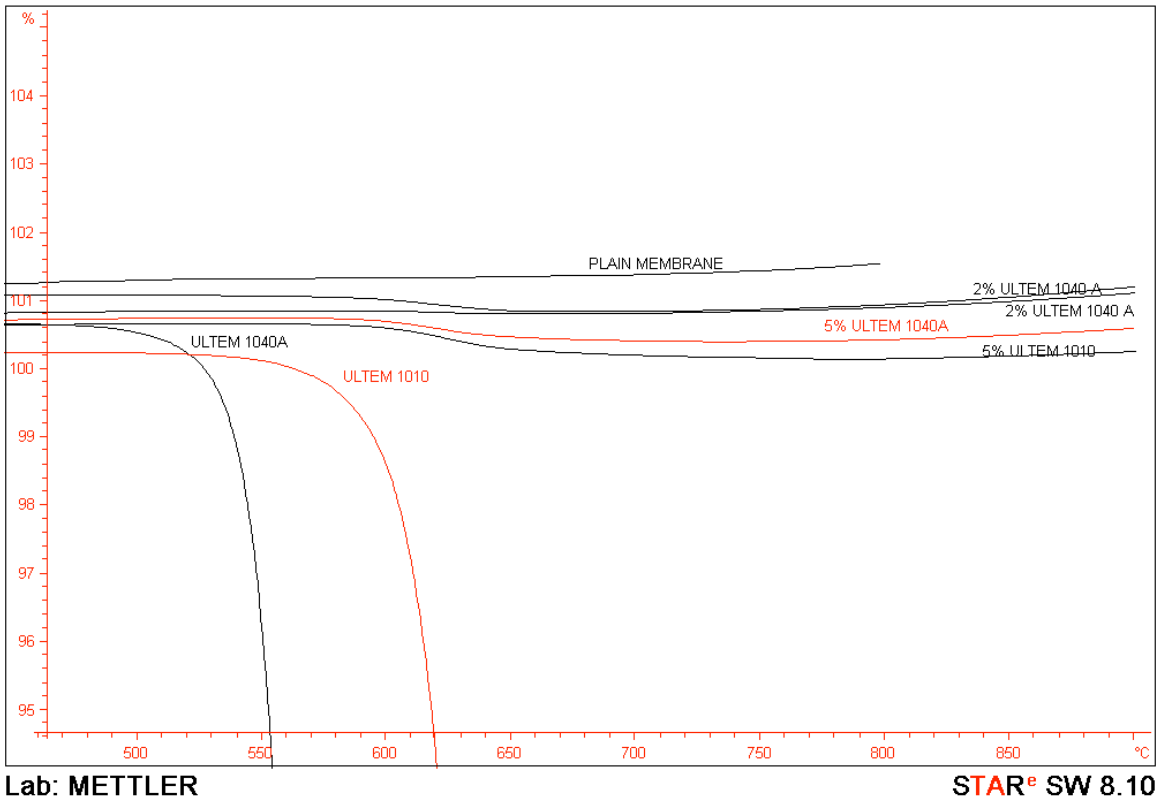

Figure 4.12 TGA Graph showing percentage weight loss as a function of temperature for membrane coated with varying concentration of polymer Ultem 1010 and Ultem 1040A

4.4 Membrane performance

4.4.1 Pore size and pore size distribution

The pore size and pore size distribution of the membranes obtained from Pall Corporation, were verified by desorption isotherm permporometry equipment. The pore size of the uncoated membrane (I30NM6) was determined to be 156 nm and after coating with 0.25% Ultem 1010 solution, the pore size has been reduced to 145 nm as shown in figure 4.13. A second membrane (I30NM5) of similar size was determined to have pore size of 157 nm before coating and 148 nm after coating as shown in figure 4.14. The pore size distribution is, however, more varied in the coated membrane. This is because of the altered pore geometry caused by the coating on the surface of the membrane, which changes the surface morphology.

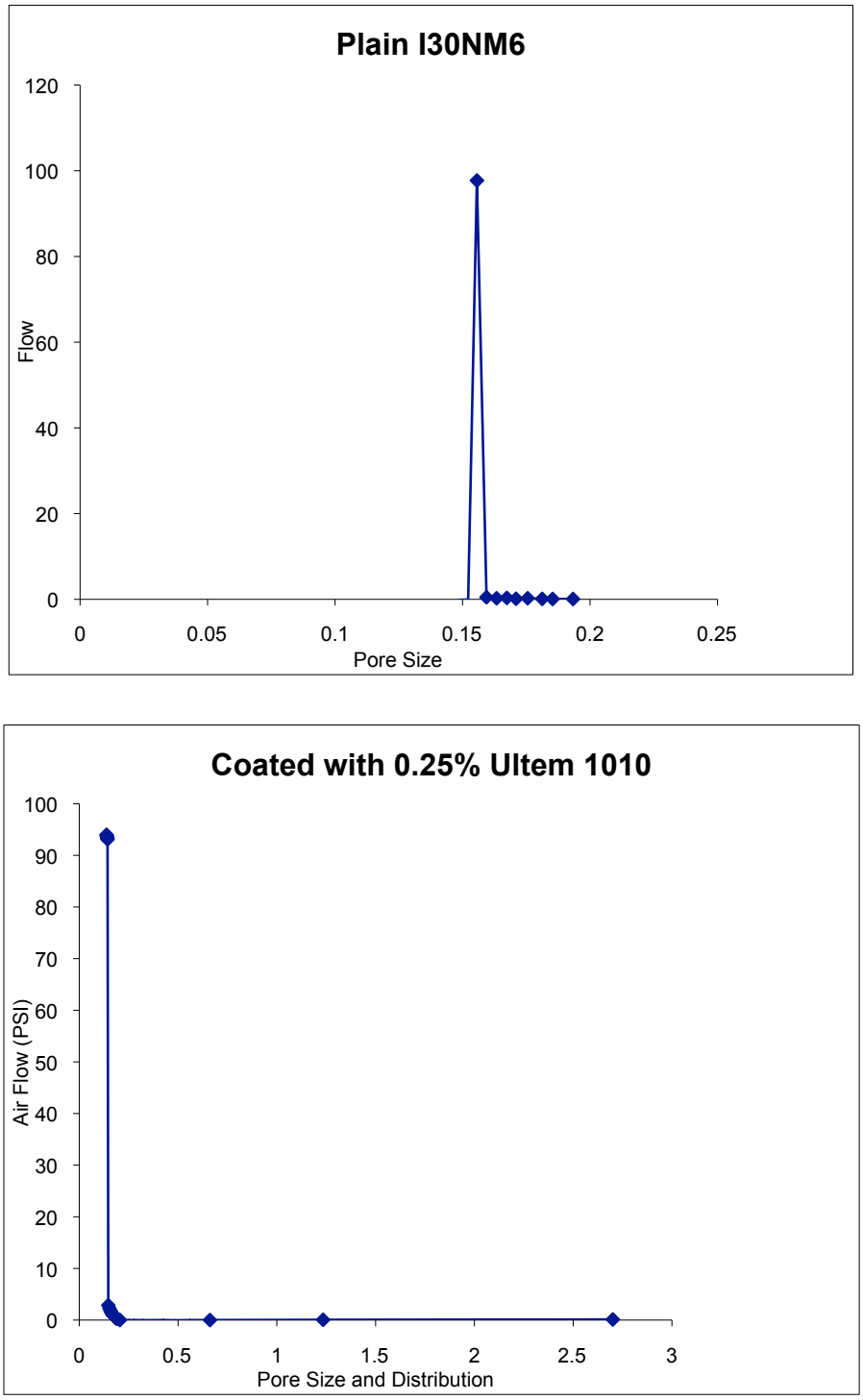

Figure 4.13 Pore size and pore size distribution of plain (above 156nm) and coated (145nm) membrane I30NM6.

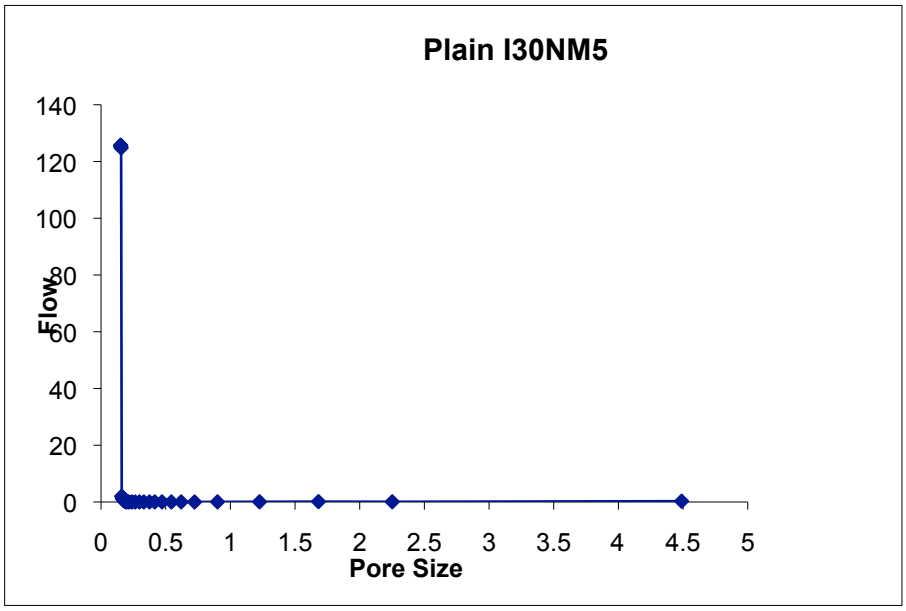

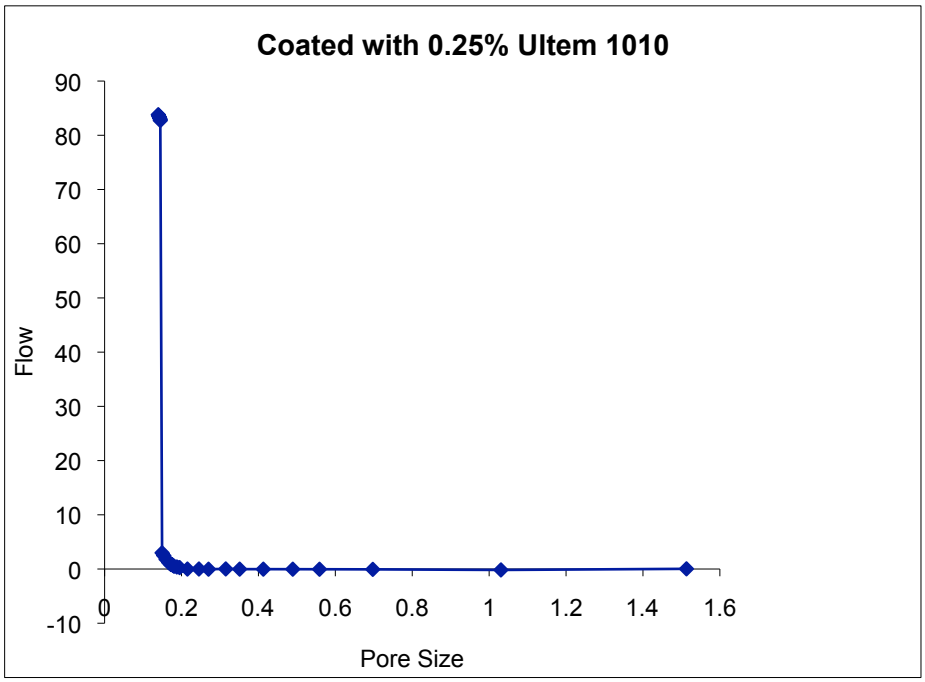

Figure 4.14 Pore size and pore size distribution of plain (top 157nm) and coated (148nm) membrane I30NM5.

The gas permeance of the membranes was measured before and after coating and it has been observed in both membranes that even though there is only about 7% decrease in the pore size of the membrane after coating with the Ultem coating, the decrease in the gas permeation characteristics is about 33% as shown in figure 4.15 and 4.16.

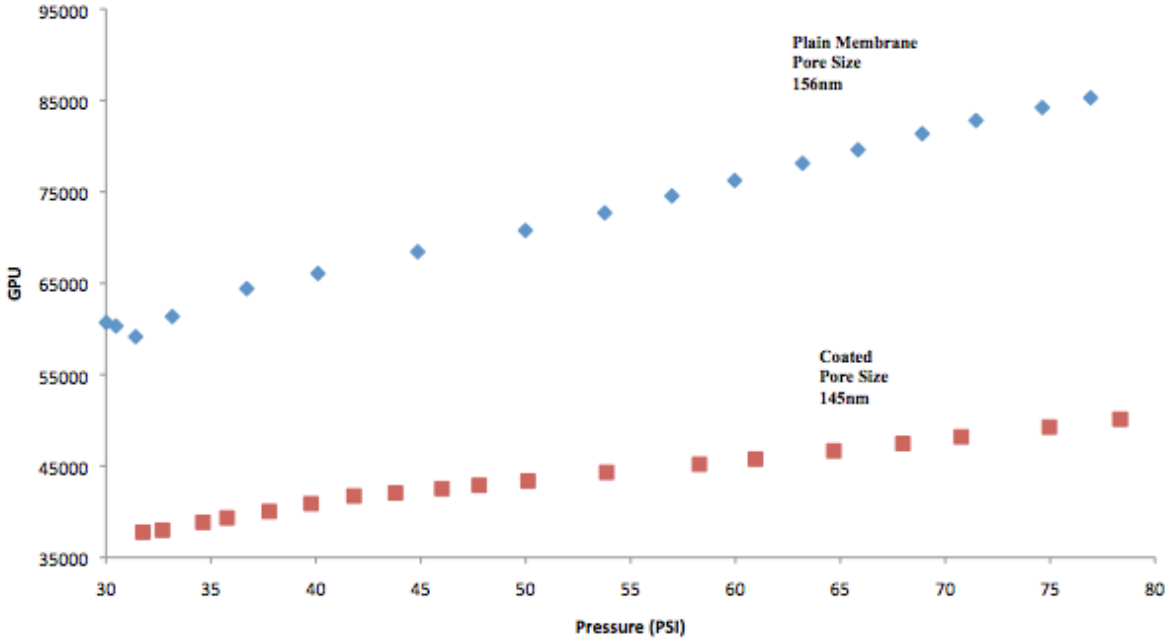

Figure 4.15 Gas permeance characteristics of coated and plain membrane (I30NM6).

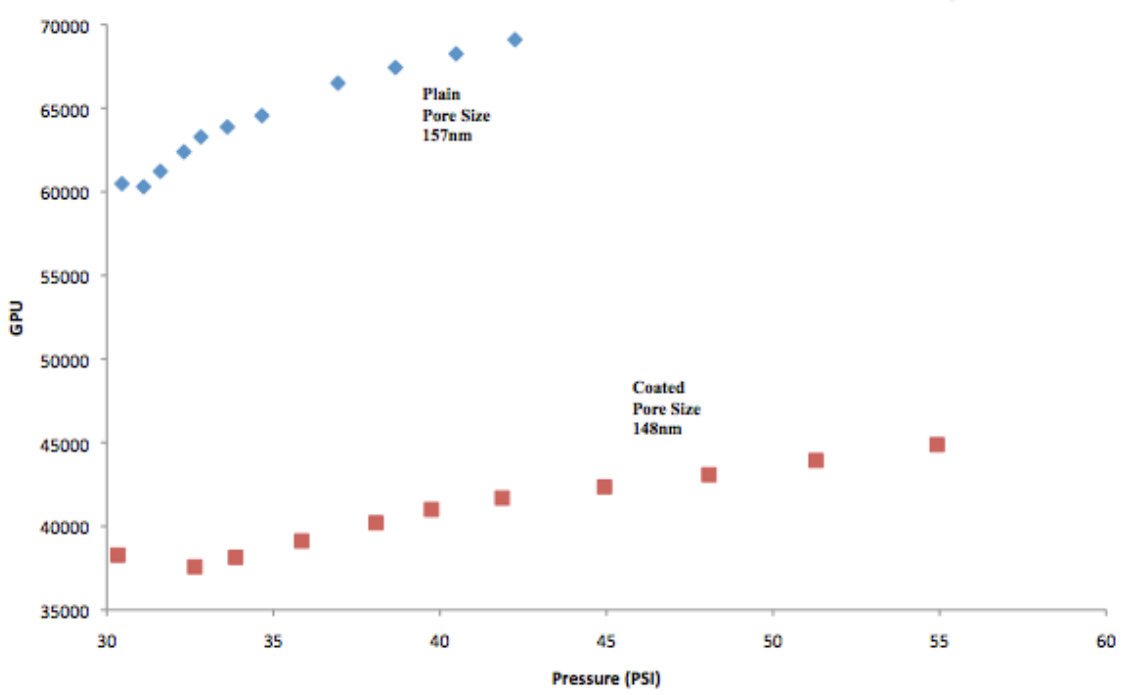

Figure 4.16 Gas permeance characteristics of coated and plain membrane (I30NM5).

These results are consistent with the literature where the gas permeance for uniformly coated membranes have reduced by a factor ranging from 5-25 compared to the uncoated membranes [103]. The SEM images show that the coating on the membrane is uniform and has been measured to be in the lower nanometer range in thickness. The overall change in gas transport in the membrane has not decreased significantly because the coating is only situated on the surface and does not penetrate into the membrane structure as shown by crossectional SEM images.

4.4.2 Flux measurement and characterization

The performance of the coated and the uncoated membrane in separation of the lignin was measured by analyzing the feed and permeate characteristics at various pressure and temperature. The flux has been measured after continuously performing the separation for one hour and after two hours. The coated membrane shows a significantly improved performance compared to the membrane that has not been coated. Although there is a reduction in the flux when the lignin solution was introduced into the system as compared to the water flux, the coated membrane performs separation better than the uncoated membrane. The amount of the lignin permeated after one hour and after two hours was the same for the coated membrane while in the uncoated membrane, the permeate volume dropped continuously as the permeation time increased. This means that the fouling is reduced when there is coating compared to when the membrane has not been coated. The sharp decline in flux in the first few minutes in the uncoated membrane is due to the formation of the polymerization layer, while the further declining of the flux, yet at a smaller rate, can be associated with the gradual adsorption of the lignin into the membrane structure. Although the same trend is observed in the coated membrane, the rate at which the initial and the consequent decline in flux occur is lower than in the uncoated membrane. This result confirms that the coating on the membrane is of great benefit. The same trend is observed at temperatures of 50, 70, and 90 ^{0}C as shown in figure 4.17, 4.18, and 4.19.

The effect of the operating pressure on the permeate flux shown in the results indicates that the flux increases steadily with increase in pressure, but at higher pressures, the increment in flux is gradual. This is because at higher pressures, the rise in the concentration polymerization results in an increase in membrane surface concentration. This will result in an the overall increase in the osmotic pressure of the lignin solution at the surface of the membrane, causing a decrease in the net driving force to the driving of the solute hence a decrease in flux. Since there is a nonlinear variation between the concentration and the osmotic pressure, a gradual increase in flux at higher pressure is observed. This trend is also reported elsewhere in literature [104].

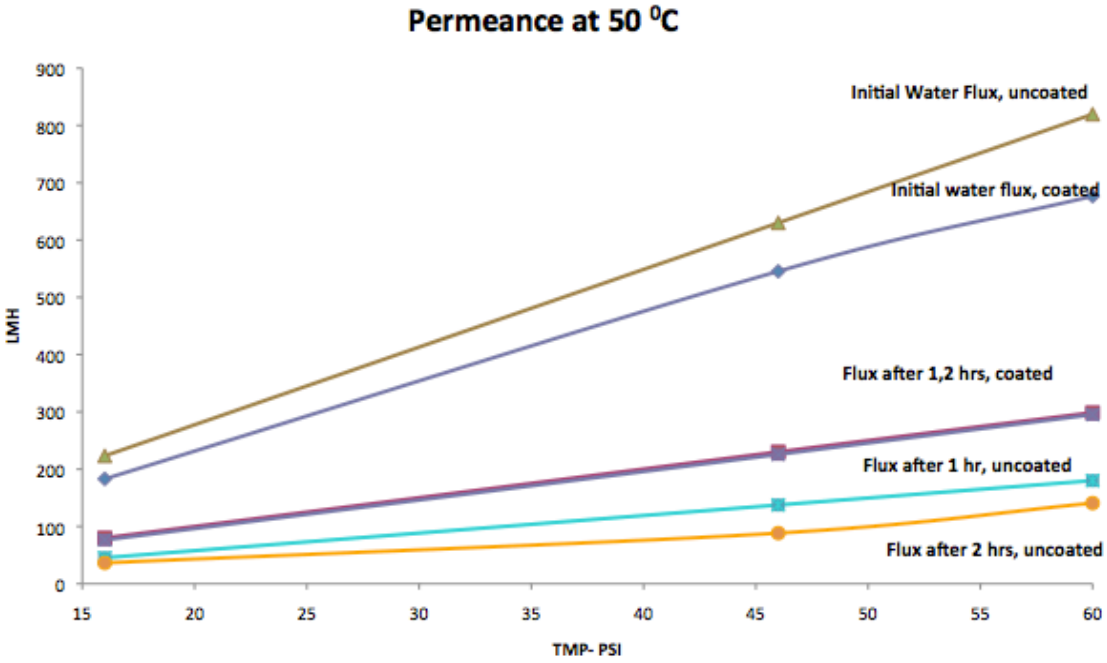

Figure 4.17 The membrane performance at 50 °C.

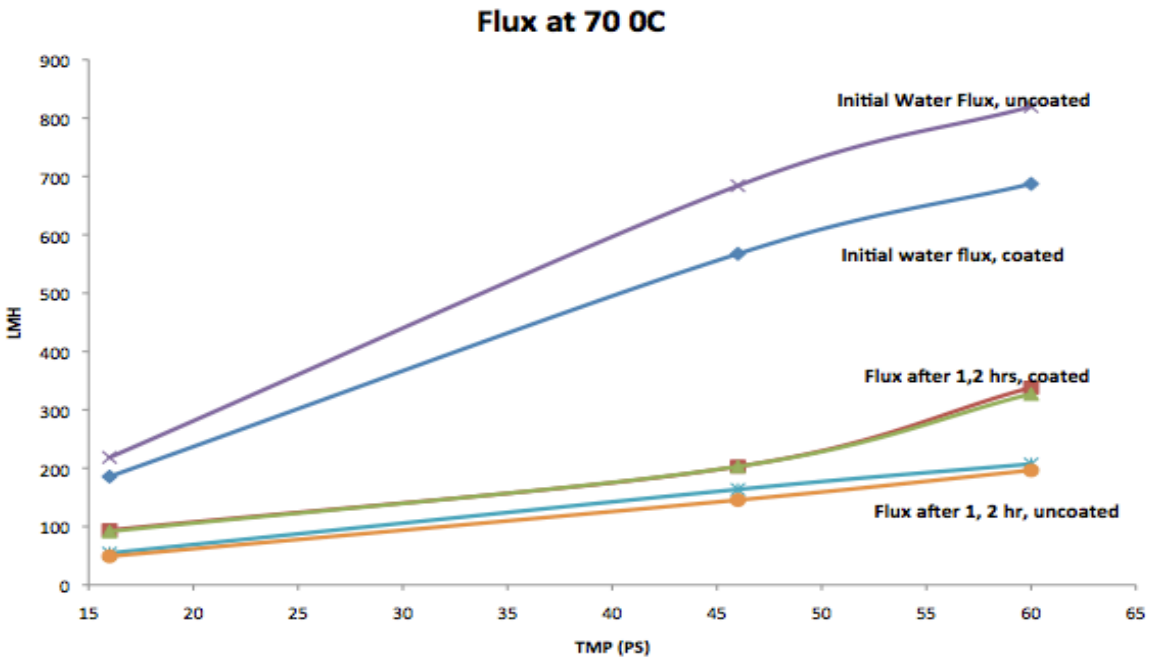

Figure 4.18 The membrane performance at 70 °C.

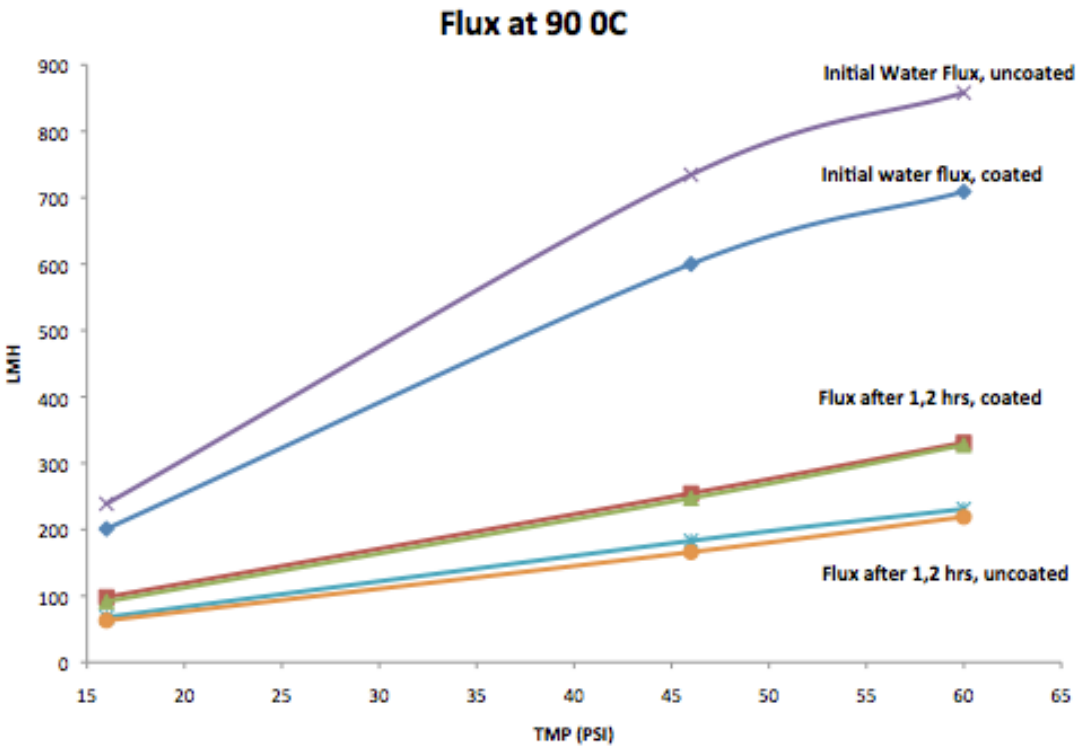

Figure 4.19 The membrane performance at 90 °C.

There is also a significant improvement in the recovery of the membrane conditions after cleaning. After using the membrane in the lignin separation for several hours, the membranes were cleaned using water at 70 ^{0}C. The water flux of the coated membrane was recovered to about 80% of the initial conditions after repeating the cleaning protocol twice as shown in figure 4.18. This can be attributed to the polymer coating on the surface of the membrane, which does not allow a chemical interaction/attachment of the lignin on the surface of the membrane and therefore making it easy for the foulant to be removed. The fouling tendency on the coated membrane is also significantly reduced and therefore less foulant is attached on the surface of the membrane compared to the same conditions on the uncoated membrane.

From figure 4.17, 18, and 19 above, it is observed that increasing the temperatures generally results in an increase in the permeate flux and hence an improved separation. Increasing the temperature will cause the permeate viscosity to be lowered, which is important in improving the flow rate. It will also cause an increase in the diffusivity, enhancing the dispersion of polarized layer. Fouling on the coated membrane surface has been reduced due to lessened concentration polymerization and increased diffusivity. The coating also may have caused a reduction in the membrane internal fouling.

The effectiveness of increased transmembrane pressure (TMP) is evident from the three figures above, which shows that increasing the TMP in the low-pressure range, initially results in an increase in the permeate flux, but also an increase in the fouling rate. It is also observed that the initial membrane retention decreases as the TMP is increased, probably due to increased concentration polymerization. The coating on the membrane surfaces has lowered this effect compared to the uncoated membrane.

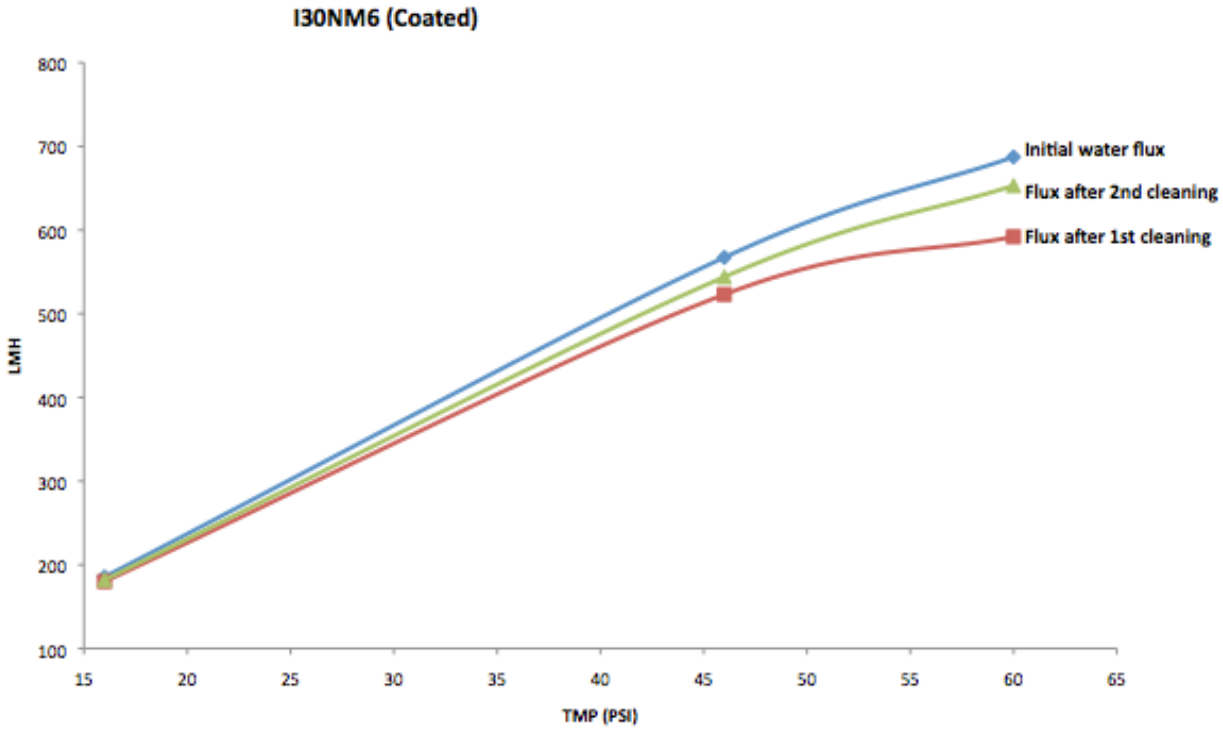

Figure 4.20 Water flux recovery in the coated membrane after cleaning it with water at 70 °C.

The uncoated membrane, however, shows a very minimal recovery of the original water flux as shown in figure 4.21. This results shows that the coating of the membrane does not only show improved performance in separation, but also in reducing the cleaning steps and process.

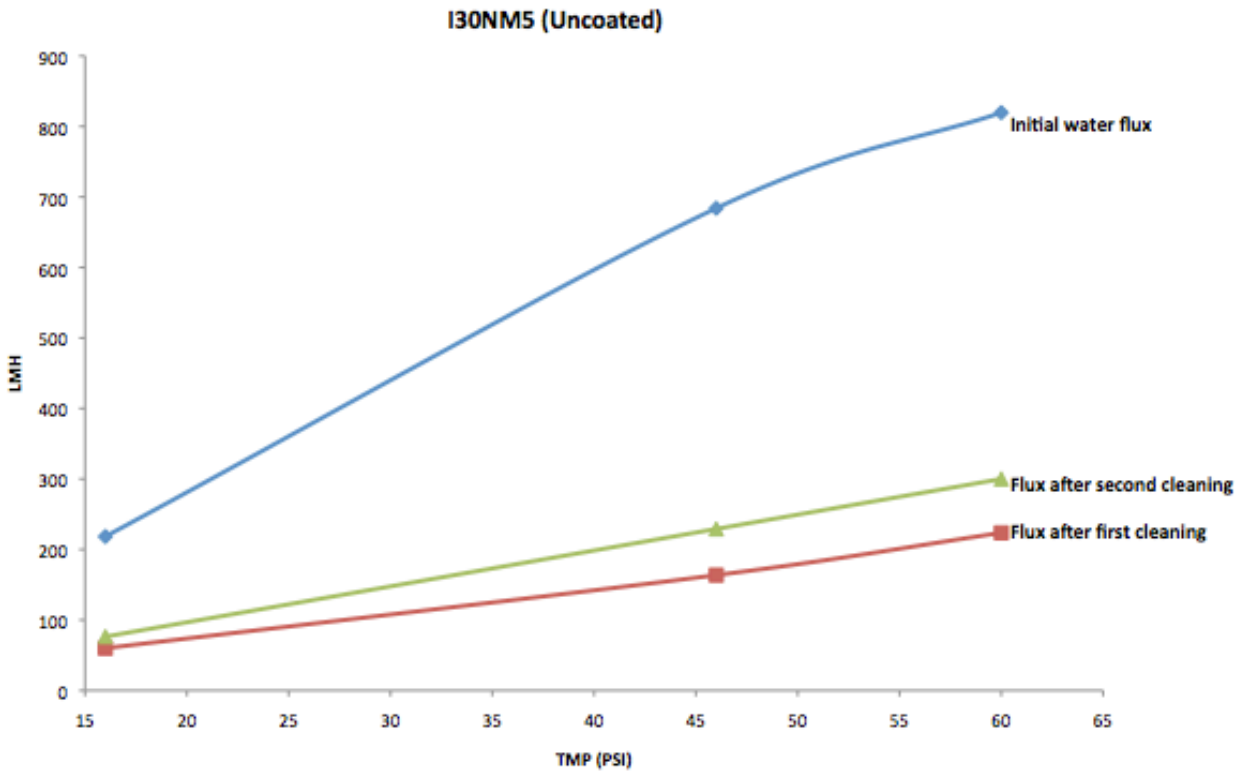

Figure 4.21 Water flux recovery in the uncoated membrane after cleaning it with water at 70 °C.

The effect of the lignin feed concentration on the permeate flux for the coated and the uncoated membrane modules is described in figure 4.22 below. It is observed that the permeate flux, and therefore the rejection, decreases with the increases in feed concentration. As the feed concentration increases, the membrane surface concentration increases, resulting in an increase in the osmotic pressure of the lignin close to the membrane, causing a reduction in the net driving force of the flux.

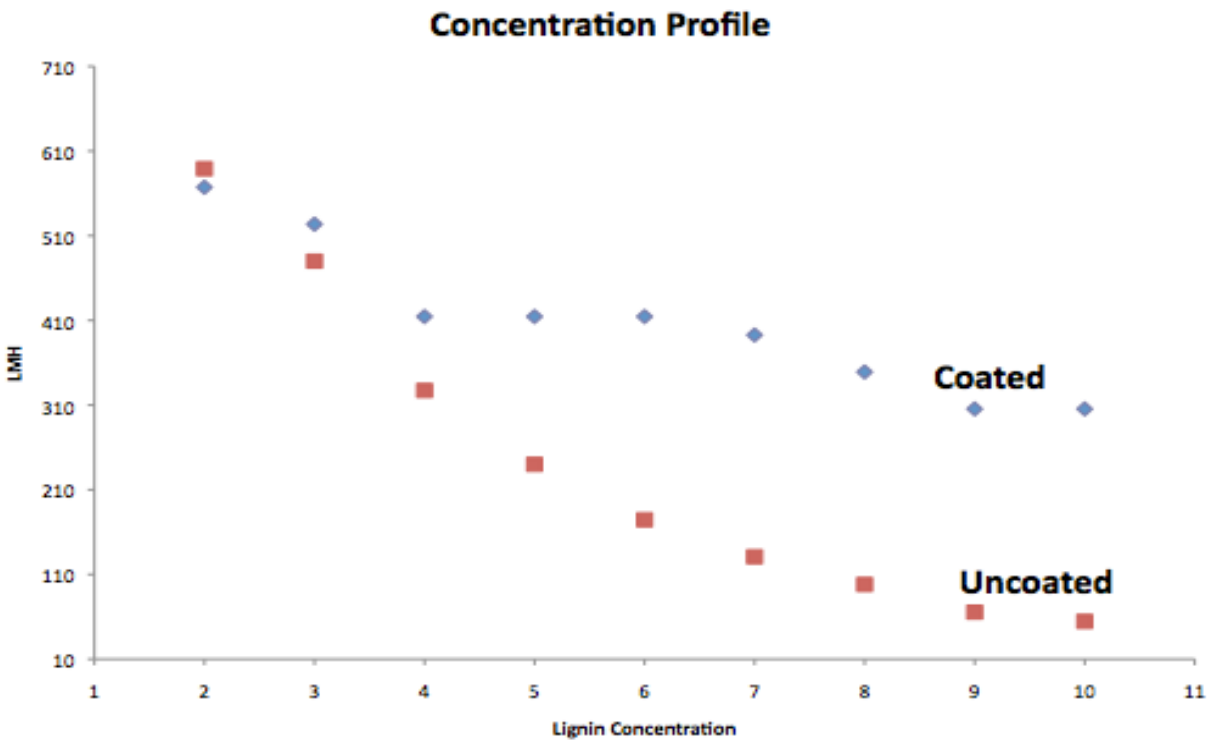

Fig 4.22 Variations of permeate flux with lignin concentration at 70 °C and TMP of 60 PSI.

It is evident from the graph that the coated membrane performs better at different concentration levels of the lignin feed and the separation property of the coated membrane is better as compared to the uncoated membranes. At lower concentration up to 4%, both membranes show a similar decrease in flux but as the concentration continues to increase, the coated membranes permeates almost in a constant manner until the maximum concentration of 10% is achieved. The uncoated membrane, however, shows a continuous decrease in the permeate flux as the concentration continues to increase. The initial decline in permeate flux in both the coated and the uncoated membranes can be associated mainly to the build up of osmotic pressure of the solution whereas the gradual decline may be considered as a combined effect of build up of deposited layers on the membrane surface and deposition of solute particles in the membrane pores. These combined effects reduce the permeation of solvent. Finally, the permeate flux attains a steady state value, which is limited by the external hydrodynamic conditions like cross flow velocity. In the coated membranes, it can be concluded that the coating on the surface of the membrane prevents the build up of the deposited layer on the surface of the membrane thus preventing the gradual decline in the permeation as seen in the graph above [105].

4.5 Data Reproducibility

In order to confirm the reproducibility of the coated membrane performance, another coated membrane I30NM3 of similar pore characteristics as the I30NM6 was coated with the high performance polyetherimide Ultem 1010 solution of 0.25% by weight of the polymer. The pore size in the I30NM3 was also slightly reduced after the coating and it was measured to have a pore size of 138nm. The membrane was used to separate the lignin as in the previous experiment and only a few data points were selected. The lignin separation was doe at temperatures of 70 ^{0}C. Figure 4.23 summarizes the performance of the membrane at different TMP pressure as was done in the previous experiments where the membrane I30NM6 was done.

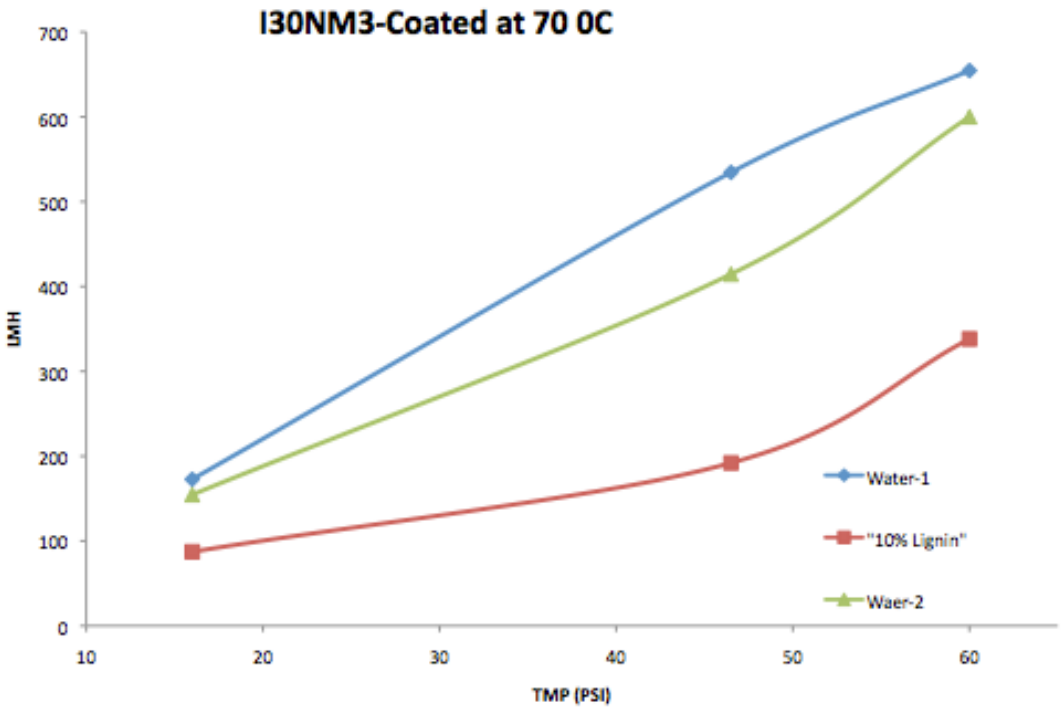

Figure 4.23 Performance of coated membrane I30NM3 for data reproducibility.

It is observed above that the membrane performance is very similar to that of the coated membrane I30NM6, except that the permeation is slightly reduced because the pore size of the I30NM6 membrane is 145nm and that of the I30NM3 is 130nm. All the other data points are similar in trend for both the coated membranes. After the membrane was used in the lignin separation for an extended period of time, it was cleaned with water at 70 °C, and then the water flux was measured. The results show that the water flux measured after the cleaning compares to the clean-coated-unused membrane in both I30NM6 and I30NM3. This confirms that when any of the inorganic membrane is coated with the high performance PEI, the overall membrane separation characteristics are improved.

The membrane I30NM3 was also used to separate the lignin for 9 hours to determine its performance over extended period of continuous operation at 3GPM and at 70 °C. The result in figure 4.24 show a similar pattern as in the I30NM6 membrane where there is a 5 percent reduction in flux in the first 2 hours and thereafter the flux continues to remain almost constant throughout the experiment. Compared to the uncoated membrane where the flux continues to drop as time progresses, this coated membrane displays a different characteristic, showing that overall; there are improved benefits in coating the membrane.

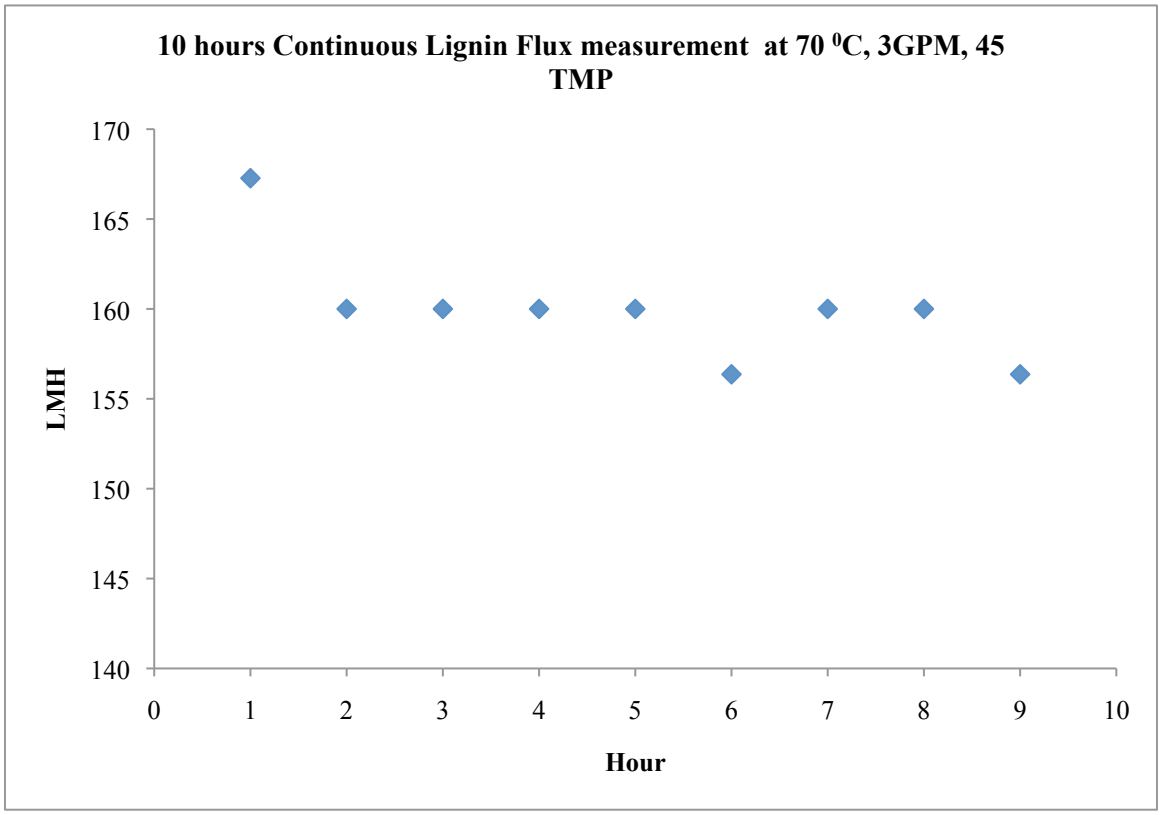

Figure 4.24 Performance of coated membrane I30NM3 for data reproducibility: 10 hours continuous lignin separation

The effect of the feed temperature on the membrane performance was also investigated by measuring the change in flux as the temperature increases. The feed temperature was varied between room temperature and 90 °C, which is below the boiling point of water and that of the lignin solution. The graph 4.25 below shows that the increase in temperatures has a slight effect on the flux in the uncoated membrane. Between 50 and 70 °C, the flux increases a little, but as the temperatures increases to 90 °C, the flux declines a little. Although it is expected that the flux would increase due to a decrease in viscosity of the lignin solution as the temperature increases, however, the flux has reduced here because of other factors such as pore blocking as it takes a longer time to increase the lignin temperatures while circulating it in the system. However, this decline in flux as the temperature increases is observed in the uncoated membrane. In the coated membrane, there is a small overall increase in the flux as the temperature increases, which can be directly associated with the increase in the lignin viscosity. This is due to an increase in the vapor pressure of the feed solution, (which increases with an increase in the temperature) resulting in an increase in the transmembrane pressure.

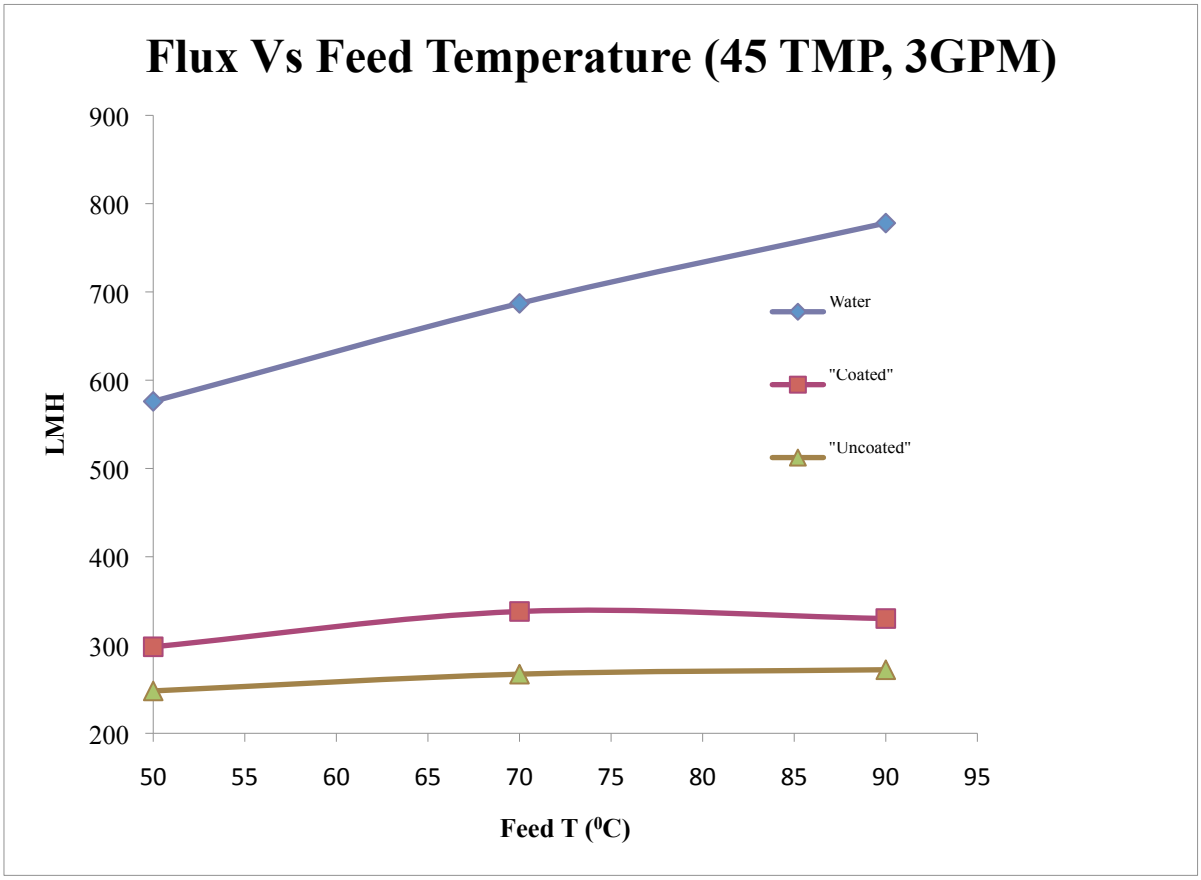

Figure 4.25 Change in flux with solution temperatures.

The water flux has increased with increase in temperature as expected. Although the viscosity of water as described by Poiseulle's law is supposed to reduce by a factor of almost half when the temperature increases from 50-90 °C as shown in table 4.3, the flux is theoretically expected to increase by a factor of 2 according to the Poiseulle's equation below. From the experimental results above, the water flux has increased from about 600 LMH to about 800 LMH an observation that is in line with the theoretical expectations.

$$Q = \pi R^4 \Delta P / (8\eta L)$$

Where Q = the volumetric flow rate, R and L are the tube radius and length, ΔP = the pressure drop in the direction of low, and η = the fluid viscosity.

Table 4.4 Viscosity of water at different temperatures [106].

Temperature t °C	Viscosity μ(μPa s)	Temperature t °C	Viscosity μ(μPa s)
−8	2421. 0	75	378. 5
−5	2144. 0	80	355. 1
0	1791. 5	85	334. 1
5	1519. 3	90	315. 0
10	1307. 0	95	297. 8
15	1138. 3	100	282. 1
20	1002. 0	105	267. 8
25	890. 2	110	254. 4
30	797. 3	115	242. 3
35	719. 1	120	231. 3
40	652. 7	125	221. 3
45	596. 1	130	212. 0
50	547. 1	135	203. 4
55	504. 4	140	195. 5
60	467. 0	145	188. 2
65	433. 9	150	181. 4
70	404. 6		

Chapter Five

Conclusion

5.0 Summary

In the last decade membrane as a separation tool for different application has become an attractive option including in production of drinking water of good quality, bio-oil separation and other functions at very economical costs. Although membranes are already used for some of these applications, many improvements in the design and operation of installations are possible that could increase the lifetime of the membrane and the overall performance over increased period of time so that the cost of using membranes as a separation tool becomes accessible for day-to-day application.

The focus for this research was to apply monolayer coating of high temperature stable, chemically and mechanically robust polyetherimide (Ultem) on nanoporous membranes using a solution-based coating method and to understand the effect of various process variables on the structure and properties of the coating. We have successfully demonstrated that among the different grades of the Ultem polymer that may be used to coat the membrane (i.e. Ultem 1010, 1285, and 1040A), Ultem 1010 was determined to be the best in forming an ultrathin coating. The ease in processing Ultem into a solution and then coating of inorganic membranes with ultrathin layers was verified by FTIR and SEM, which showed that a nanolayer coating was deposited on the surface of the membrane. The characterization showed that thin coating of Ultem 1010 on the membrane was uniformly deposited using a simplified dip coating method. It was also demonstrated that the coatings are very robust, durable and are able to withstand the chemical, and thermal exposures for prolonged periods. The coated membrane was successfully used in lignin separation and showed a 30% improvement in the flux characteristics compared to the uncoated membrane.

After coating the membrane with the polymer solution of varying weight percentage (5%, 2%, 1%, 0.5%, and 0.25%) of Ultem 1010, it was determined experimentally that 0.25% polymer solution by weight of the polymer resulted in the

thinnest uniform coating on the membrane that did not significantly reduce the original pore size while still giving the benefit of improved membrane performance in separation of lignin at high temperatures.

The benefit of the coating on the membrane was studied extensively in different membrane modules for a wide range of operating conditions including different transmembrane pressure, temperature and extended periods, and an overall improved membrane performance was recorded compared to the uncoated membrane.

Although there is a slight reduction in the permeate flux during the filtration of a 10% lignin solution; the overall performance of the coated membrane is significantly improved in that compared to the uncoated membrane which shows a continuous reduction in flux when the membrane is continuously in use. This has been possible because of the ultrathin layer coating of this high temperature polymer on the membrane surface. The coated membrane shows a great reduction in the fouling tendency, as the chemicals are not able to adhere to the membrane surface. Another benefit was in the overall recovery of the membrane performance when cleaned after being in use for extended period of time. As Ultem is engineering plastic with very little attraction to fouling components, the tendency for deposition of fouling materials on the membrane surface is eliminated. Cleaning the membrane with water showed that the coated membrane flux performance was recovered up to 95% of the original flux compared to the uncoated membrane where the flux was recovered by about 10%. This eliminates the continuous use of chemical based cleaning solutions that are normally associated with membrane deterioration and which also result in contamination of products being separated. When chemical cleaning solutions are used to clean the membranes, the membrane and the membrane support are subjected to chemical attack. The Ultem coating eliminates this in two ways: by eliminating use of chemicals as a cleaning protocol because it allows water to be used for cleaning the membranes, and also in the case where chemical solutions have to be used, the Ultem coating which has been proved to be resistant to chemical attack cushions the membrane from these chemical attacks.

Although the fouling process is a complex mechanism where the physico-chemical properties of the membrane, the type of the membrane, the quality of the feed

solution, the type of solute molecules, and the operating conditions play a role and it is difficult to point at a specific effect that contributes to fouling, we have shown that there is an improved benefit in coating the membrane with the high temperature performing polymer which has resulted in reduced fouling.

5.1 Limitations

Although there is an overall improvement in the performance of the membrane after coating, the optimization of the membrane coating and cleaning protocol requires an in depth understanding of the complex physical and chemical interaction of the specific foulant and the membrane. A detailed economic analysis of the impact of the improvement in the cleaning protocol and the increase in the membrane lifetime and efficiency should be carried out in the industrial scale for both the coated and the uncoated membranes in order to determine the overall benefit of the coating process. This study was limited by the inability to access industrial scale settings and models.

Chapter Six

Recommendations for Future Research

The idea of coating a surface or pore is a novel technology and its application is not just limited to protecting the surface of the membranes. The use of polymer coating as a controlled means of reducing the pores size needs to be investigated and researched. Since the preliminary investigations have revealed that the coating thickness can be controlled, it is also possible to apply this technique to establish a process that can be used in reducing the pore size of other filtration media to desired output characteristics by manipulating the polymer solution characteristics and the coating method. Apart from membranes, nanosize fabrics, that are also becoming popular in separation applications, can be coated with the polymer solution in order to enhance their performance characteristics. This should be explored.

Different grades of the Ultem obtained from Sabic were analyzed and their chemical, thermal, and mechanical stability combined with the ease in processing it into solution makes it potentially useful in making nonwoven membranes for different application. The chemical resistant characteristics in particular will be very applicable in fabricating a membrane for applications where high chemical resistant characteristics are desired.

The force of coating removal needs to be determined. The friction that the membrane can be subjected to due to the pressure, and also due to the corrosion from the chemical exposure has to be understood in order to optimize the coating conditions. It is therefore essential that the force of removing the polymer be carefully studied so as to make sure that the monolayer coating can withstand the chemical and mechanical forces. Since the ULTEM coating on the surface of the membrane is very thin, it is almost impossible to quantify the force of removal using conventional means. The AFM probing tip may be used to abrade the surface of the polymer coating while also simultaneously imaging the area where the polymer may be progressively damaged by the scanning tip. This technique will allow the observation of the following wear properties qualitatively, and when possible, quantitatively:

- Formation of ripples on the surface of the polymer,
- Qualitative evolution of the surface before and after the test
- Evaluate wear volume, and
- Study the adhesion effect and subsequent degradation of probe tip.

The chemical force of removal should also be studied by subjecting the coated and cured membrane to different levels of acidic environments and solvents to evaluate if the cured ULTEM coating can be removed. The research should also focus on establishing the effect of partial removal of the coating and model how the coating of the membrane will prolong its lifetime and the overall benefit that will be achieved by the coating.

In this work, the lowest Ultem concentration that was investigated was 0.25% of the polymer weight. A further lower concentration should also be investigated in order to establish the performance of a lower concentration. This can allow the coating of membranes with smaller pores for gaseous separation application. The smaller coating can also be used effectively to reduce nanosize pores membranes for specific gas or acid separation Transmission Electron Microscopy (TEM) can be used to analyze the smaller coatings on the surfaces.

REFERENCES

1. Porter, M.C., *Handbook of industrial membrane technology*. 1990, Park Ridge, N.J., U.S.A.: Noyes Publications. xx, 604 p.
2. Johnson, J. and M. Busch, *Engineering aspects of reverse osmosis module design.* Desalination and Water Treatment, 2010. **15**(1-3): p. 236-248.
3. Mulder, M., *THE USE OF MEMBRANE PROCESSES IN ENVIRONMENTAL-PROBLEMS - AN INTRODUCTION*, in *Membrane Processes in Separation and Purification*, J.G. Crespo and K.W. Boddeker, Editors. 1994. p. 229-262.
4. Cartwright, P.S., *Membrane separation technologies - Practical applications*. Providing Safe Drinking Water in Small Systems: Technology, Operations, and Economics, ed. J.A. Cotruvo, G.F. Craun, and N. Hearne. 1999. 233-239.
5. Asatekin, A. and A.M. Mayes, *Oil industry wastewater treatment with fouling resistant membranes containing amphiphilic comb copolymers.* Environ Sci Technol, 2009. **43**(12): p. 4487-92.
6. Ju, H., et al., *Crosslinked poly(ethylene oxide) fouling resistant coating materials for oil/water separation.* Journal of Membrane Science, 2008. **307**(2): p. 260-267.
7. Huang, H.J., et al., *A review of separation technologies in current and future biorefineries.* Separation and Purification Technology, 2008. **62**(1): p. 1-21.
8. Bacchin, P., P. Aimar, and R.W. Field, *Critical and sustainable fluxes: Theory, experiments and applications.* Journal of Membrane Science, 2006. **281**(1-2): p. 42-69.
9. Scott, K. and R. Hughes, *Industrial membrane separation technology*. 1996, London: Blackie Academic & Professional. xiii, 305 p.
10. Baker, R.W. and Wiley InterScience (Online service), *Membrane technology and applications*. 2012, Wiley-Blackwell,: Oxford. p. 1 online resource (xiv, 575 p.).
11. Vaccari, D.A., *Membrane technology and environmental applications.* Choice: Current Reviews for Academic Libraries, 2013. **50**(5): p. 909-909.
12. Choi, S., et al., *SAO network analysis of patents for technology trends identification: a case study of polymer electrolyte membrane technology in proton exchange membrane fuel cells.* Scientometrics, 2011. **88**(3): p. 863-883.

13. Bhave, R.R., *Inorganic membranes synthesis, characteristics, and applications*. 1991, New York: Van Nostrand Reinhold. xx, 312 p.
14. Lira, H.D.L. and R. Paterson, *New and modified anodic alumina membranes - Part III. Preparation and characterisation by gas diffusion of 5 nm pore size anodic alumina membranes.* Journal of Membrane Science, 2002. **206**(1-2): p. 375-387.
15. Bowen, W.R. and Q. Gan, *Properties of Microfiltration Membranes - the Effects of Adsorption and Shear on the Recovery of an Enzyme.* Biotechnology and Bioengineering, 1992. **40**(4): p. 491-497.
16. Yu, Q., Y.Y. Mao, and X.S. Peng, *Separation Membranes Constructed from Inorganic Nanofibers by Filtration Technique.* Chemical Record, 2013. **13**(1): p. 14-27.
17. Pickering, P.J. and C.R. Southern, *Clean-up to chirality - Liquid membranes as a facilitating technology?* Journal of Chemical Technology and Biotechnology, 1997. **68**(4): p. 417-424.
18. Adamson, A.W., *The physical chemistry of surfaces.* Abstracts of Papers of the American Chemical Society, 2001. **221**: p. U320-U320.
19. Nystrom, M., M. Lindstrom, and E. Matthiasson, *Streaming Potential as a Tool in the Characterization of Ultrafiltration Membranes.* Colloids and Surfaces, 1989. **36**(3): p. 297-312.
20. Leenaars, A.F.M. and A.J. Burggraaf, *The Preparation and Characterization of Alumina Membranes with Ultrafine Pores .2. The Formation of Supported Membranes.* Journal of Colloid and Interface Science, 1985. **105**(1): p. 27-40.
21. Thomas, D.G. and J.J. Lander, *Hydrogen as a Donor in Zinc Oxide.* Journal of Chemical Physics, 1956. **25**(6): p. 1136-1142.
22. Hamilton, H., *Palladium-Based Membranes for Hydrogen Separation.* Platinum Metals Review, 2012. **56**(2): p. 117-121.
23. Kainourgiakis, M.E., et al., *Transport properties of reconstructed alumina and Vycor membranes*, in *Membranes-Preparation, Properties and Applications*, V.N. Burganos, et al., Editors. 2003. p. 155-160.

24. Ahn, C.H., et al., *Carbon nanotube-based membranes: Fabrication and application to desalination.* Journal of Industrial and Engineering Chemistry, 2012. **18**(5): p. 1551-1559.
25. Hilder, T.A., D. Gordon, and S.H. Chung, *Synthetic cation-selective nanotube: Permeant cations chaperoned by anions.* Journal of Chemical Physics, 2011. **134**(4).
26. Kofstad, P., *Nonstoichiometry, diffusion, and electrical conductivity in binary metal oxides*. Wiley series on the science and technology of materials. 1972, New York,: Wiley-Interscience. xi, 382 p.
27. Burggraaf, A.J. and L. Cot, *Fundamentals of inorganic membrane science and technology*. Membrane science and technology series. 1996, Amsterdam ; New York: Elsevier. xviii, 690 p.
28. Clever, M., et al., *Process water production from river water by ultrafiltration and reverse osmosis.* Desalination, 2000. **131**(1-3): p. 325-336.
29. Nystrom, M., L. Kaipia, and S. Luque, *FOULING AND RETENTION OF NANOFILTRATION MEMBRANES.* Journal of Membrane Science, 1995. **98**(3): p. 249-262.
30. Strathmann, H., *Introduction to membrane science and technology*. 2011, Weinheim, Germany: Wiley-VCH Verlag & Co. xxiii, 473 p.
31. Zhong, Z.X., et al., *Crossflow filtration of nanosized catalysts suspension using ceramic membranes.* Separation and Purification Technology, 2011. **76**(3): p. 223-230.
32. Bolduan, P. and M. Latz, *Ceramic membranes and their application in food ard beverage processing.* Filtration & Separation, 2000. **37**(3): p. 36-38.
33. Schaefer, A.I., A.G. Fane, and T.D. Waite, *Nanofiltration : principles and applications*. 2003, New York: Elsevier Advanced Technology.
34. Sen Gupta, B. and M.A. Hashim, *Numerical simulation of separation factor of NaCl in surface force pore flow model.* Chemical Engineering & Technology, 2006. **29**(9): p. 1061-1065.

35. KastelanKunst, L., et al., *Preparation and porosity of cellulose triacetate reverse osmosis membranes.* Journal of Membrane Science, 1996. **109**(2): p. 223-230.
36. Wu, Q.L. and B.M. Wu, *STUDY OF MEMBRANE MORPHOLOGY BY IMAGE-ANALYSIS OF ELECTRON-MICROGRAPHS.* Journal of Membrane Science, 1995. **105**(1-2): p. 113-120.
37. Sheldon, J.M., *THE FINE-STRUCTURE OF ULTRAFILTRATION MEMBRANES .1. CLEAN MEMBRANES.* Journal of Membrane Science, 1991. **62**(1): p. 75-86.
38. Yin, X.L., et al., *Morphology and properties of hollow-fiber membrane made by PAN mixing with small amount of PVDF.* Journal of Membrane Science, 1998. **146**(2): p. 179-184.
39. Combe, C., et al., *The effect of CA membrane properties on adsorptive fouling by humic acid.* Journal of Membrane Science, 1999. **154**(1): p. 73-87.
40. Koros, W.J., Y.H. Ma, and T. Shimidzu, *Terminology for membranes and membrane processes.* Pure and Applied Chemistry, 1996. **68**(7): p. 1479-1489.
41. Van der Bruggen, B., L. Braeken, and C. Vandecasteele, *Flux decline in nanofiltration due to adsorption of organic compounds.* Separation and Purification Technology, 2002. **29**(1): p. 23-31.
42. Gwon, E.M., et al., *Fouling characteristics of NF and RO operated for removal of dissolved matter from groundwater.* Water Research, 2003. **37**(12): p. 2989-2997.
43. Kim, K.J., V. Chen, and A.G. Fane, *Characterization of Clean and Fouled Membranes Using Metal Colloids.* Journal of Membrane Science, 1994. **88**(1): p. 93-101.
44. Rabiller-Baudry, M., et al., *Characterisation of cleaned and fouled membrane by ATR-FTIR and EDX analysis coupled with SEM: application to UF of skimmed milk with a PES membrane.* Desalination, 2002. **146**(1-3): p. 123-128.
45. Plakas, K.V., et al., *A study of selected herbicides retention by nanofiltration membranes - The role of organic fouling.* Journal of Membrane Science, 2006. **284**(1-2): p. 291-300.
46. Manttari, M., et al., *Fouling effects of polysaccharides and humic acid in nanofiltration.* Journal of Membrane Science, 2000. **165**(1): p. 1-17.

47. Sherwood, T.K., et al., *Salt Concentration at Phase Boundaries in Desalination by Reverse Osmosis.* Industrial & Engineering Chemistry Fundamentals, 1965. **4**(2): p. 113-&.

48. Sablani, S.S., et al., *Concentration polarization in ultrafiltration and reverse osmosis: a critical review.* Desalination, 2001. **141**(3): p. 269-289.

49. Koyuncu, I. and D. Topacik, *Effect of organic ion on the separation of salts by nanofiltration membranes.* Journal of Membrane Science, 2002. **195**(2): p. 247-263.

50. Bacchin, P. and P. Aimar, *Critical fouling conditions induced by colloidal surface interaction: from causes to consequences.* Desalination, 2005. **175**(1): p. 21-27.

51. Contreras, A.E., A. Kim, and Q.L. Li, *Combined fouling of nanofiltration membranes: Mechanisms and effect of organic matter.* Journal of Membrane Science, 2009. **327**(1-2): p. 87-95.

52. Nghiem, L.D. and A.I. Schafer, *Adsorption and transport of trace contaminant estrone in NF/RO membranes.* Environmental Engineering Science, 2002. **19**(6): p. 441-451.

53. Belfort, G., R.H. Davis, and A.L. Zydney, *The Behavior of Suspensions and Macromolecular Solutions in Cross-Flow Microfiltration.* Journal of Membrane Science, 1994. **96**(1-2): p. 1-58.

54. Chang, Y.J. and M.M. Benjamin, *Modeling formation of natural organic matter fouling layers on ultrafiltration membranes.* Journal of Environmental Engineering-Asce, 2003. **129**(1): p. 25-32.

55. Field, R.W., et al., *Critical Flux Concept for Microfiltration Fouling.* Journal of Membrane Science, 1995. **100**(3): p. 259-272.

56. Kochkodan V, e.a., *Polymeric membranes: Surface modification for minimizing (bio)colloidal fouling.* Advances in Colloid and Interface Science, 2013.

57. Aimar, P., *Some Kinetics Aspects in the Concept of Critical Flux, Fouling and Critical Flux.* 2004.

58. Jefferson, B., et al., *Methods for understanding organic fouling in MBRs.* Water Science and Technology, 2004. **49**(2): p. 237-244.

59. Meiereles, M., P. Aimar, and V. Sanchez, *MEMBRANE TECHNOLOGY - MICROFILTRATION AND ULTRAFILTRATION.* Biofutur, 1992(111): p. S1-&.
60. Roudman, A.R. and F.A. DiGiano, *Surface energy of experimental and commercial nanofiltration membranes: Effects of wetting and natural organic matter fouling.* Journal of Membrane Science, 2000. **175**(1): p. 61-73.
61. Tiller, C.L. and C.R. Omelia, *Natural Organic-Matter and Colloidal Stability - Models and Measurements.* Colloids and Surfaces a-Physicochemical and Engineering Aspects, 1993. **73**: p. 89-102.
62. Beckett, R. and N.P. Le, *The Role of Organic-Matter and Ionic Composition in Determining the Surface-Charge of Suspended Particles in Natural-Waters.* Colloids and Surfaces, 1990. **44**: p. 35-49.
63. Shahalam, A.M., A. Al-Harthy, and A. Al-Zawhry, *Feed water pretreatment in RO systems: unit processes in the Middle East.* Desalination, 2002. **150**(3): p. 235-245.
64. Maartens, A., E.P. Jacobs, and P. Swart, *UF of pulp and paper effluent: membrane fouling-prevention and cleaning.* Journal of Membrane Science, 2002. **209**(1): p. 81-92.
65. Razavi, S.K.S., J.L. Harris, and F. Sherkat, *Fouling and cleaning of membranes in the ultrafiltration of the aqueous extract of soy flour.* Journal of Membrane Science, 1996. **114**(1): p. 93-104.
66. Kilduff, J.E., et al., *Photochemical modification of poly(ether sulfone) and sulfonated poly(sulfone) nanofiltration membranes for control of fouling by natural organic matter.* Desalination, 2000. **132**(1-3): p. 133-142.
67. Chen, J.P., S.L. Kim, and Y. Ting, *Optimization of membrane physical and chemical cleaning by a statistically designed approach.* Journal of Membrane Science, 2003. **219**(1-2): p. 27-45.
68. Lindau, J. and A.S. Jonsson, *Adsorptive fouling of modified and unmodified commercial polymeric ultrafiltration membranes.* Journal of Membrane Science, 1999. **160**(1): p. 65-76.
69. Tragardh, G., *Membrane Cleaning.* Desalination, 1989. **71**(3): p. 325-335.

70. Lee, Y.G., et al., *Application of hybrid systems techniques for cleaning and replacement of a RO membrane.* Desalination, 2009. **247**(1-3): p. 25-32.
71. Merlo, C.A., W.W. Rose, and N.L. Ewing, *A Membrane Filtration Handbook Selection Guide - a Guide for Food Processors.* Abstracts of Papers of the American Chemical Society, 1994. **207**: p. 36-AGFD.
72. Ren, D.Q., *Cleaning and Regeneration of Membranes.* Desalination, 1987. **62**: p. 363-371.
73. Kosutic, K. and B. Kunst, *RO and NF membrane fouling and cleaning and pore size distribution variations.* Desalination, 2002. **150**(2): p. 113-120.
74. Weis, A., M.R. Bird, and M. Nystrom, *The chemical cleaning of polymeric UF membranes fouled with spent sulphite liquor over multiple operational cycles.* Journal of Membrane Science, 2003. **216**(1-2): p. 67-79.
75. Liikanen, R., J. Yli-Kuivila, and R. Laukkanen, *Efficiency of various chemical cleanings for nanofiltration membrane fouled by conventionally-treated surface water.* Journal of Membrane Science, 2002. **195**(2): p. 265-276.
76. Wilson, I. and T. Hasting, *Special issue - Fouling, cleaning and disinfection in food processing 2006.* Food and Bioproducts Processing, 2006. **84**(C4): p. 251-252.
77. Zhu, H.H. and M. Nystrom, *Cleaning results characterized by flux, streaming potential and FTIR measurements.* Colloids and Surfaces a-Physicochemical and Engineering Aspects, 1998. **138**(2-3): p. 309-321.
78. Cakl, J., et al., *Effects of backflushing conditions on permeate flux in membrane crossflow microfiltration of oil emulsion.* Desalination, 2000. **127**(2): p. 189-198.
79. Kumar, S.M., G.M. Madhu, and S. Roy, *Fouling behaviour, regeneration options and on-line control of biomass-based power plant effluents using microporous ceramic membranes.* Separation and Purification Technology, 2007. **57**(1): p. 25-36.
80. Singh, R., *Design of Dual-Purpose Membrane Desalination Systems.* Environmental Progress & Sustainable Energy, 2010. **29**(3): p. 349-357.

81. Li, S.G., et al., *High-pressure CO2/CH4 separation using SAPO-34 membranes.* Industrial & Engineering Chemistry Research, 2005. **44**(9): p. 3220-3228.
82. Fane, A.G., R. Wang, and Y. Jia, *Membrane Technology: Past, Present and Future*. Membrane and Desalination Technologies, ed. L.K. Wang, et al. Vol. 13. 2011. 1-45.
83. Cuny, J.-P.R.A., *Diffusion measurements using a Knudsen cell*. 1965. p. 38, 14 leaves.
84. Shiojiri, K., et al., *Separation of condensable greenhouse gases by surface diffusion and transport of capillary condensate through porous glass membranes.* Abstracts of Papers of the American Chemical Society, 2005. **229**: p. U831-U831.
85. Shiojiri, K., et al., *Separation of F-gases (HFC-134a and SF6) from gaseous mixtures with nitrogen by surface diffusion through a porous Vycor glass membrane.* Journal of Membrane Science, 2006. **282**(1-2): p. 442-449.
86. Einav, R., K. Harussi, and D. Perry, *The footprint of the desalination processes on the environment.* Desalination, 2003. **152**(1-3): p. 141-154.
87. Kumar, P., et al., *Methods for Pretreatment of Lignocellulosic Biomass for Efficient Hydrolysis and Biofuel Production.* Industrial & Engineering Chemistry Research, 2009. **48**(8): p. 3713-3729.
88. Budd, P.M., et al., *Gas separation membranes from polymers of intrinsic microporosity.* Journal of Membrane Science, 2005. **251**(1-2): p. 263-269.
89. Aerojet-General Corporation. and United States. Office of Saline Water. Division of Processes Development., *Design and construction of a desalination pilot plant, a reverse osmosis process*. United States Office of Saline Water Research and development progress report,. 1964, Washington, D.C.: Office of Saline Water. iv, 15, A-6, B-17 p.
90. Melin, T. and R. Rautenbach, *10 Ultra Filtration and Micro Filtration*. Membranverfahren: Grundlagen Der Modul- Und Anlagenauslegung, 3 Aktualisierte Und Erweiterte Auflage Ed. 2007. 309-368.

91. Wang, C.H., et al., *The performance of immobilized membrane bioreactor with different membrane operation modes.* Desalination and Water Treatment, 2013. **51**(13-15): p. 3090-3096.
92. Hsieh, H.P., R.R. Bhave, and H.L. Fleming, *MICROPOROUS ALUMINA MEMBRANES.* Journal of Membrane Science, 1988. **39**(3): p. 221-241.
93. Amy, G., *Fundamental understanding of organic matter fouling of membranes.* Desalination, 2008. **231**(1-3): p. 44-51.
94. Yebra, D.M., S. Kiil, and K. Dam-Johansen, *Antifouling technology - past, present and future steps towards efficient and environmentally friendly antifouling coatings.* Progress in Organic Coatings, 2004. **50**(2): p. 75-104.
95. Mauter, M.S., et al., *Antifouling Ultrafiltration Membranes via Post-Fabrication Grafting of Biocidal Nanomaterials.* Acs Applied Materials & Interfaces, 2011. **3**(8): p. 2861-2868.
96. Taurozzi, J.S., et al., *Effect of filler incorporation route on the properties of polysulfone-silver nanocomposite membranes of different porosities.* Journal of Membrane Science, 2008. **325**(1): p. 58-68.
97. Vandezande, P., L.E.M. Gevers, and I.F.J. Vankelecom, *Solvent resistant nanofiltration: separating on a molecular level.* Chemical Society Reviews, 2008. **37**(2): p. 365-405.
98. Cakar, F., et al., *Surface analysis of poly(ether imide) by inverse gas chromatography.* Optoelectronics and Advanced Materials-Rapid Communications, 2011. **5**(8): p. 821-826.
99. Bhat, G.S., P.G. Wapner, and W.P. Hoffman, *Processing of a high temperature imide copolymer into hollow fibers.* Materials and Manufacturing Processes, 2000. **15**(4): p. 533-545.
100. Krechetnikov, R. and G.M. Homsy, *Dip coating in the presence of a substrate-liquid interaction potential.* Physics of Fluids, 2005. **17**(10).
101. Strawbridge, I. and P.F. James, *The Factors Affecting the Thickness of Sol-Gel Derived Silica Coatings Prepared by Dipping.* Journal of Non-Crystalline Solids, 1986. **86**(3): p. 381-393.

102. Majeed, S., et al., *Multi-walled carbon nanotubes (MWCNTs) mixed polyacrylonitrile (PAN) ultrafiltration membranes.* Journal of Membrane Science, 2012. **403**: p. 101-109.

103. Jennifer, L.S., *Fouling-resistant coatings for reverse osmosis membranes: Gas and liquid permeation studies on morphology and mass transport effects*. 2011: ProQuest, UMI Dissertation Publishing.

104. E.A. Tsapiuk, M.T.B., V.M. Kochkodan and E.E Danilenko, *Separation of aqueous solution of non ionic organic solutes by ultrafiltration,.* Journal of Membrane Science, 1990. **48**(1).

105. Satyanarayana, S.V., P.K. Bhattacharya, and S. De, *Flux decline during ultrafiltration of kraft black liquor using different flow modules: a comparative study.* Separation and Purification Technology, 2000. **20**(2-3): p. 155-167.

106. J. Kestin, M.S., and W. A. Wakeham, *Viscosity of Liquid Water in the Range -8 °C to 150 °C.* Journal of Physical Chemistry, 1978. **Vol. 7**(3): p. 8.

APPENDICES

Appendix A

Sample Calculation of the Isothermal Permeability

A. Solving for n and k_P simultaneously.

1. Assumptions

2. The membrane surface is smooth.

3. The hydrogen partial pressure on the permeate side of the membrane is very small in comparison with the retentate side, therefore is negligible.

4. The governing equation for hydrogen permeation through dense media is given in terms of hydrogen flux, N_{H2}, and rate of hydrogen transport through the membrane, R_{H2}, by the following relations respectively.

$$N_{H_2} = -k_M \frac{P^n_{H_2,Ret}}{t_M} \quad \text{or} \quad R_{H_2} = -k_M A_M \frac{P^n_{H_2,Ret}}{t_M}$$

5. The following table illustrates an example of one data set collected under steady state conditions, for an array of given temperatures.

y_{H2} in Process Gas	Membrane Temperature	Process Gas Flow Rate	Process Gas Pressure	Sweep Gas Flow Rate	Sweep Gas Pressure	y_{H2} in Sweep Gas
	(K)	(smm)	(kPa)	(smm)	(kPa)	
0.90	738	1.9E-4	101.35	8.5E-5	116.52	0.009009
0.90	738	1.9E-4	652.93	8.5E-5	116.52	0.024649
0.90	738	1.9E-4	1549.25	8.5E-5	116.52	0.042609
0.90	738	1.9E-4	2928.20	8.5E-5	116.52	0.063893

6. The area of the membrane is calculated using the inside diameter of the membrane holder (0.51 inches).

$$A_M = \frac{\pi D^2}{4} = \frac{\pi (0.51\text{in})^2}{4} * \frac{(2.54\text{cm})^2}{\text{in}^2} = 1.317\text{cm}^2 = 1.317\text{x}10^{-4}\,\text{m}^2$$

7. Calculation the hydrogen partial pressures of the process gas feed.

$$p_{H2,Ret} = y_{H2,Ret} P_{Ret} = (0.90)(101.35\text{kPa}) = 91.21\text{kPa}$$

8. The rate of hydrogen passing through the membrane is then calculated

$$R_{H_2} = \frac{Q_{Sweep} y_{H2,Per}}{y_{Ar,Per}} * \frac{\text{mol}}{2.24\text{x}10^{-2}\,\text{m}^3} \Rightarrow \frac{\left(85\frac{\text{cm}^3\,\text{Ar}}{\text{min}}\right)_{STP}(0.009009\,\text{mol}\,H_2)}{(1-0.009009)\text{mol Ar}} * \left(\frac{\text{mol Ar}}{22400\text{cm}^3\,\text{Ar}}\right)_{STP}$$

$$R_{H_2} = 3.40\text{x}10^{-5}\frac{\text{mol}\,H_2}{\text{min}} = 5.56\text{x}107\frac{\text{mol}\,H_2}{\text{s}}$$

9. Calculation of the membrane permeation characteristics is accomplished by first taking the log of the permeation governing equation as follows.

$$R_{H_2} = \frac{k_M A_M}{t_M}\left(P^n_{H_2,Ret} - P^n_{H_2,Per}\right) \Rightarrow R_{H_2} = \frac{k_M A_M}{t_M}\left(P^n_{H_2,Ret}\right) \Rightarrow$$

$$\log R_{H_2} = n \log P_{H_2,Ret} + \log\frac{k_M A_M}{t_M}$$

10. Therefore, the only unknowns in the permeation governing equation are the partial pressure exponent, n, and the membrane permeability k_P. The log calculations needed for the analysis of n and k_P are give in the following table.

y_{H2} in Process Gas	Process Gas Pressure	y_{H2} in Sweep Gas	$p_{H2,Ret}$	R_{H2}	log $p_{H2,Ret}$	log R_{H2}
	(kPa)		(kPa)	(mol H_2/s)	(kPa)	(mol H_2/s)
0.90	101.35	0.09009	91.22	5.67E-7	1.96	-6.25
0.90	652.93	0.024649	587.64	1.62E-6	2.77	-5.79
0.90	1549.25	0.042609	1394.33	2.82E-6	3.14	-5.55
0.90	2928.20	0.063893	2653.38	4.34E-6	3.42	-5.36

11. An example of the log of the retentate hydrogen partial pressure, $p_{H2,Ret}$, plotted against the log of the rate of hydrogen transport through the membrane, R_{H2}, is shown below.

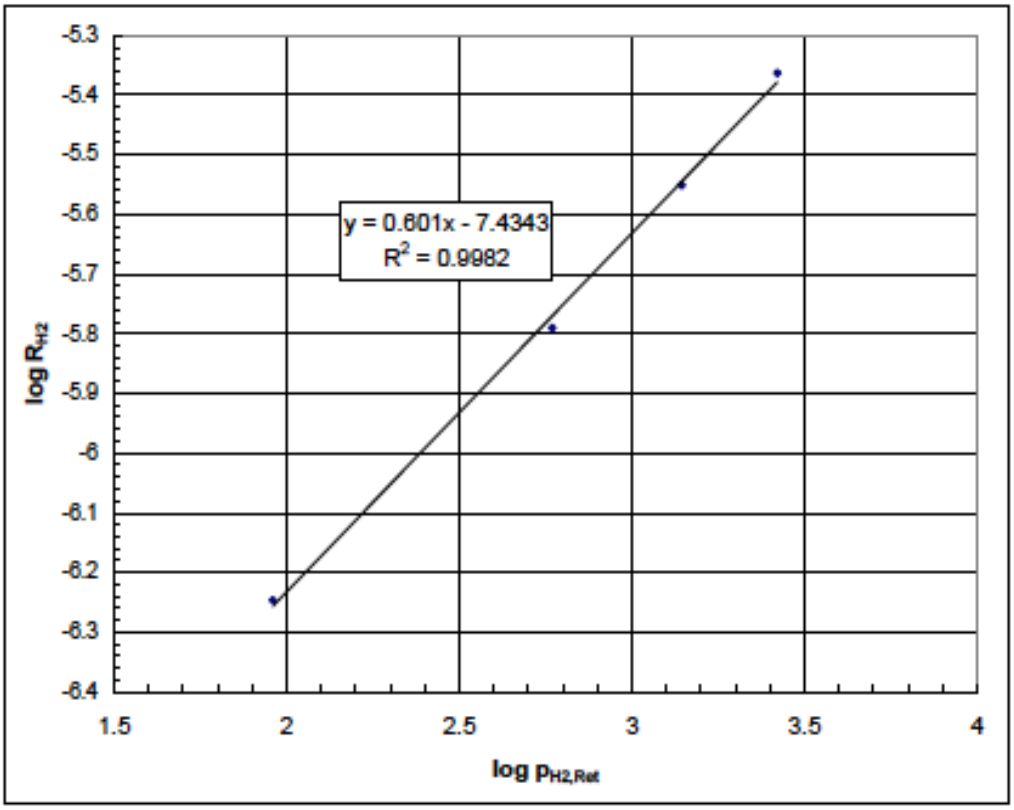

12. Thus, n and k_P are obtaind for the slope and intercept by the following relationships respectively:

$$m = n \therefore n = 0.60$$

and

$$b = \log\frac{k_M A_M}{t_M} \Rightarrow k_M = \frac{t_M}{A_M}10^b = \frac{0.001\,m}{1.317x10^{-4}\,m^2}10^{(-7.4343)}$$

$$k_M = 2.79x10^{-7}\frac{mol}{ms\,kPa^{1-0.60}} = 1.77x10^{-8}\frac{mol}{ms\,Pa^{0.40}}$$

B. Solving for k_P assuming that the rate-limiting step is diffusion (n=0.5).

5 Assumptions

13. The membrane surface is smooth.
14. The hydrogen partial pressure on the permeate side of the membrane is very small in comparison with the retentate side, therefore is negligible.

6 The governing equation for hydrogen permeation through dense media is given in terms of hydrogen flux, N_{H2}, and rate of hydrogen transport through the membrane, R_{H2}, by the following relations respectively.

$$N_{H_2} = -k_M \frac{P^n_{H_2,Ret}}{t_M} \quad \text{or} \quad R_{H_2} = -k_M A_M \frac{P^n_{H_2,Ret}}{t_M}$$

7 The following table illustrates an example of one data set collected under steady state conditions, for an array of given temperatures.

y_{H2} in Process Gas	Membrane Temperature	Process Gas Flow Rate	Process Gas Pressure	Sweep Gas Flow Rate	Sweep Gas Pressure	y_{H2} in Sweep Gas
	(K)	(smm)	(kPa)	(smm)	(kPa)	
0.90	738	1.9E-4	101.35	8.5E-5	116.52	0.009009
0.90	738	1.9E-4	652.93	8.5E-5	116.52	0.024649
0.90	738	1.9E-4	1549.25	8.5E-5	116.52	0.042609
0.90	738	1.9E-4	2928.20	8.5E-5	116.52	0.063893

8 The area of the membrane is calculated using the inside diameter of the membrane holder (0.51 inches).

$$A_M = \frac{\pi D^2}{4} = \frac{\pi (0.51\text{in})^2}{4} * \frac{(2.54\text{cm})^2}{\text{in}^2} = 1.317\text{cm}^2 = 1.317\text{x}10^{-4}\text{m}^2$$

9 Calculation the hydrogen partial pressures of the process gas feed.

$$p_{H2,Ret} = y_{H2,Ret} P_{Ret} = (0.90)(101.35\text{kPa}) = 91.21\text{kPa}$$

10 The rate of hydrogen passing through the membrane is then calculated

$$R_{H_2} = \frac{Q_{Sweep} y_{H2,Per}}{y_{Ar,Per}} * \frac{\text{mol}}{2.24\text{x}10^{-2}\text{m}^3} \Rightarrow$$

$$R_{H_2} = \frac{\left(85\frac{\text{cm}^3\text{ Ar}}{\text{min}}\right)_{STP}(0.009009\,\text{mol H}_2)}{(1-0.009009)\text{mol Ar}} * \left(\frac{\text{mol Ar}}{22400\text{cm}^3\text{ Ar}}\right)_{STP}$$

$$R_{H_2} = 3.40\text{x}10^{-5}\frac{\text{mol H}_2}{\text{min}} = 5.56\text{x}107\frac{\text{mol H}_2}{\text{s}}$$

11 Calculation of the membrane permeation characteristics is accomplished by solving the rate equation illustrated below.

$$R_{H_2} = \frac{k_M A_M}{t_M}\left(P^n_{H_2,Ret} - P^n_{H_2,Per}\right) \Rightarrow R_{H_2} = \frac{k_M A_M}{t_M}\left(P^n_{H_2,Ret}\right) \Rightarrow$$

$$R_{H_2} = \frac{k_M A_M}{t_M}\left(P^{0.5}_{H_2,Ret}\right)$$

8. Therefore, the only unknown in the permeation governing equation is the membrane permeability constant k_P. Sample values of the membrane permeability constant at various temperatures is illustrated in the table below.

y_{H2} in Process Gas	Process Gas Pressure	y_{H2} in Sweep Gas	$p_{H2,Ret}$	R_{H2}	k_P
	(kPa)		(kPa)	(mol H_2/s)	(mol H_2 / m s $Pa^{0.5}$)
0.90	101.35	0.09009	91.22	5.67E-7	1.43E-8
0.90	652.93	0.024649	587.64	1.62E-6	1.60E-8
0.90	1549.25	0.042609	1394.33	2.82E-6	1.81E-8
0.90	2928.20	0.063893	2653.38	4.34E-6	2.02E-8

relation enables one to calculate the membranes permeability at any temperature within the temperature range of the experiments.

Appendix B

Methods of measurement for critical flux: a comparison

Method	Advantages	Disadvantages	Form measured	Suitability
Flux–pressure profile: deviation from linearity (Section 3.1.1)	Simplicity	Can be subjective. No link with reversibility	Strong and weak form J_{cs}, J_{cw}	Feeds with low osmotic pressure
Flux or pressure vs. time: flux stepping (Section 3.1.2)	With up and down steps, fouling hysteresis found. Resistance should be determined for each step	Unlike flux cycling, points of transition to irreversibility can be missed	Strong and weak form J_{cs}, J_{cw}	Feeds with low osmotic pressure; if correction is to be made for osmotic pressure flux cycling is to be preferred
Flux or pressure vs. time: flux cycling (Section 3.1.2)	Rigorous when allowance made for osmotic pressure	Time consuming and complex	All forms J_{cs}, J_{cw} and J_{ci}	All kinds of feed
Direct observation through the membrane (Section 3.2)	Direct observation of flux giving deposition. Potential for measuring J_{ci} yet to be exploited	Limited to particulate feeds and membranes that are transparent when wet	Linkage to J_{cs}, J_{cw} or J_{ci} not obvious, but value determined is significant	Particulate feeds
Mass balance (Section 3.3)	Linked to a complementary parameter, the deposited mass	Needs to be used in conjunction with another method	Linkage to J_{cs}, J_{cw} or J_{ci} not obvious, but value determined is significant	Particulate feeds
Determination by fouling rate analysis (Section 3.4)	If a flux for "low fouling" is not found then determination of dP/dt (under fixed fluxes) may identify a point of sustainable flux. Absolute "no fouling" corresponds to a critical flux	Can be subjective. No link with reversibility	Strong and weak form J_{cs}, J_{cw} also J_{sus}	All feeds

Appendix C

Viscosity of water at different temperatures

TABLE 4. Re-evaluation of viscosities from the original data of L. D. Eicher and B. J. Zwolinski [6] with the aid of eq (3)

Temp. °C	Density ρ, kg/m³	Viscosity μ, μPa s from [6]	Re-evaluation				
			Viscosity μ, μPa s	Kinematic viscosity ν, mm²/s	Uncertainty $\Delta\nu$	Relative uncertainty $\Delta\mu/\mu$ or $\Delta\nu/\nu$, %	Deviation from [6] %
−8. 280	0. 998502	2455. 1	2456. 6	2. 4603	0. 0002	0. 01	−0. 06
−6. 647	0. 998878	2296. 0	2297. 3	2. 2999	0. 0002	0. 01	−0. 06
−4. 534	0. 999329	2113. 7	2114. 9	2. 1164	0. 0002	0. 01	−0. 06
−1. 108	0. 999752	1863. 0	1863. 9	1. 8644	0. 0002	0. 01	−0. 05
0	0. 9998396	1791. 9	1792. 7	1. 7930	0. 0002	0. 01	−0. 04
5	0. 9999641	1519. 0	1519. 6	1. 5196	0. 0002	0. 01	−0. 04
10	0. 9997281	1306. 7	1307. 1	1. 3075	0. 0002	0. 01	−0. 03
15	0. 9991286	1138. 0	1138. 4	1. 1393	0. 0002	0. 01	−0. 04
20	0. 9982336	1002. 0	1002. 1	1. 0039	0. 0001	0. 02	−0. 01
25	0. 9970751	890. 20	890. 2	0. 8928	0. 0001	0. 02	0. 0
30	0. 9956783	797. 23	797. 2	0. 8006	0. 0002	0. 02	0. 01
35	0. 9940635	719. 11	719. 0	0. 7233	0. 0002	0. 02	0. 01

TABLE 5. Re-evaluation of original data of L. D. Eicher and B. J. Zwolinski [6] on a relative basis

Reference temperature: 20 °C

Temp. t °C	Density ratio $\rho(t)/\rho(20\ °C)$	Viscosity ratio $\mu(t)/\mu(20\ °C)$	Ratio of kinematic viscosities $\nu(t)/\nu(20\ °C)$	Uncertainty $\Delta[\nu(t)/\nu(20\ °C)]$	Relative uncertainty %
−8.280	1.00027	2.4508	2.4502	0.0007	0.03
−6.647	1.00065	2.2920	2.2905	0.0007	0.03
−4.534	1.00110	2.1103	2.1080	0.0006	0.03
−1.108	1.00152	1.8596	1.8568	0.0005	0.03
0	1.00161	1.7886	1.7857	0.0004	0.03
5	1.00173	1.5161	1.5135	0.0003	0.02
10	1.00150	1.3042	1.3023	0.0002	0.02
15	1.00090	1.1359	1.1348	0.0001	0.01
20	1.00000	1.0000	1.0000	0.0000	0.00
25	0.99884	0.8884	0.8894	0.0001	0.01
30	0.99744	0.7957	0.7977	0.0002	0.02
35	0.99582	0.7178	0.7208	0.0002	0.03
40	0.99400	0.6516	0.6555	0.0003	0.05

VITA

Vincent C. Kandagor Chesire was born on June 20 1980 in Kabarnet, Baringo County-Kenya to Christina Kandagor and the late Chief-Councilor L.K Chesire. He graduated with an accelerated Master of Science Degree in Material Science and Engineering from Missouri State University in December 2008. In January 2009, he took a Post Masters Research Associate position at the Oak Ridge National Laboratory and in September 2009 he joined The University of Tennessee - Knoxville as a Graduate Research Fellow at The Bredesen Center for Interdisciplinary Research and Graduate Education to pursue his PhD in Energy Science and Engineering under the guidance of Professor Gajanan Bhat.